Mirijam Zickel

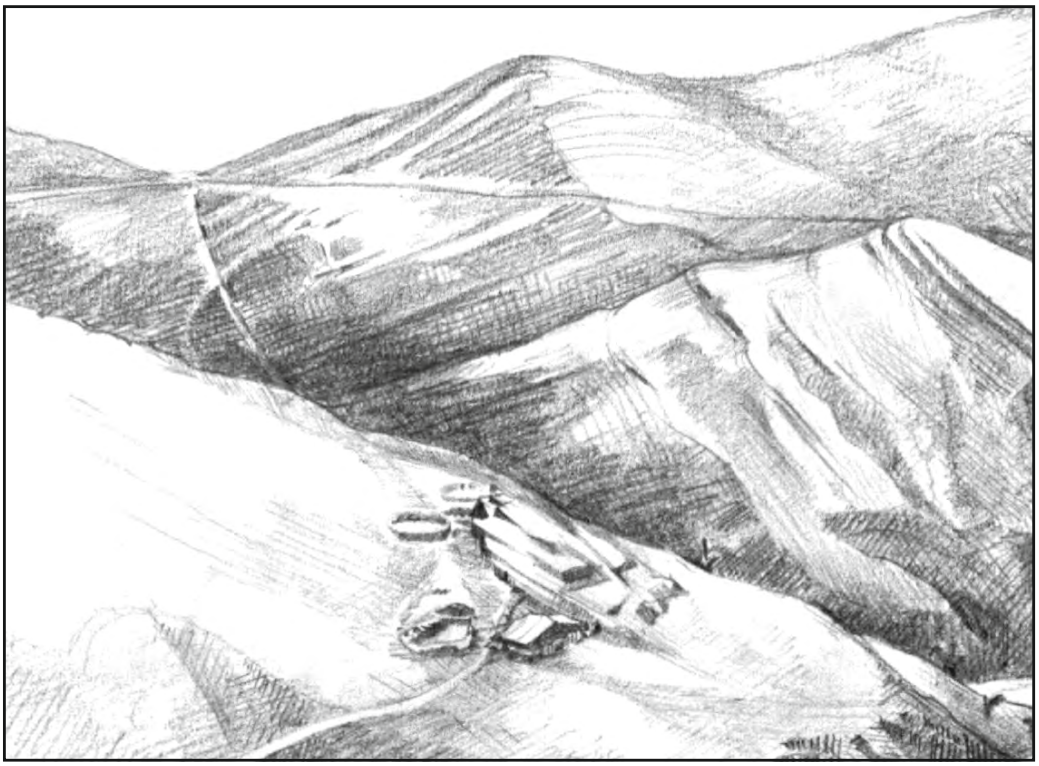

SPATIAL PATTERNS OF MOROCCAN TRANSHUMANCE

Geoarchaeological field work & spatial analysis of herder sites in the High Atlas Mountains of Morocco

KÖLNER ETHNOLOGISCHE BEITRÄGE

Herausgegeben von Michael J. Casimir

Heft 58

2020

Drawing: Laura Meier, 2017. The nomads' camp on the summer pastures of the Aït Atta in the High Atlas Mountains. Sketches from the field.https://laurameier.allyou.net/9374319/ait-atta-nomads

Mirijam Zickel

SPATIAL PATTERNS OF MOROCCAN TRANSHUMANCE

Geoarchaeological field work & spatial analysis of herder sites in the High Atlas Mountains of Morocco

KÖLNER ETHNOLOGISCHE BEITRÄGE

Herausgegeben von Michael J. Casimir

Heft 58

Zu beziehen durch:
Institut für Ethnologie
Universität zu Köln
Albertus-Magnus-Platz
D-50923 KÖLN

2020

Vorwort

Seit geraumer Zeit, nicht zuletzt unter dem Einfluss des Klimawandels, nimmt das Interesse der Ethnologie an den Methoden einiger Nachbardisziplinen im Sinne der interdisziplinären Zusammenarbeit zu. Hierbei spielen die Geographie und in besonderem Maße fernerkundliche Methoden sowie räumliche Analysen eine herausragende Rolle. Ebenso wie, im Kontext diachroner Analysen, die Methoden der Geoarchäologie zur Erfassung der lokalen Historie.

Um diese Forschungsansätze den Studierenden der Ethnologie nahezubringen habe ich Frau Mirijam Zickel gebeten mir ihre Masterarbeit, die von Herrn Prof. Dr. Georg Bareth und Frau Dr. Astrid Röpke betreut und mit dem zweiten Platz des Dr. Prill Preises 2020 der Gesellschaft für Erdkunde ausgezeichnet wurde, in leicht veränderter Form, für meine Reihe zur Verfügung zu stellen.

Nach einer allgemeinen Darstellung der Methoden der Fernerkundung zeigt Frau Zickel am Beispiel transhumanter Aït Atta auf deren Sommerweiden im Hohen Atlas, wie durch die räumliche Analyse von Fernerkundungsdaten und unter Einbezug von geoarchäologischen Informationen, Erkenntnisse über die Aufenthaltsplätze der Nomaden im Sommerlager gewonnen werden können. Hierbei zeigt sich, dass die Viehpferche der Nomaden eine zentrale Rolle für die räumliche und zeitliche Erfassung von Transhumanz im Untersuchungsgebiet spielen können. Weiterhin ist es ihr gelungen, mit unterschiedlichen, einander ergänzenden Methoden der Fernerkundung die ökologische Situation des Gebietes und insbesondere der Pferchstandorte zu beleuchten. Ihre Arbeit eröffnet eine neue Perspektive, um die Mensch-Umweltbeziehung im semiariden Bergland von Marokko zu erfassen.

Michael J. Casimir

Acknowledgements

I am much obliged to all of those who supported me in carrying out my master thesis. Mostly, the gratitude goes beyond this intense period.

First of all, I want to express my greatest thanks to Touda, Brahim and their family who have been extremely hospitable. With great serenity they have accepted my interest in the deposits of their livestock pens, and still invited me to their tent. I would like to thank Abdellah Benalla, who tirelessly translated my various questions into Tamazight. Many thanks go to Thomas Reitmaier as he invited me to participate in the AREHHAL project and provided the WorldView-2 data. I thank Laura Meier, our talented illustrator, for her assistance in the field and for making a digital herbarium of local plant communities. Moreover, I would like to thank Wolfram Lobin, who supported the subsequent plant identification.

I would like to mention my first supervisor Georg Bareth in particular. Despite his many commitments, he has a far-reaching and inspiring enthusiasm, not exclusively in GIS and remote sensing, but for interdisciplinary work as well. Thank you for accepting my master thesis, sharing your wide experiences with me, and for constructive criticism.

Many thanks are addressed to the outstanding guidance of my second supervisor Astrid Röpke. In sharing her knowledge, I gained a lot of experience in the field of geoarchaeology and she constantly supported my work with expertise and creativity. Her openness to new approaches and other disciplines has set this study in motion.

Of course, the patient proofreaders and advisors who supported me in copy-editing, contributed to the completion of this thesis as well. Thank you, my dear friends, family and colleagues: Michael Casimir, Marina Herbrecht, Christoph Hütt, Ulrike Lussem and especially Hauke-Peter Vehrs. Moreover, my favourite archaeologist Thomas Wolter, who supported my work even from far away Athens must be emphasised here. Just as Vera Krieger, who provided advice in schedule organisation, LaTeX and layout matters. Concluding, I am grateful for continuous intellectual exchange and teamwork experience, which largely contributes to good research conditions.

Contents

Abbreviations

A.m.s.l. .....Above Mean Sea Level
AD .....Anno Domini (Christian Era)
AOI.....Area Of Interest
CRS .....Coordinate Reference System
DEM .....Digital Elevation Model
DLR.....German Aerospace Center
(Deutsches Zentrum für Luft- und Raumfahrt)
ESA .....European Space Agency
ESP .....Earth Surface Process
GCP.....Ground Control Point
GIS.....Geographic Information System
GPS .....Global Positioning System
GUI.....Graphical User Interface
LMVM.....Local Mean and Variance Matching
MFD.....Multiple-Flow-Direction
MFC.....Morphological Feature Contrast
MTC .....Morphological Texture Contrast
NDVI.....Normalized Difference Vegetation Index
NIR.....Near-infrared
NIR-1.....Near-infrared region: WV-2 band 7, 765-901 nm
NIR-2.....Near-infrared region: WV-2 band 8, 856-1043 nm
OTB.....Orfeo Toolbox
QM .....Quantitative Modelling
Radar.....Radio Detection And Ranging
RGB.....Red-Green-Blue band composite
ROI.....Region Of Interest
RPC.....Rational Polynomial Coefficients
SAR .....Synthetic Aperture Radar
SWIR.....Short-wave Infrared
TDX.....TanDEM-X
UTM .....Universal Transverse Mercator
Uint .....Unsigned Integer
WGS 84.....World Geodetic System 1984
WV-2.....WorldView-2

List of Figures

List of Tables

1 Introduction

In many parts of the world, various forms of pastoralism have developed since Neolithic times. About a quarter of the earth land surface is used for livestock grazing (reported for 2000, compare Ramankutty et al. 2008), which occurs in many different forms, such as mobile pastoralism, agropastoral livelihood, or permanent rangeland grazing.

This study is concerned with a transhumant pastoral system in the Moroccan Central High Atlas Mountains. Transhumant pastoralism implies seasonal mobility between summer and winter pastures whereby the herder community, choose the migration routes according to the actual climatic conditions which are related to the availability of fodder and water. Migration can take place over a short or a long distance and often occurs between the low- and highlands (Akasbi et al. 2012: 315).

In 2017, the interdisciplinary project AREHHAL (an acronym which stands for: 'transhumant herder' in Tamazight) started to document the life of one pastoral family of the ethnic group of the Aït Atta, whereby the one family was accompanied on their annual migration routes. The project has the task to document the pastoral way of life of the Aït Atta, which was exposed to significant change in the last decades. Many of the formally nomadic Aït Atta families have now settled down and earn their living as subsistence farmers. Whereas the ethnoarchaeological part of the project is generally concerned with the documentation of the everyday life and the material culture, geoarchaeology focuses on the livestock pens of the transhumant nomads (compare Reitmaier et al. 2017). The analysis of the sediments below the pens are understood as landscape archives whereby the contemporary regional flora and fauna provide the analysis with reference data. Specifically, herder camps and related livestock pens on the communal summer pastures of the Aït Atta are concerned (see Chapter 3.2). These pastures are situated in a semiarid steppe landscape (see Chapter 3.1) at an altitude of approximately 2 500 m above mean sea level (a.m.s.l.).

Ethnoarchaeological and geoarchaeological documentation enables insights in trans-humance practices in a mountainous semiarid environment. In general, this knowledge can be used in the archaeological study of prehistoric transhumant herder camps. At the same time, it must be noted that in

contrast to sedentary lifestyles, the use of tents as dwellings is common in Moroccan long distance transhumance (Akasbi et al. 2012: 315). Permanent or extensive habitation structures and related material culture do not occur in the pastoralist's territory. Thus, in a narrow sense, transhumant pastoralists hardly leave considerable traces of their activity in the archaeological context. In contrast to the few remnants of pastoralists on pasture land, livestock pens build by the herders consist of durable dry-stone-walls. Thus, to investigate environmental and human history in the region (compare Marshall et al. 2018 and Kothieringer et al. 2018), geoarchaeological methods can be applied on these livestock pens or rather their sediments (see Chapter 2.7).

According to the geoarchaeological investigations of livestock pens performed in the AREHHAL project in 2017, their sediments seem to represent a special ecological habitat with increased organic content and humidity (see Chapter 3.3), especially, in contrast to the surrounding ground of the semi-arid environment. Considering that livestock pens and their sediments are the major material remains of a herder camp, they provide a key to record transhumant pastoralists archaeologically (compare Shahack-Gross 2011).

To contextualize the geoarchaeological results of 2017 (see Chapter 3.3) in the region, further herder camp sites must be investigated. Since, the mountainous study area is difficult to access, a targeted approach to determine potential key sites is required. Potentially, remote sensing and geographic information system (GIS) methods can specifically contribute to these requirements of interdisciplinary research with the analysis of satellite image data and the detection of possible study sites in a vast and inaccessible research areas (compare Luo et al. 2014). Furthermore, ethnographic data about pastoral groups in Morocco and the Aït Atta in particular is considered to complement the GIS analysis with insights of pastoral land use practices in the region.

In the sense of digital geoarchaeology (compare Siart 2018), the study's aim is, to create a link between the fields of remote sensing, GIS and geoarchaeology. In this work, it will be further investigated to what extent remote sensing and GIS can contribute to research in the study area and in the context of digital geoarchaeology.

Objectives of this study

In more detail, this study focusses on the investigation of the herder camp distribution in the Central High Atlas study area (see Chapter 3) and the research of spectral livestock pen tracers in the region (see Chapter 2.2). In the following, the working hypotheses and main steps will be discussed.

In a region with predominant pastoral land use (see Chapter 3), it is assumed that recent land use patterns can be investigated by a remote-sensing-based detection of livestock pens. Since the area under study is a mountainous terrain, which poses specific challenges to the analysis of remote sensing data, a combined analysis of high-resolution multispectral WorldView-2 (WV-2) imagery and high-resolution elevation data of TanDEM-X (TDX) will be performed.

From a remote sensing perspective, the dry-stone walls of the livestock pens seem to be difficult to detect. Their spatial extension is limited to a few square metres, they have a circular shape and the wall thickness does rarely exceed 1 m in width (see Fig. 1). Additionally, they are often built from stones taken from the surrounding surface and are therefore difficult to distinguish spectrally from their environment (see Chapter 2.6). This is a challenge for pixel-based satellite image classification (see Analysis III in Fig. 17 in Chapter 4).

Therefore, a spectral edge extraction approach will be carried out additionally. Subsequently, the shapes of livestock pens can be isolated and therefore herder camps can be detected. To specify the detection results, it is planned to intersect the results with suitable herder camp terrain parameters in a GIS analysis (see Analysis II in Fig. 17 in Chapter 4). Since it is expected that pen sediments could last over several epochs (compare Marshall et al. 2018), their traces are assumed to be visible on the surface even after decades after their last use.

These 'pen imprints' were frequently observed during field work (Chapter 3.1). Often the dry-stone walls were dismantled over time, occasionally, remains of the pen wall are still visible. In most cases, only a specific ground signature can be determined, which differs from the surrounding surface (see Fig. 1). Accordingly, a further interest of this work is the question to which extent recently used pen locations can spectrally be distinguished from pen imprints, respectively former livestock pen locations (see Accuracy Assessment and Statistics in Fig. 17 in Chapter 4).

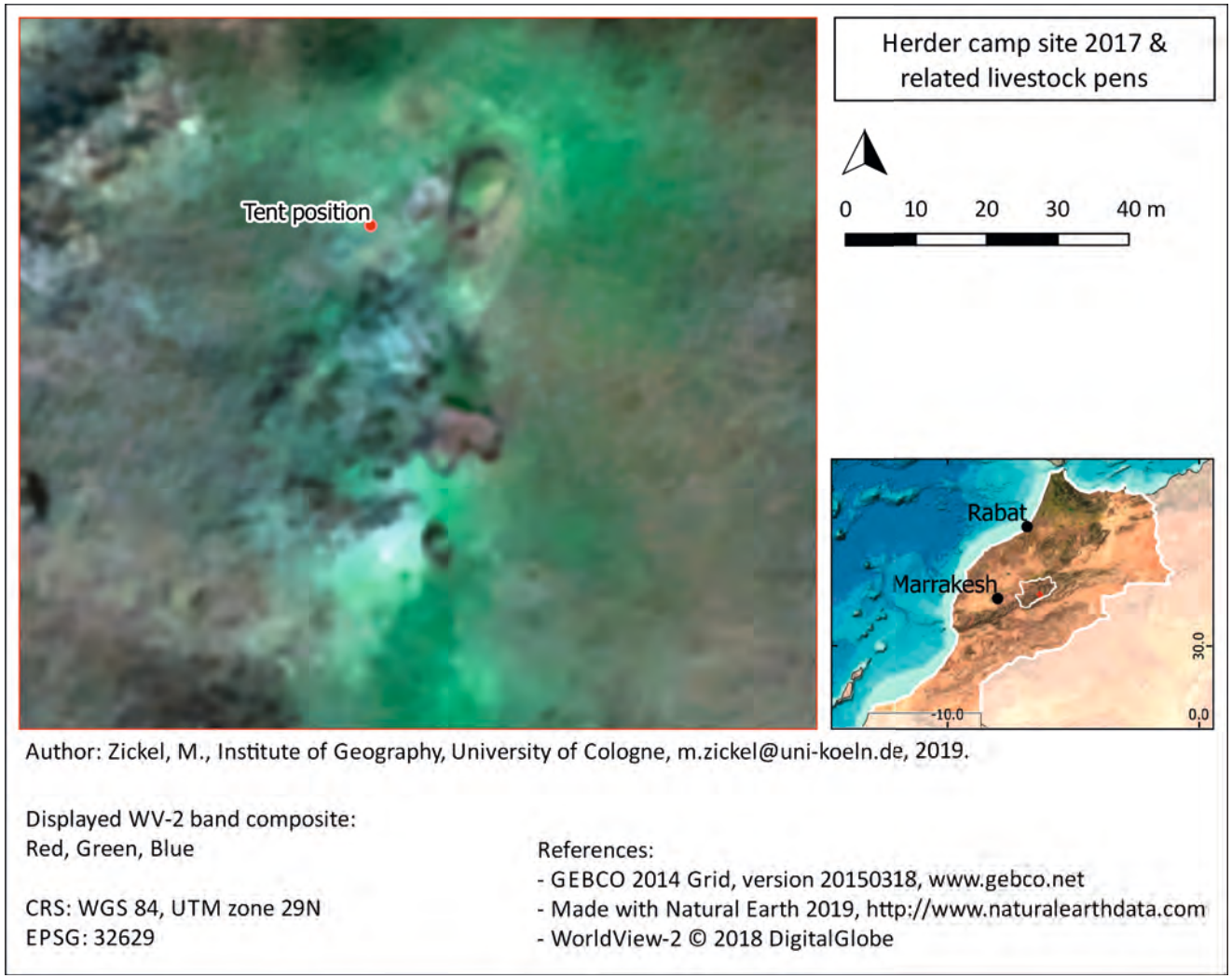

Figure 1: WV-2 RGB (red-green-blue band composite) image of the herder camp area investigated in 2017. The circular black shapes in the map centre represent livestock pens. The visible green ground signature frequently occurs at herder camp sites in the region.

As mentioned above, the pen sediments have a rich organic content respectively they are possibly rich in plant nutrients. Related to this, it will be investigated if the consistence of the specific, patchy-green spectral signature (see Fig. 1) on herder camp sites can be determined by remote sensing techniques (see Chapter 2.2) For this purpose, the normalized difference vegetation index (NDVI) will be used to examine, to what extent the ground signature is caused by plant growth (see Analysis IV in Fig. 17 in Chapter 4). Probably the signature can be used as livestock pen tracer. In addition to this part of the study plan, the mentioned TDX data is used to explore, if the sharply bordered ground signature is caused by the local relief, for instance the presence of natural depressions (see Analysis I in Fig. 17 in Chapter 4).

In the following Chapter 2, the basic study information is explained and the study area is furthermore geographically described in Chapter 3. In addition, the geoarchaeological fieldwork of 2017 and regional archaeology are described in this chapter to complement the comprehensive description of the study area. Subsequently, Chapter 4 illustrates the satellite data set properties and the methodological approach in detail, while Chapter 5 presents the results of the remote sensing and GIS analysis. The results are then discussed in Chapter 6. Concluding, the outcome and scope of this work is reconsidered against the background of the wider research project mentioned above (Chapter 7). It is supplemented by a brief outlook (Chapter 8) on possible improvements and future geoarchaeological research in the region.

It can be observed that remote sensing and GIS have been used frequently in the field of archaeology for some decades now. Often, an analysis of remote sensing data with GIS proves to be a powerful method for archaeological prospection. The big advantage here is the possibility to prospect even very large areas and especially poorly accessible terrain. This enables systematic search for sites in the study area. Locations with a high archaeological potential, probable key sites, can be determined under certain aspects, such as a high occurrence of stone rows (building remains) or mound deposits (tumuli, tells).

'Moreover, the permanent increase in spatial resolution of available datasets also helps to overcome the traditional problems of scale (e.g. Stein 1993; Schlummer et al. 2014) between archaeologists, who mainly work on specific and spatially restricted sites over distinct human-related time slices, and geoscientists, who rather focus on specific environments and/or landscape-forming processes.' (Siart 2018: 3)

As Siart 2018 mentioned, today high-resolution geospatial data can be combined with archaeological and geoarchaeological field data. The combination of data from different scales yields the possibility to link and contextualise excavation, or rather research results of several sites within a specific space. For example, such a combined approach was used, in the northeast of Dunhuang oasis in China. Among other geospatial data, the advantage of high-resolution WV-2 data let to the discovery of several previously unknown archaeological sites. These were mainly building remains identified as courier stations along a medieval road system Luo et al. 2014.

Furthermore, remote sensing and GIS, or rather spatial analysis has a high potential in geoarchaeology, the discipline of landscape archaeology or paleoenvironment reconstruction (Siart 2018: 1). In which remotely sensed data displays traces of past landscapes on today's land surface, it facilitates the exploration of prehistoric geography. The publication of textbooks, such as Siart 2018's work on digital geoarchaeology, shows the trend towards a sustainable implementation of GIS and remote sensing methods in the everyday work of geoarchaeology. Also, within this textbook Verhagen 2018 does explain a critical perspective on the future of digital geoarchaeology. He

presupposes a paradigm shift with regard to digital methods in archaeology in general. Thus GIS & remote sensing should be seen as a possible focus of archaeological work rather than an auxiliary tool that supports intrinsic archaeological interpretation (see quote on next page).

'The emphasis placed by postprocessual theoreticians on narrative, at the expense of scientific methods, has led to a rift between 'science-based' and mainstream archaeology that is still very evident today. It has also led to an attitude amongst archaeologists of seeing 'hard science' methods and techniques as auxiliary tools that provide helpful data to be used in the construction of an historical narrative, rather than as a possible focus of archaeological research.' (Verhagen 2018: 21)

Since, this study unites remote sensing, or rather GIS methods and geoarchaeology, the data analysis provides the basis for future geoarchaeological site search in the study area. The successful combination of data from different survey levels: field work, satellite remote sensing and GIS requires certain knowledge about the nature of the respective data sources and methods. Accordingly, this chapter explains the basics necessary to perform the preprocessing and analysis steps listed in Chapter 4. Furthermore, ethnological and geoarchaeological background information are provided.

2.1 Satellite remote sensing

The field of remote sensing essentially involves collecting information about an object, area or phenomenon without being in direct contact with it. This is often done with sensors mounted on drones, aircraft or satellites. A simple photo camera can be called a remote sensing sensor as well as a human eye that works according to the same principle of contactless exploration and information reading. Whereas the human brain stores and analyses sensed data, sensor collected data requires a computer and storage media to perform this task. The two examples given and WV-2 that is used in this study belong to the group of passive optical sensors that record reflected light. In addition to these and among others, it exists a variety of sensor systems (compare Lillesand et al. 2015: 1). However, the focus of this study is on the analysis of electromagnetic signals (see Fig. 2) collected by the satellite mission WV-2

(DigitalGlobe 2019a). Additionally, digital elevation data of the satellite mounted, active TDX radar (radio detection and ranging) sensor of the DLR 2019 was implemented in this study, and which will be concerned in Chapter 2.3.

In general, electromagnetic energy is radiated or reflected as waves. The electromagnetic spectrum can be differentiated by its wavelength, the distance from one wave peak to the other. Mostly, it is measured in micro- (µ) or nanometres (nm). Besides the wavelength, or spectral region of visible blue, green or red light (400 to 700 nm), the sensing of other wavelengths regions (see Fig. 2) can be very useful in image analysis of the earth surface for different purposes. Therefore, multispectral optical sensors such as WV-2 do not only sense visible light. For example, they record in the Ultraviolet (UV), near Infrared (NIR), infrared (IR), or shortwave infrared (SWIR) region. The different regions are split in several sensor bands. Their number and width determines the spectral resolution of the sensor. Reflection differences of certain wavelength regions produce specific spectral signatures for various landcover types and objects (see Fig. 3) that can be analysed (Lillesand et al. 2015: 4-6).

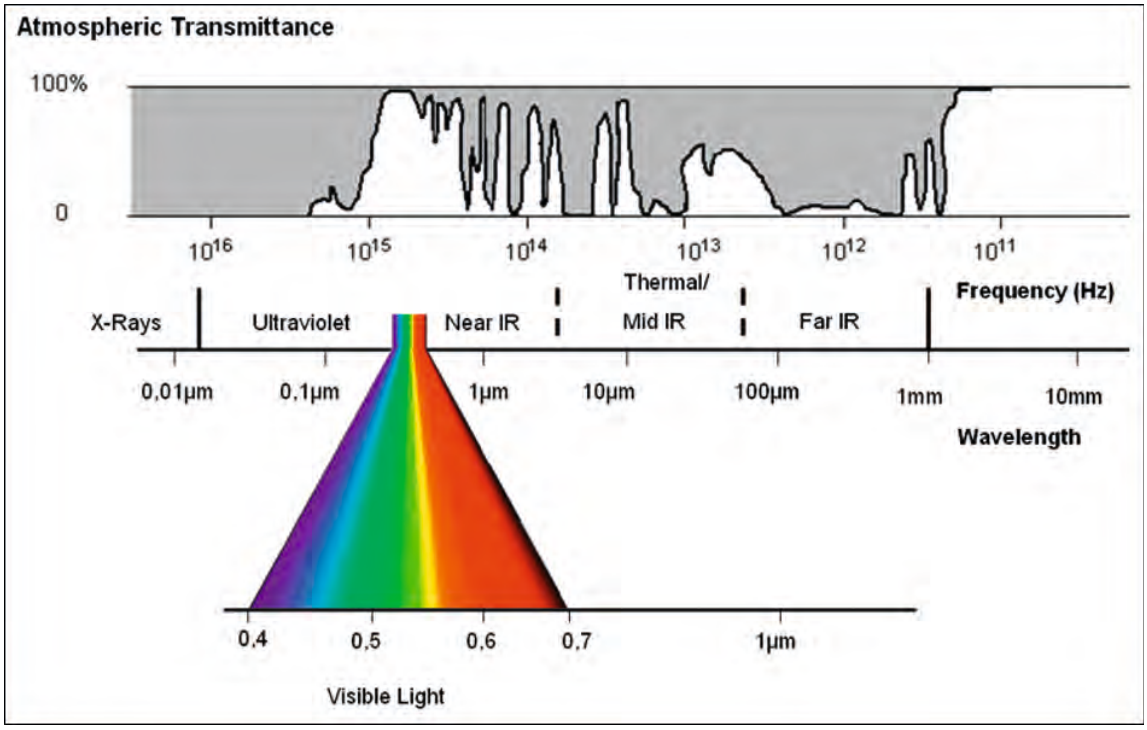

Figure 2: The electromagnetic spectrum: Spectral regions and wavelengths (modified version of SEOS 2019b)

2.2 Spectral properties and image classification (WorldView-2)

Spectral signatures are material- or object-related patterns that result from the reflection intensity variation across the electromagnetic spectrum. In Fig. 3 the spectral signatures of exemplary main landcover types are displayed. The figure illustrates how landcover types can be distinguished by comparing the specific reflection intensity per wavelength region, or rather per sensor band covering this. In particular, the spectral signature curve of vegetation shows a distinctive course (compare Fig. 3).

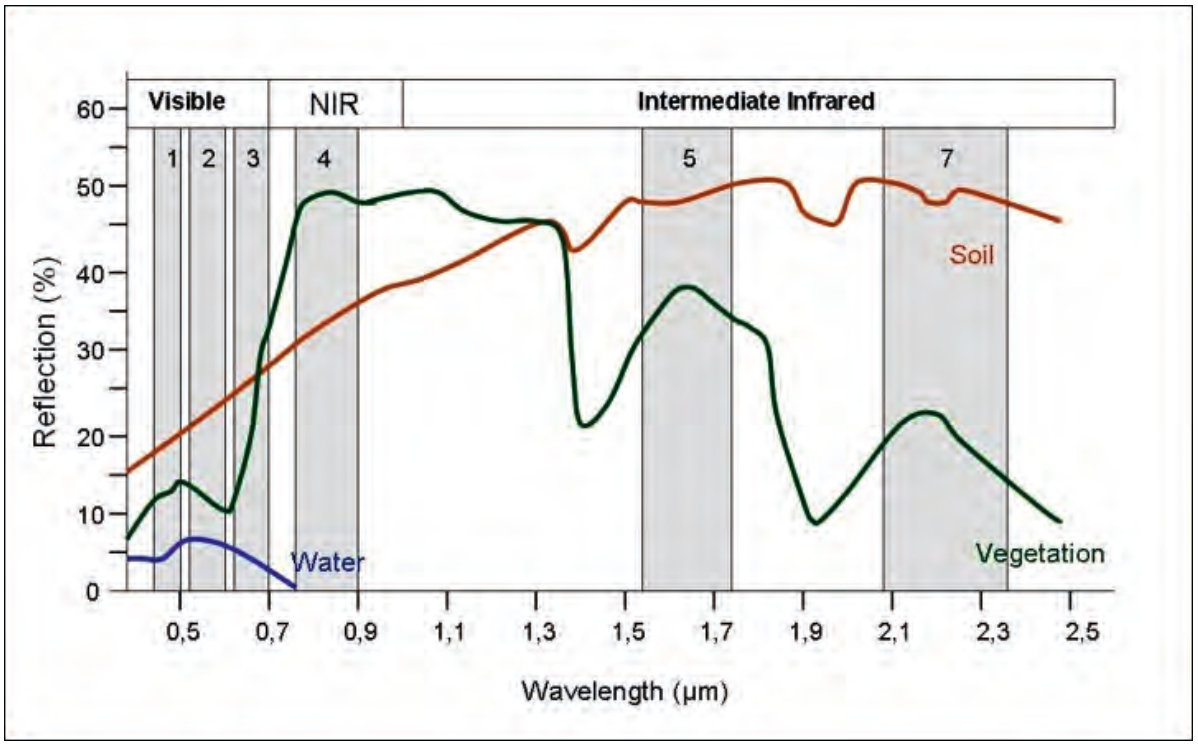

Figure 3: Spectral signatures of main landcover types. The grey, numbered columns (1-7) represent band allocation and width of an exemplary multispectral sensor (SEOS 2019a).

Most materials or rather objects on the earth surface, for example plants, do not only reflect sunlight. Transmission and absorption of certain wavelength regions can play a role in remote sensing too. In general, the ratio of reflected, absorbed, and transmitted wavelength regions depend on the incidence angle of sunlight but also on the actual leaf structure and the plant's health. According to this, different plant species can be determined and their condition can be assessed (Jones & Vaughan 2010: 37f). With regard to the NDVI vegetation index that was used in this study refmethods42, mostly light reflection and

absorption of plants will be discussed here (see Fig. 4). However, a good overview about remote sensing techniques and electromagnetic properties is given by the textbooks of Jensen 2004, Albertz 2009 and Lillesand et al. 2015.

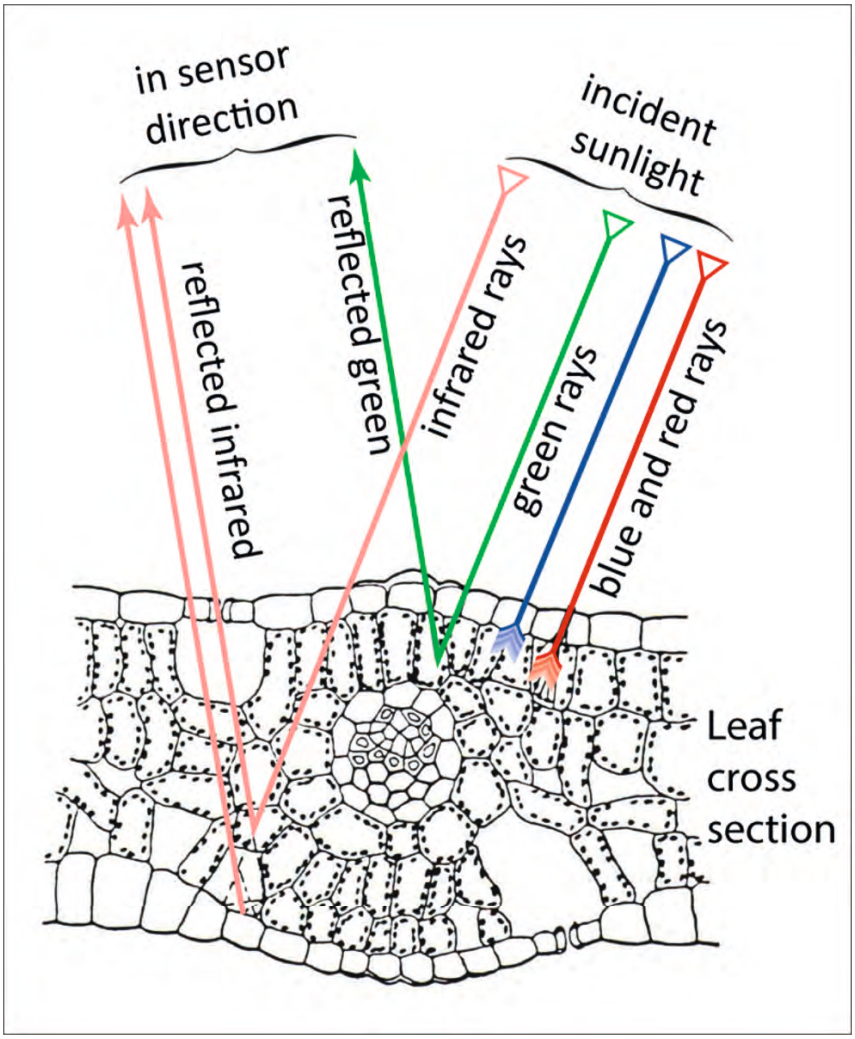

Figure 4: Illustration of sunlight - plant interaction. Whereas green and infrared wavelengths are reflected by the leaf structure, blue and red are absorbed to a large extent (modified version of Albertz 2009: 19).

Mainly, blue and red light of the visible light spectrum are absorbed, the big part of green light is reflected also as infrared light (see Fig. 4) from whom a small part is transmitted (Jones & Vaughan 2010: 37f). Thus, the difference between low reflection in the red and high reflectance in the infrared wavelength region is significant, which can be seen in Fig. 3. Red edge is situated at about 700 nm, it has the shortest wavelength in the Infrared region. In contrast to the neighbouring red region, the plant's reflection abruptly

increases in the Red edge region (see Fig. 4).

The ratio between low red and high infrared reflection can be used to calculate vegetation indices. In this study the advantages of one of the most established vegetation indices, the NDVI, were used (see Chapter 4.4). The NDVI ranges from -1 to 1, and shows very low values for non-vegetated or bare soil areas and high index values are produced where plants occur (Lillesand et al. 2015: 520).

Furthermore, the specific reflection properties of certain surfaces and materials, which manifest themselves in spectral signatures, can also be used in image classification. The varying reflection values of a certain group of pixels, or rather of an object type that have a similar spectral signature, for example buildings, can be combined in one single class. The result can be a simplified output raster image that consists of land cover areas. These areas are represented by different classes, in which each pixel has the respective class value instead of an individual value. The grouping is done according to rules, which can be conducted by a supervised classification algorithm for example.

'Random forest', known as a very frugal machine learning algorithm, is frequently used in image classification, and has been applied to a small part of this study (see Chapter 4.4). First, it was considered because, it builds decision trees that are less influenced by the total ROI (region of interest) coverage per class. ROIs are user defined areas, which consist of training pixels per class for the algorithm. In random forest, ROI classes with a relatively small coverage, for example livestock pens, can achieve a good classification accuracy (Pal 2005: 218).

Moreover, significant spectral value differences from pixel to pixel can occur, for example at the boundaries of neighbouring land cover types or the edges of objects. These spectral edges can be filtered out or classified using edge extraction functions (see Chapter 4.4.

Both the quality of spectral signatures and classification results are determined by the spectral resolution. But, another point that affects all remotely sensed imagery data and their classification is the spatial resolution that varies a lot. For example, WV-2 data has a very high spatial resolution of approximately 2 m in the multispectral bands and approximately 0.5 m in the panchromatic band. Furthermore, the analysis of data from different regions

of the electromagnetic spectrum requires disparate sensor systems that allows the processing of different tasks. Thus, the nature of sensors systems, their spectral and spatial resolution defers.

2.3 SAR and the high-resolution digital elevation model TanDEM-X

Radar technology differs greatly from optical remote sensing. A special advantage of radar is the availability of its own energy source and the possibility to penetrate almost all atmospheric components. This leads to the fact that the active system is independent of the time of day and certain weather phenomena such as cloud cover. In contrast, optical sensing is often limited by the absence of sunlight and a dusty or cloudy atmosphere. Since radar technology is a very complex and wide field, for detailed study Lillesand et al. 2015 and Albertz 2009 as well as the TDX Mission presentation of (Bartusch et al. 2010) are recommended for detailed study.

Radar is an active sensor system, basically it emits microwave pulses via an antenna. The signal reflection of the earth's surface, the echo, is then registered back at the satellite. The distance to the object on the surface is measured by the time the echo needs to return to the satellite (Lillesand et al. 2015: 389f).

In general, radar products have a coarser spatial resolution than optical sensed images. The beam width and thus the spatial resolution of a radar antenna is limited by its length. Therefore, the satellite mounted synthetic aperture radar (SAR) uses a modified data recording. It simulates an antenna array, and special processing techniques synthesise a high-resolution result by artificially increasing the beam width. In addition, bistatic data acquisition is applied which means one satellite mounted antenna transmits while two satellites receive. The recording from two slightly different positions can be equated in a baseline function (see Fig. 5). Furthermore, this implies a time offset and a phase difference. This information is required to compute an interferogram (Lillesand et al. 2015: 399f).

The most widely known interferometric SAR products are probably digital elevation models (DEM). This is a digital topographic model, a grid of the Earth's surface that consists of surface elevation values that are stored in pixels (Lloyd 2010: 17). It allows the study of landscape morphology and its

quantification (Pelletier 2008: 66).

Compared to common SAR applications, TDX is a new, slightly different approach to obtain very high-resolution elevation data from the Earth's surface. The mission is operated by the German Aerospace Center (DLR). As the name TanDEM-X indicates, the x-band in the microwave region, at approximately 3 cm wavelength, is recorded (Albertz 2009: 62). The mission subsists of two radar satellites, TDX and TerraSAR-X, in formation flight (see Fig. 5). Besides this bistatic SAR system (compare Lillesand et al. 2015: 399f), the TDX satellite also has a radar interferometer addon (compare Bartusch et al. 2010) that takes advantage of the helix shaped orbit (see Fig. 5) of the two satellites (Bartusch et al. 2010: 7). As displayed in Fig. 5, the specific orbit enables horizontally and vertically variable cross-track baselines. This results in multiple phase differences (compare Lillesand et al. 2015: 401), which are essential to generate a precise, high-resolution DEM (see Chapter 4.2) out of thus obtained interferograms (Krieger et al. 2007: 3317). The result is a global DEM with a spatial resolution of approximately 12 m with a vertical (height) accuracy of approximately 2 m (Bartusch et al. 2010: 3).

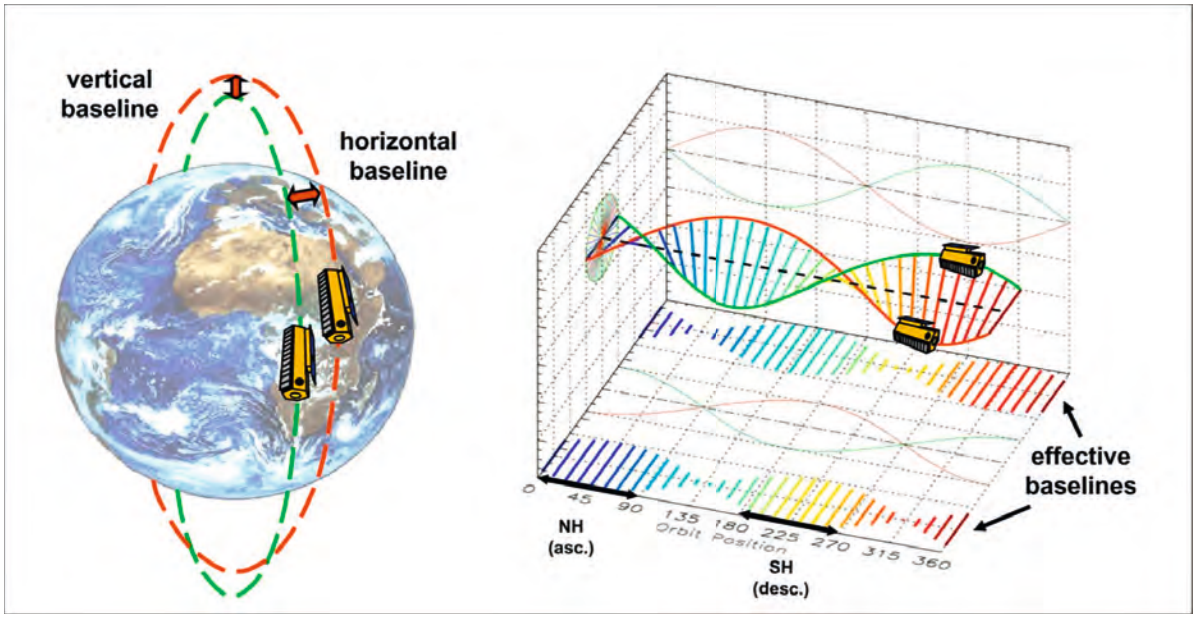

Figure 5: The helix shaped formation flight of TanDEM-X and TerraSAR-X. NH is northern and SH southern hemisphere (Krieger et al. 2007: 3324).

2.4 Processing of remote sensing data

As mentioned in Chapter 2.1, WV-2 is a passive sensor system that only records reflected light. At the satellite sensor, the signal is picked up of several bands (see Fig. 3 in Chapter 2.2) and converted in digital information. Each band dataset produces a separate raster image, in which each pixel stores the measured intensity within the band's spectral region.

Since the entire radiation arrives at the sensor in space, it must be taken into account that the signal, in addition to the reflection of the earth's surface, includes reflections of the atmosphere among others. For example, aerosol reflection and diffuse at sensor radiation. Sometimes atmospheric correction is necessary to reach pure surface or top of canopy reflection. Exemplary, for detailed vegetation studies or multitemporal analysis (Jensen 2004: 202). Moreover, atmospheric correction can result in a better image quality in general. For example, the angle, in which the satellite captured the scene, can also be important. In general, there is no satellite imagery capture of 0 ° off-nadir, which means the satellite sensor looks straight down (compare Jensen 2004: 234). In contrast, a small acquisition angle in combination with a mountainous terrain can result in extensive shadows in the imagery (see Chapter 4.1). Thus, as it was the case for the WV-2 scene, a correction attempt was made to improve image quality, but this was unsuccessful (see Chapter 4.1).

Whereas the WV-2 imagery was delivered as ortho-ready standard by Digitalglobe, still geometric correction or rather orthorectification has to be made (see Chapter 4.3). Therefore, RPCs (rational polynominal coefficients) provide measurement values of the orbital position and imaging geometry in metadata of DigitalGlobe, which should be implemented in the orthorectification process.

In addition, to increase the spatial accuracy or resolution of satellite imagery the high spatial resolution panchromatic band can be combined with the spectral information of the multispectral bands. This process is called 'Pansharpening'. However, because of its very fine resolution of 0.46 m WV-2's panchromatic band can add noisy texture information too. It can cause processing issues that can be avoided using LMVM (local mean and variance matching) 'Pansharpening' (see Chapter 4.3). After the performance of these pre-processing steps, the actual analysis, including spectral edge extraction

and NDVI analysis, can be conducted to detect livestock pens and herder camp related spectral signatures.

2.5 GIS and spatial analysis

As Lloyd 2010 comments in the quotation below, GIS is the base to carry out spatial analyses. Using GIS techniques, characteristics of a certain landscape can be highlighted, and their spatial relationships can be analysed and illustrated.

> *'GIS provide a mean of generating, modifying, managing, analysing, and visualising spatial data.'* (Lloyd 2010: 1)

GIS data uses different coordinate reference systems (CRS) and projections. This has to be considered if working with GIS because they spatially register the datasets. CRS and projection have to be adjusted if datasets with different CRS are used. In this study the Universal transverse mercator (UTM) system was used with the World geodetic system of 1984 (WGS 84) reference ellipsoid. UTM provides metric units, equally for latitude, longitude, and altitude, which can simplify the application. Especially in terrain analysis where the pixel position, or rather latitude, longitude, and altitude play a role in the calculations.

Raster and vector data are the main datatypes that are used and analysed in GIS. WV-2 also as TDX data are provided as imagery raster data. They consist of pixels that have individual values. In the case of multispectral imagery (WV-2) this is spectral information, DEM pixels (TDX) content surface elevation values. Pixel in Raster datasets are identified by the row and column position of the cells (pixels). Whereas, a lot of data can be stored in raster format, for some applications it is suitable to convert categorized raster data in vectors, such as it was done in this study (see Chapter 4.4). In contrast to raster, vector data consists of points that have spatial coordinates, and related attributes can be stored in an attribute table. If the vector objects are lines or polygons, their vertices follow the same principle (Lloyd 2010: 7f).

Often GIS uses set theory approaches, among others this is discussed by Usery 1993. Basically, two principles are mentioned: Set theory and cognitive category theory that can be very useful when it comes to face the

abilities of GIS (compare Usery 1993). Mostly, this study is based on set theory. Especially subset, intersection, and set difference operations were used to process the random forest classification, spectral edge extraction, NDVI calculation, and DEM derived datasets. Most of these mentioned overlay functions can be performed with vector data. As mentioned above, data type conversion is required to use both data type dependant toolkits (De Smith et al. 2018: 132f).

For detailed study of GIS theory and practice, further reading is recommended. For example, in the textbooks of Lloyd 2010 and De Smith et al. 2018. The GIS techniques and tools used in this study are concerned briefly in the following.

To carry out a GIS analysis with data from different sources, these must first be prepared and harmonised. First of all, this implies an approximation of the spatial expansion, which can be done by georeferenciation. Moreover, there are different ways to adjust the spatial resolution, for example through pixel interpolation and expansion, for example in cutting down the dataset to a certain area, or rather extend with a 'Clip' function (see Chapter 4.4). The actual analysis can then take place on the basis of spatially harmonised datasets.

The spatial analysis steps, used in this study consists essentially of the operation categories neighbourhood, terrain, overlay, and distance analysis also as reclassification, editor, and query functions. Map algebra is a global function, and was applied to categorise or group raster values in classes for example (compare De Smith et al. 2018: 234).
Neighbourhood analysis is a common method to assign new values to pixels in accordance to their neighbourhood and a user defined function (De Smith et al. 2018: 69).

DEM terrain analysis functions include for example 'Slope', 'Curvature', and 'Flow accumulation' calculation. In the latter case it is a matter of quantitative modelling (QM) of earth surface processes method (ESP), and often used in hydrological analysis (Pelletier 2008). The result of this analysis shows where potential river valleys are located. Slope is 'the amount of rise' or change in elevation over a given distance, and can be computed to investigate the steepness of a given terrain(De Smith et al. 2018: 351).

Curvature means the profile curvature in this case. It depends on the calculated DEM slope, and shows if the profile of a surface has a concave, convex or flat shape (compare De Smith et al. 2018: 360).

Overlay functions, such as 'Clip' and 'Difference' are basic GIS functions that work after the set theory principle. The output of these tools will only include vector geometries or parts of a raster that prepossess a certain condition(De Smith et al. 2018: 133). To define the condition another dataset, or rather GIS layer can be used. For example, these functions are useful to add or subtract areas, objects, or to isolate overlapping ones.

In contrast, 'Shapes buffer' are distance operations, and create one or more zones around vector features. The output is a polygon layer with a specific radial difference to the original polygon, line or point (De Smith et al. 2018: 217f). The buffer distance and the amount of output vertices can be set, if a 'fixed distance buffer' is applied (QGIS Development Team 2019). For example, neighbouring polygons can be merged to connect and/ or dissolve them (De Smith et al. 2018: 218). Reclassification is a simple way to extract, group, or filter values, for example if a threshold was set, to create a newly classified raster as an output (compare (GRASS Development Team 2017)). Different data types, such as float or integer, require different reclassification methods (see Chapter 4.4).

'Editing' functions allow the creation and modification of user defined spatial data. For example, an artificial vector grid can be created with a user defined spacing. This can provide an overview of the distribution of certain objects in a given area (see Chapter 4.5. In addition, vector data can be created or adjusted for specific tasks, for example to create GCPs (ground control points) to assess classification accuracy . Moreover, raster derived polygons often include voids or sliver polygons that prevent the proper use of overlay or distance operations and should be therefore adjusted using 'Editing' functions (compare QGIS Development Team 2019).

Various tools provide functions to query pixel or attribute values of vector geometries by a second raster or vector dataset. The output, mainly in form of a table, can be used to create spatial data statistics. Also, an error matrix can be created based on a set of GCPs or second raster and the classification result. In this study, an error matrix was created to assess the random forest

classification and the pen detection accuracy (see Chapter 4.5 and 5). It is a basic function to get information about the accuracy of a classification result per class and in form of a matrix (compare CNES 2018). Regarding the matrix, the overall accuracy can be determined.

2.6 Transhumant pastoralism and the ecology of pasture lands

Transhumance, is a variation of mobile pastoralism, can be found in the Alps focusing on cattle or in the French Cevennes with the focus on sheep (Macphail & Goldberg 2018: 444). Other forms of transhumance are listed in Akasbi et al. 2012: 315, and will not be discussed in detail.

Since the study has the goal to detect herder camp locations, using remote sensing data and methods described above, essential, context-related information about the way nomadic pastoralism and especially transhumance can be observed in Morocco is presented.

A large part of Morocco's land area, about 40%, is covered by steppe. It is hardly suitable as a permanent pasture or rangeland. The steppe environment needs a lot of time to regenerate, and the sparse vegetation can quickly be overgrazed (Dutilly-Diane 2007: 1). Thus, in a mostly subsistence driven form, transhumant pastoralism is widespread in Morocco. Seasonal migration between summer and winter pasture lands determines the herder's annual cycle. Therefore, and in contrast to sedentary lifestyles, many Moroccan transhumant pastoralists live in tents (Akasbi et al. 2012: 308).

Often, summer pasture lands are to find in high altitudes, such as the High Atlas Mountains, where water and forage availability is relatively high in summer. In contrast, winter pastures are situated in relative low altitudes. For example, close to the Sahara Desert in southern Morocco. Additionally, there are also differences in the migration distance, some pastoral groups ascend and descend only over a distance of a few kilometres. Others migrate several hundred kilometres, which can be categorised as long-distance migration (Akasbi et al. 2012: 311). For example, some Aït Atta herders cover a distance of about 130 km between the winter pasture land in the Jbel Sarhro region (see Chapter 3.2) and their summer pastures in the Central High Atlas (see Fig. 13 in Chapter 3.2). Migration routes depend strongly on the communal land property (*Agdal*, see Chapter 3.2) of the respective ethnic

group and their pasture land rights (compare Akasbi et al. 2012: 311, Hvezda 2007: 93). Moreover, subsistence types can differ within the ethnic groups or extended family. Agropastoral or pastoral subsistence forms occur in Moroccan transhumance, which does not rule out transitions between these forms, or exchange relations (Akasbi et al. 2012: 308).

This draws a spatially and temporary very variable pattern of transhumant pastoralism in Morocco. However, after the grazing season in the particular pasture land, the vegetation has many months to regenerate until the herders and their livestock return. Thus, this can be a basis for the sustainability of pastoral livelihoods in fragile Moroccan steppe landscapes (Akasbi et al. 2012: 315). In contrast to the only seasonal presence of herders and livestock, livestock pens are constantly present on the pasture land. Thus, they can be used every year anew. Livestock pens can also be described as enclosures, or animal gathering enclosures. They are *'fenced areas where domestic animals are corralled'* (Shahack-Gross 2017: 265). In Morocco, pens are often built by layering stones into dry-stone walls. Often, stones from the surface of the pen's environment are used for this purpose. In such, often round to oval structures, the livestock is kept at night (see Fig. 6).

Figure 6: Dry-stone wall forming a typical livestock pen in the Jbel Sarhro region.

An aspect that is sometimes underestimated, is the role of herd animals, or rather their consumption of plants and the production of dung, for the local flora. Typical livestock animals in the Moroccan transhumance are goats, sheep, and dromedaries Akasbi et al. 2012: 311. Their excrements accumulate components derived from the ingested fodder plants for example nitrogen. Additionally, plant nutrients, which originate from the animal's digestive system, such as phosphate and calcium, are further components of the excrements (Spedding 1971: 102). In general, the transhumant system implies that during the day the livestock is mobile, respectively grazes on the pasture land. As mentioned above, at night it is corralled in pens. Therefore, the nutrients are returned to the soil in the form of dung or urine in two ways. During the day, dung is distributed throughout the region, at night it is accumulated in the livestock pens.

'The nutrient cycle is thus a dynamic process of circulation of all elements within and between soil, plants, and animals. The rate at which this circulation occurs is important and so are the gains and losses which are associated with different parts of the cycle.' (Spedding 1971: 101f)

A selective accumulation, such as in livestock pens, can deeply influence soil formation and thus the water storage capacity of the ground. In addition to herbivore mammals, other faunal actors such as dung beetles and soil microorganisms are involved in the nutrient cycle respectively in the nutrient provision to plants. A complete absence of herbivores can lead to the formation of mats from dead plants. In contrast, a balanced ratio of the above-mentioned parties can have a positive influence on plant growth (Spedding 1971: 99f). With regard to herbivore excrement accumulation in livestock pens, a strongly increased nutrient content is not demanded by all plant species. However, if the nutrients are distributed over the whole area of origin, thus the pasture, or if high erosion rates lead to diffusion of nutrients from the pens, overfertilization can be prevented. Essentially, the key to a balanced nutrient cycle is the mobility of herbivores, or rather herd animals (Jones 2000).

With regard to the possibilities of remote sensing, as described in Chapter 2.2, the distribution of plants in the study area can be determined, if the NDVI is calculated and analysed. Thus, if increased nutrient availability, in the form

of herd animal excrements, at pen locations affects plant growth, then it can be visible in the vegetation patterns.

Considering excrement accumulation in livestock pens, this can also be visualised elsewhere, namely through geoarchaeological analyses as described in the following chapter.

2.7 Geoarchaeology of herder camps

As described at the beginning of this chapter, the focus of this work is on digital geoarchaeology. By Siart 2018's state out however, it should become clear that geoarchaeology provides the geoscientific basis in the field of archaeology:

> *'Above all, the geosciences became an indispensable counterpart of archaeology and cultural heritage management. As to the investigation of past archaeological landscapes and palaeoenvironments, the term Geoarchaeology [...] is commonly used, representing the utilization of traditional and the development of new geoscientific applications for archaeological purposes.'*
> (Siart 2018: 1)

In the following, however, the geoarchaeological possibilities offered by the study of recent herder camps, their distribution, and the methods that can be applied for this purpose are described in more detail.

To study the history of herders and transhumance, the archaeology of pastoral camps, one must first imagine what mobile herders can leave behind. In the archaeological context, material culture, for example in the form of building remains or extensive dumb deposits, can be ruled out. In general, these can be perceived to display human activity. At least, as described in Chapter 3.3, ceramic fragments and lithic artefacts can be found on the surface of the study area, which indicate a longer history of spatial use. However, with regard to the permanent presence of livestock pens in the study area today (see Chapter 2.6), it can be expected that former livestock pens, and especially their sediments, form major livelihood remains in the archaeological context.

Livestock pens *'[. . .] have been ubiquitous in the archaeological record since animals were domesticated. [. . .] The best studied area of animal domestication is the Old World, and especially the Near East where the first domesticated animals were sheep, goats, cattle and pigs. Since the Neolithic, animals, mostly domestic, have been kept in a variety of gathering enclosures, [. . .]. A common phenomenon in all types of animal gathering enclosures is the accumulation of dung deposits within these structures.'* (Shahack-Gross 2017: 265)

Considering Shahack-Gross 2017's statement that pens were already used in the Neolithic period, the question now is how to recognize a pen even after several hundred, or rather thousand years. If organic matter is still present in the original shape, e.g. under very humid or very arid conditions, it can be relatively easily assigned to dung. Since this is rarely the case after several hundred or thousand years, it is often worth analysing the mineral components of dung residues (see Fig. 7).

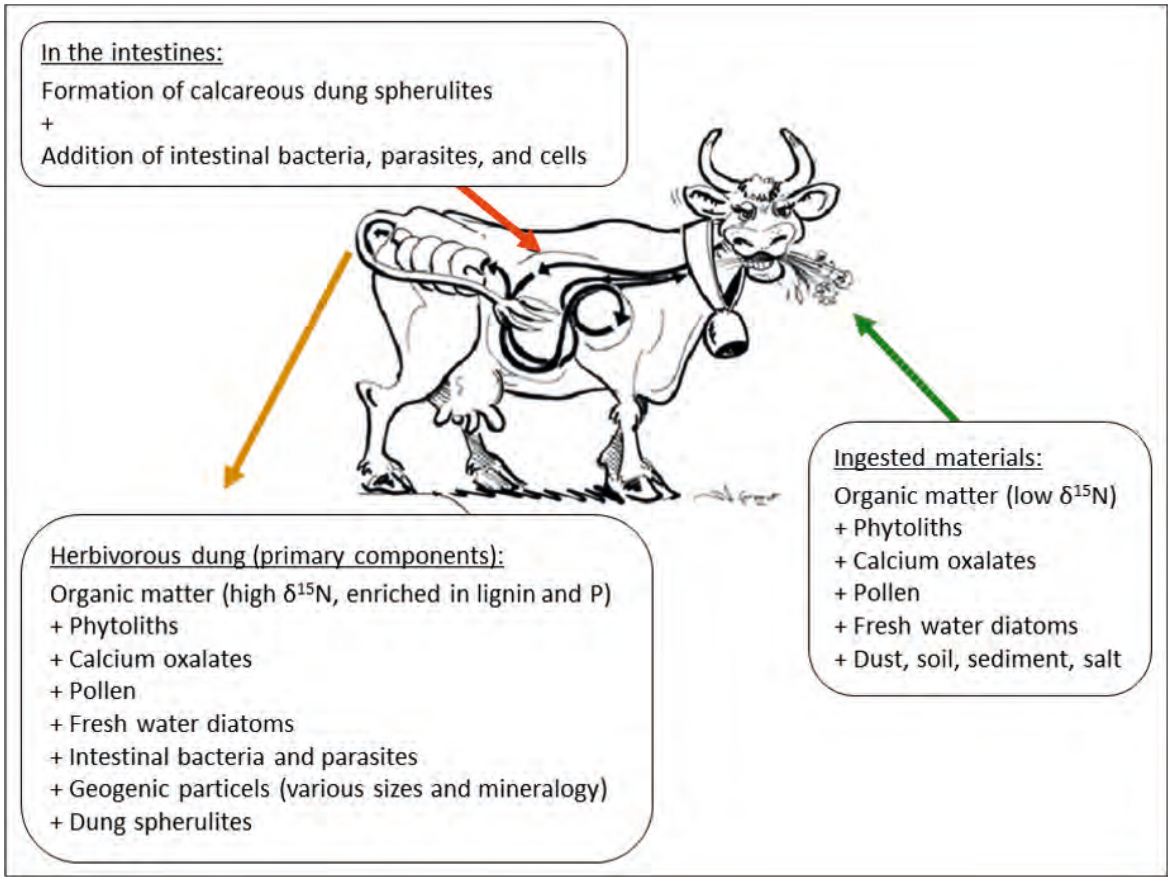

Figure 7: Ingredients of herbivorous manure and their origin (modified version of Shahack-Gross 2011: 207).

Sometimes plant pollen and fungal spores are also preserved and can be palynological analysed. Calcite spherulites, phytoliths (compare Shahack-Gross 2017: 266), and a high content of phosphate in the sediments are indicators for the digestive activity of herbivores (see Fig. 7). A high accumulation of phosphate in a sediment layer may indicate that many herbivores were kept in one place, for example a livestock pen (compare Kothieringer et al. 2018). However, this can only be proofed by the analysis of further tracers pointing to herd keeping. Thus, for example high zinc and nitrogen concentrations in sediments or soils can be mentioned as geochemical tracers (Pastor et al. 2016: 51). A typical pen-like concentration of certain mineral components can be validated in comparison with off-site (natural sediment from the surroundings) measurements. Calcite spherulites, phytoliths, and characteristic soil microstructure (compare Macphail & Goldberg 2018) can be determined using micromorphology. After such exemplary identification, one can date a pen sediment layer by the presence of organic carbon using the radiocarbon method.

However, the composition and concentration of the components in dung varies according to herd species and diet. Thus, on the one hand it is easier to distinguish which animals were kept and which fodder plants were used. This requires further comparative studies on recent material. For example, there are hardly any studies on Camelidae dung residues (Shahack-Gross 2017: 265). However, as can be seen in Fig. 8, dromedary dung forms a macroscopic visible, durable crust. Therefore, it has the potential to be detectable over centuries. In the archaeological context it often helps to be able to recognize the layers of dung correctly in order to date them. This allows to record the temporal depth of local human land use history. But, if it is possible to carry out further comparative studies, it may be possible to make more precise statements about herd structures, pasture environment, and the transhumant annual cycle of herders of past epochs.

Figure 8: Deposited white, platy dromedary excrements in a livestock pen.

With regard to spatially concentrated herbivore excrements, and therefore a high concentration of plant nutrients, such as phosphate and nitrogen, livestock pens are a special ecological site. In particular in semi-arid environments. Due to the increased input of organic material and its processing, soil formation can take place. Furthermore, he walls of the livestock pen provide a segregated, and therefore erosion protected, area. The result might be an Anthrosol sequence as described in Chapter 3.3. Thus, it is possible that the same camp location, containing increased biomass, which can be taken up by plants, stay attractive for pastoralists over hundred or thousand years (compare Marshall et al. 2018: 389). Accordingly, recent herder camps and related livestock pens could be the best locations where to find geoarchaeological key sites.

3 Study site

As part of the ethnoarchaeological work of the AREHHAL project, geoarchaeological investigations were carried out in a region locally called Tamda, which is situated in the Moroccan district Azilal (see Fig. 9). The major part of the district is located in the Central High Atlas Mountains, a subdivision of the Moroccan Atlas belt. It is seasonally frequented by transhumant herders as well as some agriculture, mostly horticulture in terraced gardens take place. The geoarchaeological survey in the region was carried out in September 2017. It mostly focused on one herder camp, including related livestock pens and the surrounding environment, in an altitude of approximately 2 500 m. In contrast, the spatial basis for the remote sensing and GIS analysis embraces approximately 25 km^2, and is centred on the geoarchaeological site of 2017. Since, regional human-environmental interaction is to be scientifically examined, geographic parameters such as climate, lithology, flora, fauna in connection to human activity should be considered, and will be explained in this chapter.

3.1 Geography of the study area

The examined area, at an approximately height of 2 300 to 3 000 m (see Fig. 9), shows a summer-dry, Mediterranean climate. Accordingly, after the effective climate classification of Köppen-Geiger from 1918 (modified by Rubel & Kottek 2010), it can be ranked to a 'Csa' climate (compare Rubel & Kottek 2010). Precipitation, also as snow, occurs mainly in the winter half-year, about 400 mm are reached in the annual average (Maroc Météo 2019). Surface water entirely in the form of small mountain rivers. The temperatures in late summer reach approximately 25 ° to 30 ° C at day. During the night temperatures could cool down to approximately 10 ° C. Therefore, one can speak of a relatively high day temperature amplitude. In general, a semiarid climate prevails in the region.

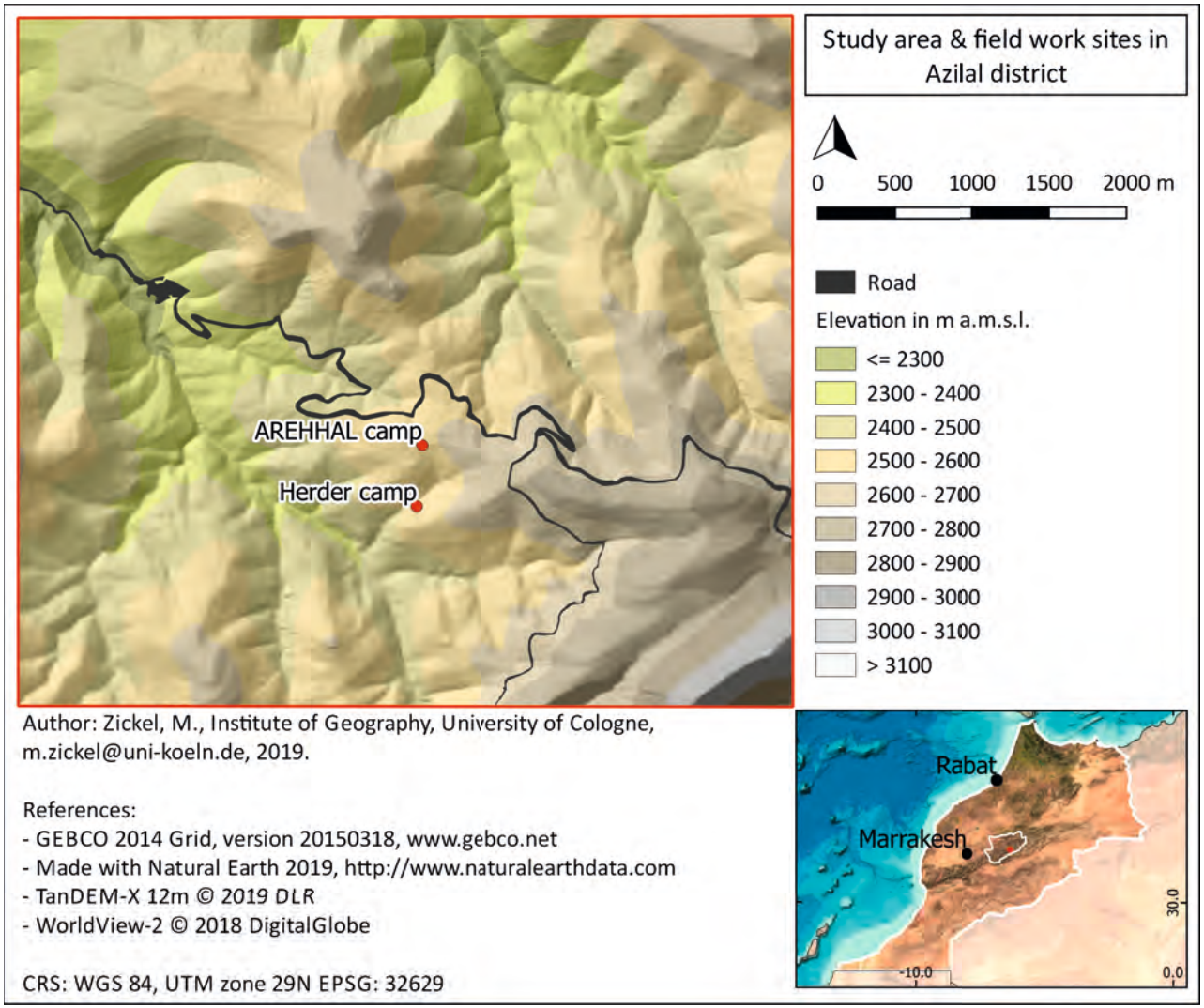

Figure 9: The selected study area extends approximately 25 km^2, and is located in the Moroccan district of Azilal (see small overview map). Displayed is the mountainous terrain of the area together with the main traffic axis (see 'Road') and the project sites from 2017.

The geological basis consists mainly of Mesozoic marine sediments respectively cretaceous limestone and calcareous marl which are deposited on this montane level (Schlüter 2006: 163ff). As a consequences of subsequent uplift and strong fluvial erosion, troughs in the Atlas foredeeps, developed extended alluvial fan systems (Schlüter 2006: 165). As a result, a variety of desert gorges determines the landscape image, and functions as a witness of past humid eras. Today, the hillslopes show detritic sediment layers that alternate stratigraphically with elevated calcareous rock strata. In addition to seasonal fluvial erosion and other physical weathering, aeolian dynamics, or rather deflation play a formative role. In general, the landscape type resembles that of a mountainous Hamada. It is characterized by coarse weathering debris respectively small rocks and gravel stones on the surface (Eitel 2011: 459). Whereas a semiarid climate prevails, and the surface is widely covered by debris, only sparse vegetation occurs (see Fig. 10).

Figure 10: View of the landscape southwest of the investigated herder camp.

The vegetation cover consists of steppe species that show some mountain specific adaptions. Especially, the shrubs and bushes form hemispheric canopies, and grow short branches that stand close together (see Fig. 11). The mountain steppe vegetation consists of spiny xerophytes for example *Arenaria pungens* or *Astragalus augustifolius* occur. *Bupleurum spec.* and diverse *Artemisia* shrubs can be found too.

Figure 11: The foreground shows hemispherical xerophytes; the background shows a circular area cleared of stones with greyish sediment.

Occasionally, inconspicuous *Campanula filicaulis* and *Malva spec.* grow close to the ground. *Juniperus thurifera*, the so-called Spanish juniper tree (see Fig. 12), determines the tree stock of the region. Mostly, junipers are loosely distributed among hillslopes. Besides various *Poaceae* species, typical fodder plants for goats and sheep, are some *Asteraceae* species, or for example *Trifolium spec.* and *Plantago coronopus*. Mostly, *Launaea arborescence* is used as forage for dromedaries. It is a thorny shrub, which the herders first burn in order to remove the thorns. Before it is given to the dromedaries, it is

processed with a hammer to soften it. In addition to herd animals mentioned above, the herders possess donkeys that graze on the pastures. In contrast, other large grazing herbivores respectively wild species could not be observed. In accordance to the annual temperature and precipitation variation, the extension of the vegetation cover differs. Developed soils are rare and if they occur, then alkaline, but low in nutrients.

Figure 12: A single growing *Juniperus thurifera* on a hilltop.

Long-term human influence and the presence of herd animals can be seen in many places. For example, sparse vegetation, probably decreased by grazing, was observed on the investigated herder camp site in September. Additionally, trampled paths between the camp, river, and the road occur. Moreover, camp sites are frequently cleared of larger. In contrast to off-site sediments, the ground is of a greyish colour (see Fig. 11 and Chapter 3.3). However, and in contrast to the mostly less developed soils of the study area, Anthrosol (see Chapters 2.6 and 3.3), rich in organic matter, can be observed in the livestock pens of the investigated herder camp. In addition, many dung

beetles (*Scarabaeinae*) can be found there. It seems that the nutrient cycle, respectively the conversion of biomass into nutrients (see Chapter 2.5), is decisively accelerated, which manifests in thick, dark layers, enriched with organic matter. In contrast to the off-site sediments, an increment of soil humidity can be observed too. In more detail, the stratigraphical properties of livestock pens are described in Chapter 3.3. Ecologically, livestock pens represent specific habitats in the semiarid environment of the study area (see Chapter 2.5). Especially, in combination with the above mentioned sedimentological specifications of herder camps in general.

3.2 Transhumant Aït Atta herders

The family accompanied by the project belongs to the ethnic group of the Aït Atta. This is one of the native groups in Morocco, known as 'Berber', who practice transhumance. Aït Atta means the people of Dadda (grandfather) Atta. They are socially organised in a segmentary system consistent of different genealogical branches or divisions (compare Hart 1981). Whereas Morocco's national language is Arabic, Aït Atta almost exclusively speak a certain Tamzight dialect (Hart 1981: 1). The community's administrative center (capital) is Igharm Amazdar that is located in their area of origin, the Jbel Sarhro region (see Fig. 13 on page 47) in southern Morocco (Hart 1981: 1f).

It has to be added that not all of the Aït Atta are mobile pastoralists. Some are farmers that are sedentary all over the year. Of other families or clans, one part does transhumance while others are sedentary farmers or agropastoralists (Hart 1981: 7). In the further course of this chapter, the transhumant Aït Atta will be concerned. Mostly, the Jbel Sarhro region is where the winter pasture lands are located. Here, the winter camp of the accompanied family is situated, in relatively low altitudes of approximately 1 600 m (a.m.s.l.). As a relatively large and powerful community, the Aït Atta claim several, extensive, communal pasture lands in other parts of Morocco too (Hart 1981: 1f). For example, in the Central High Atlas Mountains where the summer camp of the family is located in an altitude of approximately 2 500 m (a.m.s.l.).

Nevertheless, most of their pasture lands are located in southern Morocco, but expand to the Central High Atlas Mountains in the North too (Hart 1981: 1f). There, the summer pasture land is frequented approximately be-

tween May and October. The annual migration movements respectively the pasture land rotation system follows the *Agdal* concept, a common way to manage pasture lands in pastoral Morocco (Hvezda 2007: 207). The pasture's or *Agdal*'s opening and closing times are decided within the ethnic group respectively the Aït Atta community. The dates and individual place assignments on the pasture land results from intra community, respectively majority, votes that are mainly driven by customary law. Variable forage and water availability on the actual pasture land are considered (Akasbi et al. 2012: 308, and Dominguez 2013). Additionally, grazing prohibitions can be issued related to history, religion, territorial heritage, political structure, social issues, knowledge, and annual economic strategies. Thus, the temporal use of the specific pasture land depends on the migration calendar. These factors are considered to be important to ensure the continuity of the pastoral system (Dominguez et al. 2012: 278f). Non-compliance to *Agdal* regulations, such as unauthorized crossing or grazing of animals by other ethnic groups (Hart 1981: 7), is fined by communal, Islamic, or national law (compare Hvezda 2007).

The artificial 25 km^2 study area seizes Aït Atta pasture land, but also territories of neighbouring mobile or semi/ -pastoralists, agropastoralists and sedentary farmers of different ethnic groups. The Aït Atta's local pasture land was mainly appropriated through annexations, contracts, or pacts (Hart 1981: 3). But, as it is the case with many other transhumant groups in Morocco, the use of the *Agdals* by the Aït Atta has decreased considerably. Many families have already become sedentary farmers, and less people substitute themselves through transhumance. Many *Agdals* are now considered overgrazed, and can no longer be used. Probably, the reason for this is the transformation of pastoral strategies through modernization (Dominguez et al. 2012: 279). For example, today herds can be moved more quickly between pasture lands by truck instead of by foot. Water pumps facilitate the use of groundwater, and therefore the grazing season can be prolonged. Thus, the livestock no longer graze along the migration route, but only on the summer and winter pasture lands, where they can stay longer as more water is available. In general, the strong effects of global warming on (semi-) arid landscapes in particular should be taken into account. Nevertheless, the accompanied family by the

AREHHAL project still practice transhumance in the traditional way. In Fig. 13 a row of mapped GPS sourced point coordinates show their seasonal long-distance migration route, approximately 160 km in length, between the Jbel Sarhro in the south and the Central High Atlas in the centre of Morocco. This family lives in a tent made of wool canvas (sheep, goat) and accompany their grazing animals throughout the day on the pasture land. During the night the livestock is corralled in dry-stone wall pens build of rocks that were collected from the surrounding surface. The structure of their camp, which forms the starting point for the detection of camps in the remote sensing analysis, is shown schematically in the sketch plan Fig. 14.

3.3 Geoarchaeological field work and archaeological survey

As mentioned above, the field work was carried out on site in the summer of 2017. In the archaeological context, a noteworthy point, which is also visible in the sketch plan (Fig. 14), are the numerous rock art sites (see Fig. 15) near the camp. These, however, are difficult to date. According to the herder family, they date back to the time when the pasture right pact, the tat'a, was concluded with local ethnic groups. Thus, the pictograms would have been created between AD (anno domini) 13th and 16th century. However, much older rock art, which dates back to the Bronze Age and the late Neolithic, was found in the region (compare Auclair et al. 2013). It illustrates the extensive land-use history of the area and the cultural function of pastoralism.

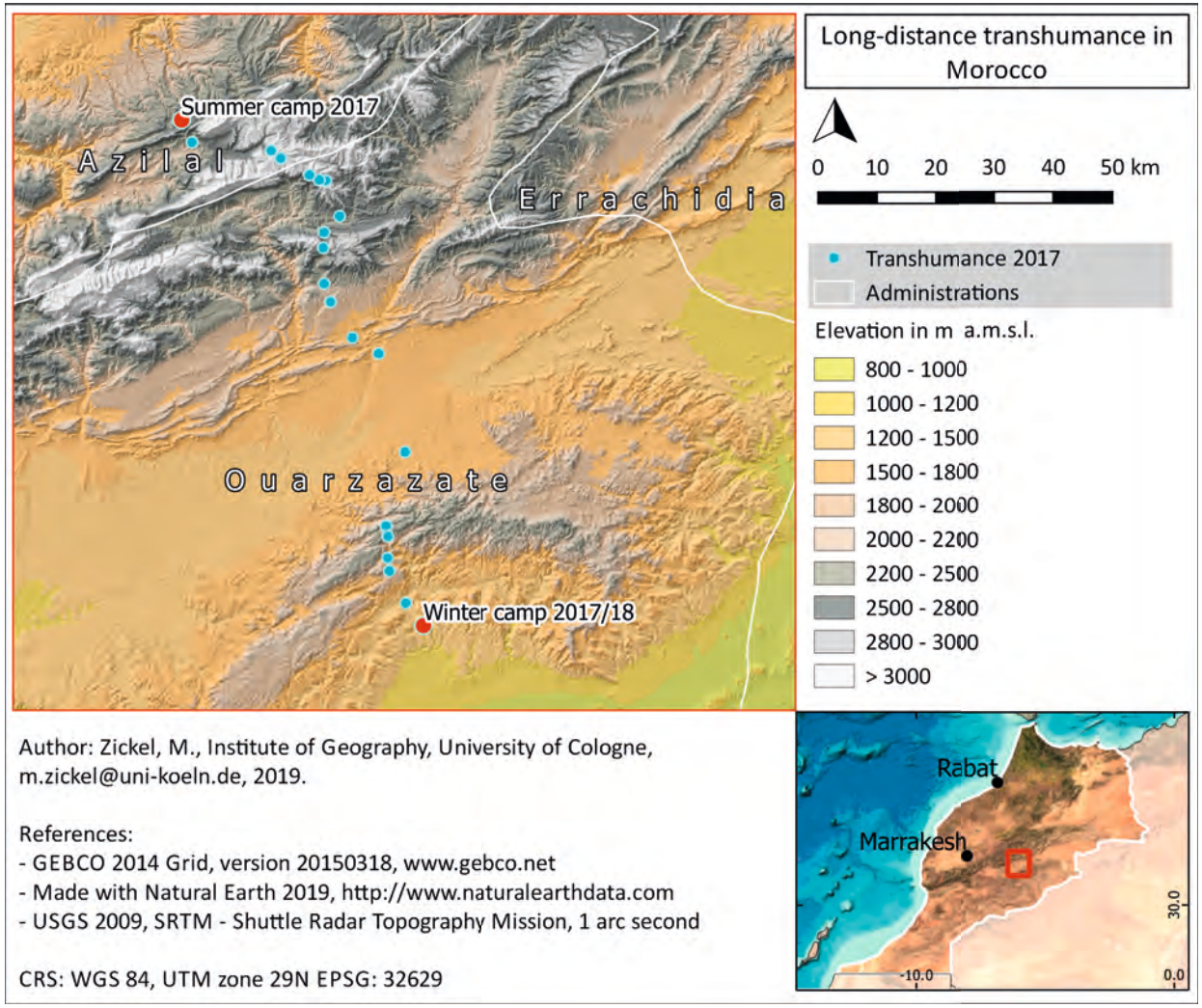

Figure 13: Transhumant long-distance migration from the Jbel Sarhro region to the summer pasture land in the Central High Atlas Mountains. It was tracked by the AREHHAL project team in the year 2017. Mapped GPS points from intermediate camps are dyed blue. The positions of the two longer-term stays in winter and summer are dyed red.

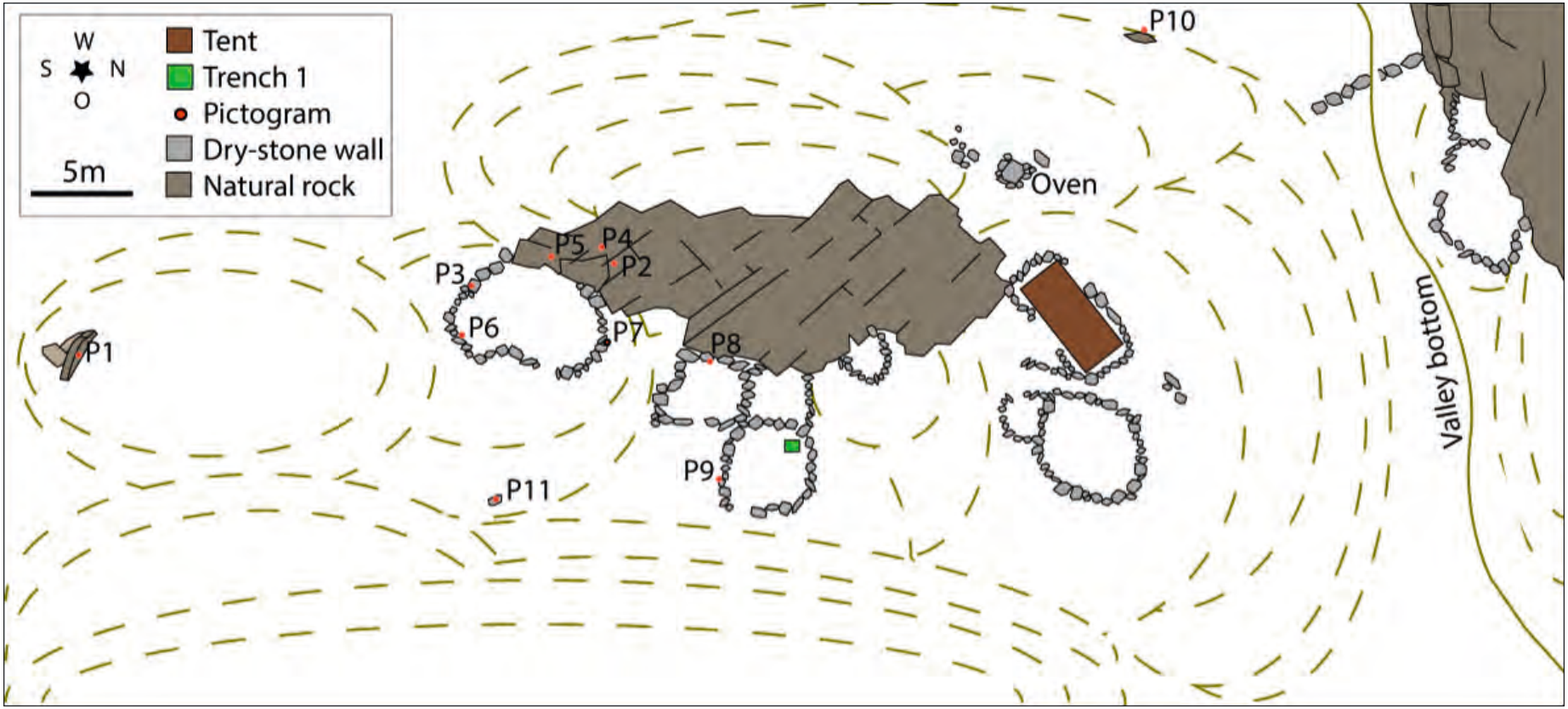

Figure 14: Sketch plan of the herder camp investigated in 2017, at an altitude of approximately 2 500 m. The sketched isolines (dashed lines) show the approximate elevation profile of the hill, on which the herder camp is located (based on field-sketches of Meier 2017).

Other archaeological material found on the surrounding surfaces of the camp were mainly undated prehistoric lithic artefacts from mostly pinkish white or black Chert and weathered ceramic fragments Whereas the ceramic finds are widely spread, some lithic artefact finds accumulate at a hill close by the camp. Probably latter stands in relation to a partial result of this study, and is discussed in Chapter 6.3.

Figure 15: Pictograms (P2, see Fig. 14) in the form of sandals. The ritual exchange of sandals is closely related to the historic pasture right pact (Auclair et al. 2013: 296 and Hart 1981: 186f).

The main geoarchaeological work, however, is focused on the constitution of the livestock pen sediments in the herder camp. Among others, in Fig. 14) the position of test trench 1 is tagged. It is situated in the north-eastern part and close to the wall of a pen used for donkeys and goats. In the final state, Trench 1 had a depth of 65 cm with a width of 50 cm and a length of 65 cm. The stratigraphy is displayed in Fig. 16.

The stratigraphy shows seven clearly recognizable layers. The upper layers 1, 2, and 3 are relatively dry. The layers 4, 5, 6, and 7 show increasing

downward moisture. In accordance, Scarabaeinae larves and pupa were found in the moist layers. Dung pellets can be found in the upper layer 1, in all lower layers, especially in layer 2, 4, and 6 dung is degraded, but macroscopically identifiable. Layer 3, 5, and 7 are in light colour, relatively unsorted and variable in the grain size fractions from silt to gravel. The detailed stratigraphy of the trench's profile was sketched (see Fig. 16) and described as follows:

1. A: Loose topsoil, dung pellets, dried plant stems and stalks, smaller rounded stones, overall of greyish colour.

   B: Compressed, dry clayey layer of beige colour.

2. Quite homogeneous, compact clayey layer with visible dung residues, moist, greyish-brown to black colour.

3. Mostly homogeneous silt layer package of beige to greyish colour. A horizontal subdivision is determined by loose and unsorted silt, fine gravel and small stones.

4. Quite homogeneous moist clayey layer with dung residues, moist and of brown-greyish colour.

5. Relatively thick (approximately 20 cm), mostly homogeneous, moist and clayey layer. Some horizontally adjusted, flat stones stuck in the profile. Of a greyish colour.

6. Crumbly, clayey, moist layer with larger horizontally adjusted stones that stuck in the profile. Dung remains can be identified. Of dark to brown colour.

7. Clearly more homogeneous layer than 6. But, also moist and larger horizontally adjusted stones are visible, and dung remains can be identified. Of greyish colour.

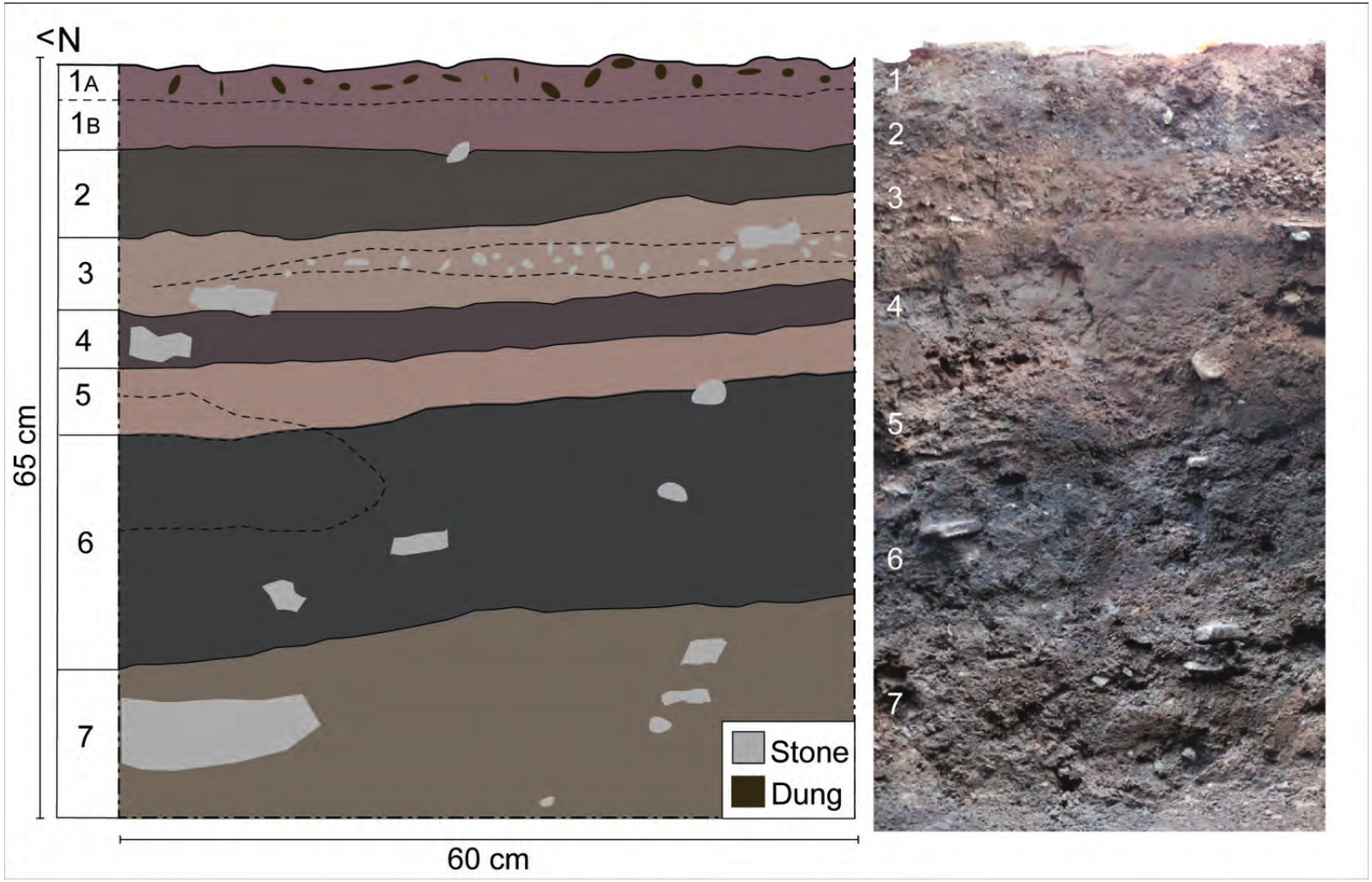

Figure 16: Stratigraphy and components of Trench 1. The figure on the left side is a sketch of the east profile (based on field-sketches of Meier 2017). On the right side, a photogrammetrically merged image shows the same soil profile (Zickel et al. 2018).

So far, the layers have not been dated. However, their apparent durability suggests that this is a sensible next step. Sediment samples and related geochemical analysis (see Chapter 2.7) could also clarify the site formation. In particular, the unsorted grain sizes of layer 3 have a fluvial depositional character and could represent accumulated surface erosion. Possibly then, this layer originates from the last precipitation-rich phase respectively the last winter. In general, the described multi-layered stratigraphy shows a high geoarchaeological potential besides ongoing soil formation, from which plants can profit (see Chapter 2.7). This soil can be best described as Anthrosol, whereas the ongoing soil formation process is based on the addition of organic matter having an anthropogenic origin (FAO 2015: 148). Therefore, pen sediments may be visible indirectly through increased plant growth, and certainly preserved in this landscape. Accordingly, it suggests that livestock pens represent a tracer for pastoral activity, or rather herder camps as well as their sediments can be used to investigate the regional land use history in connection with local archaeology. In order to overview recent pastoral land use, and to determine ancient pen sediments, the remotely sensed detection of livestock pens will be performed, and which related methodical workflow is described in the following chapter.

4 Data and methods

In view of the aim of this study, which is the detection of livestock pens and other herder camp related characteristics, such as the green ground signature or special terrain properties (see Chapter 1), the following methods were applied. To answer the related research questions, two satellite image datasets with different alignment were considered suitable, and therefore selected to be analysed. WV-2 imagery provides high-resolution multispectral data (see Chapter 2.2) and TDX supplies a high-resolution DEM (see Chapter 2.3) for the study area. The properties of the mentioned remote sensing data sets will be presented in the following, but first the methodical workflow is displayed in Fig. 17 (see next page) to provide an overview of the performed analysis steps that are presented as this chapter proceeds.

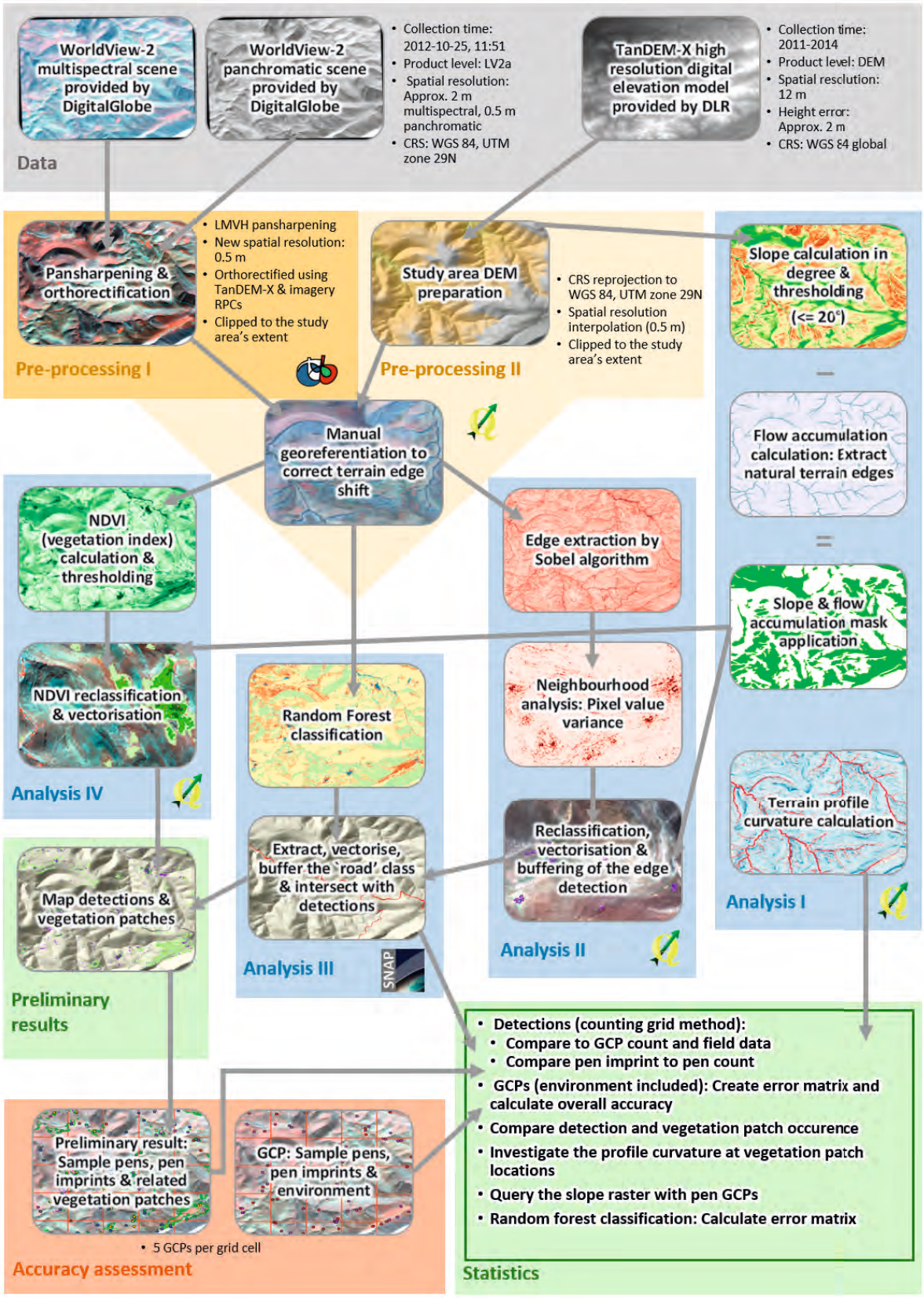

Figure 17: Methodical workflow of the performed analysis.

4.1 WorldView-2 multispectral data

WV-2 is a satellite operated by the DigitalGlobe company (DigitalGlobe 2019a). It is equipped with a passive, optical sensor (see Chapter 2.1) that scans the earth surface using a bi-directional, along-track push broom method (compare Lillesand et al. 2015: 230f) and records a multispectral band set. Therefore, WV-2 operates at an altitude of 770 km with a swath width of 16.4 km at nadir. Moreover, it has an imagery acquisition capacity of 550 000 kmm^2 per day and offers a revisit rate of 1.1 days for almost every spot on the globe (DigitalGlobe 2010: 3). For this study, an image scene was acquired that completely covers the study area (see Chapter 3), and which quality is appropriate for the analysis plan. The scene was captured on 25 October 2012 and handed over by Digital Globe as standard ortho ready (LV2a) in 16 bits uint (unsigned integer) format. It means that it has already been map projected to WGS 84 / UTM zone 29N (see Chapter 2.5), thus ready for orthorectification. The scene is cloudless and was captured, at a mean off-nadir angle of 23.6 °, around noon, at 11:51, and with a mean sun elevation angle of 45.9 °. Thus, there are no clouds or haze that reduce the image quality, but the interaction between off-nadir and sun elevation angle produces several shadow areas on the ground. Especially, the captured mountains show extensive shadows. However, WV-2 offers eight multispectral bands that partially cover the wavelength region from 400 to 1040 nm with a spatial resolution of 1.84 m (see Tab. 1). Contrary, the single panchromatic band covers a wider spectral region of 450 to 800 nm, but has a higher spatial resolution of 0.46 m (DigitalGlobe 2010). Like mentioned above, the WV-2 scene was used to investigate land cover, respectively to detect livestock pen structures and to clarify the consistency of the green ground signature on herder camp sites. With regard to these two main issues, the advantages of WV-2 bands, the mentioned high panchromatic spatial resolution, which is needed to capture the narrow pen dry-stone walls (see Chapter 1 and the high spectral resolution of the multispectral bands (see Chapter 2.4), were combined (4.3). Thus, with an increased spatial resolution, the wavelengths regions of the eight bands (see Tab. 1) can be analysed to investigate the study area from these points of view, but also for a wide range of other purposes (see DigitalGlobe 2010: 4).

Table 1: The spectral and spatial resolution of WV-2 satellite imagery.

Spatial resolution (m, approx.)	multispectral: 1,84				panchromatic: 0,46			
Band no.:	1	2	3	4	5	6	7	8
Band name:	Coastal	Blue	Green	Yellow	Red	Red edge	NIR-1	NIR-2
Band spectral region (nm):	400 - 450	450 - 510	510 - 580	585 - 625	630 - 690	705 - 745	770 - 895	860 - 1 040
Center wavelength (nm):	427	478	546	608	659	724	833	949

Especially, for the study of vegetation properties WV-2 offers four valuable bands in the electromagnetic red region: Red, red edge, NIR-1 (Near-infrared 1), and NIR-2 (Near-infrared 2). With those, the NDVI can be calculated (see Chapter 2.2 and 4.4).

4.2 TanDEM-X high-resolution DEM

The use of a high-resolution DEM is particularly recommended in mountainous terrain, such as that of the study area. Thus, even smaller terrain varieties, such as small depressions or plateaus, which provide sufficient space for a herder camp, can also be included in the analysis.

Using specially recorded and processed SAR data of the TDX radar sensing mission (see Chapter 2.3), the DLR provides a DEM with a spatial resolution of 12 m for the study area. It is a mosaic dataset consistent of processed interferograms (see Chapter 2.3) of several captured scenes that were collected in the region from 2011 until 2014. The mean 2 m height error of TDX data, promises a high accuracy for DEM products such as slope and profile curvature (see Chapter 2.5). Besides the derivation of terrain parameters, which can limit the detection of herder camps, due to its high spatial resolution the DEM is predestined for the orthorectification of the WV-2 data set that will be presented in the following.

4.3 Data pre-processing

The methodical workflow is non-linear, but it can be described in several parts and stages. A workflow diagram to provide an overview of the processing and analysis steps is displayed in Fig. 17), in the beginning of this chapter.

To process remote sensing data the software SNAP 6.0 and OTB 6.6.1 (Orfeo toolbox) were used, to perform the GIS analysis the QGIS 2.18 GUI (graphical user interface) contains a good toolkit of own geoalgorithms. Additionally, it profits from the integration of several toolboxes from other providers such as GDAL 2.4.0, GRASS 7.6, SAGA 2.3.2. Each software mentioned above is open source based. Detailed information about tools and documentation, software or GUI, and related citations are listed in Appendix I and will not be described in detail in this chapter.

Since, shadows in the imagery (see Chapter 4.1), also as some dry-stone wall structures, show empty pixel values (no data) after running an atmospheric correction (see Chapter 2.4). Apparently, former pixel values were removed in the correction process and replaced by no data values. These 'data gaps' are interpreted as spectral edges, and therefore produce errors in the 'Edge extraction' analysis (see Chapter 4.4). Regarding the goal to detect livestock pens, this step was considered as not reasonable. Thus, the analysis was carried out with uncorrected WV-2 data. In this step, the intersection of the two data sets, WV-2 and TDX, was prepared by making them spatially compatible, and therefore adapting them to the analysis requirements. First, the originally 12 m spatial resolution of the TDX DEM was adapted to 0.5 m by bilinear interpolation. Bilinear interpolation uses four weighted values of neighbouring pixels of the input raster to determine the interpolated value of the specific cell in the output (De Smith et al. 2018: 397). The function was applied using the tool 'r.resample.interp' of GRASS 7.6.

In accordance with the RPC information provided by DigitalGlobe (see Chapter 2.4), orthorectification of the WV-2 imagery was performed. In combination with the interpolated TDX DEM it supports to increase the spatial accuracy of pixel positioning. Orthorectification was conducted using the 'OrthoRectification' algorithm of OTB 6.6.1. After this step, pansharping was applied to the WV-2 multispectral data. Using the 'Pansharpening' tool of OTB 6.6.1, the 1.84 m spatial resolution of the multispectral bands were adapted to the 0.5 m resolution of the panchromatic band. Structural details, which were previously not visible, are now identifiable and provide multispectral information. In addition, a form of salt and pepper effect (compare Lillesand et al. 2015: 489f), that is caused by the mentioned rocky stone pavement (hamada, see Chapter 3.1) in the study area has to be reduced. The pavement stones are the construction material for dry-stone walls, or rather livestock pens. Thus, with regard to that it is the same material, spectral confusion can be a consequence. Therefore, the OTB 6.6.1 'LMVM pansharpening' algorithm was used. Using a moving window, LMVM weights the mean and variance of the pixel 4 x 4 neighbourhood values before matching them to the multispectral data (compare Lillesand et al. 2015: 490f) and CNES 2018). The result is a smoothed imagery texture, from which the cattle pens stand

out better.

Caused by the strongly varying terrain of the study area and because the WV-2 and TDX dataset still showed small spatial deviation after orthorectification, additional georeferenciation with the 'Georeferencer' tool of QGIS 2.18 was necessary. It is a process to register a raster to the coordinates of a reference raster. This is done by sampling locations in one raster using reference points (similar to GCPs) that can be determined in the second raster too. The function links these assigned coordinates, and accordingly adapts the target raster (compare Jensen 2004: 234f). Thus, the WV-2 raster was registered to the TDX DEM. Additionally, in order to reduce the data volume to the essentials and to limit the spatial extent to the study area of approximately 25 km m^2, both data sets were cut using the GDAL 2.4.0 'Clip' tool. 'Clip (raster)' and 'Clip (vector)' data is a basic function to create a data subset. In this case, the spatial extend of all raster datasets was cut by the polygon extend of the study area.

4.4 Analysis

In the first part of the analysis (see Analysis I, Fig. 17 and Appendix I), terrain specific features were determined to create an area of interest (AOI) for the detection results based on these parameters. The terrain slope and profile curvature were calculated based on the interpolated TDX DEM using the GRASS 7.6 tool 'r.slope.aspect'. The slope inclination is a parameter, which if its angle becomes too large, i.e. the slope is too steep, it limits the occurrence of pens. It is computed, based on a DEM, and uses the Horn formula (compare De Smith et al. 2018: 354). Calculated slope inclination can be expressed in degree and stored as pixel value (De Smith et al. 2018: 351).

To investigate the terrain form at herder camp sites, the terrain's profile curvature was computed. The radius of profile curvature calculation is about 20 m. Convex forms are stored in positive, and concave form pixel values in negative values.

To detect natural terrain edges such as valley bottoms the 'Flow accumulation' tool of SAGA 2.3.2 was used. The flow tracing algorithm of Freeman 1991, which is called Multiple-Flow-Direction (MFD), traces the flow in multiple possible down-slope pixels that are weighted by the slope. In contrast to

other methods MFD produces continuous geometries that take topographic shape, for example the terrain steepness, into account (Pelletier 2008: 68f). Valley bottoms often show natural edges that can be interpreted as spectral edges. Therefore, these areas have to be subtracted from the slope mask in order to be able to better limit the detections later on.

Subsequently, slope values up to 20 ° and flow accumulation catchments greater than 31 592 were isolated using the possibilities of reclassification 2.5 with the tool 'r.recode' of GRASS 7.6. Both raster datasets were vectorised with the 'Polygonize' tool of GDAL 2.4.0. Polygonisation, creates vector polygons per pixel cluster, or rather groups pixels with the same class value in polygons (GDAL 2.4.0 2018).

A 'shapes buffer' (QGIS 2.18), or rather vector buffer, with a fixed distance of 15 m was then applied to the derived valley bottom polygons to provide a comprehensible coverage of these areas where no livestock pens occur.

To reduce the data volume, a shape simplification was carried out using the tool 'Simplify geometries' (QGIS 2.18) was applied with factor 3. This slightly smooths polygon edges (reduces vertices) that originate from raster pixels.

In addition to slivers and voids, computed areas smaller than 100 m^2 that offer too little space for a herder camps, or rather livestock pens, were excluded from further analysis. This was done using the 'Geometry checker' tool of (QGIS 2.18).

Subsequently, the processed slope and valley bottom information was combined to a single vector dataset using the 'Difference' tool of (QGIS 2.18). The output raster of his overlay function will only include polygons that does not overlay polygons of a second layer (De Smith et al. 2018: 133). Thus, this can be used if specific areas, such as the computed river valleys that are defined by polygons, are subtracted from the slope mask.

The produced mask area therefore only contains areas with a slope of up to 20 °, but without valley bottoms (flow accumulations), which would otherwise also fall within this value range.

In the second part of the analysis, the actual livestock pen structures detection was executed (see Analysis II, Fig. 17 and Appendix I). It is based on a spectral edge extraction 2.2 that was performed with the OTB 6.6.1 'Edge

extraction' tool. 'Edge extraction' is a process of image segmentation where edge features where computed from a spectral value threshold, a parameter that can be set. It means that a single or a group of pixels will result in an edge feature if their value is significantly lower or higher than the neighbourhood. Experimental work on the different WV-2 bands resulted in the choice of the NIR-2 band 8, whether it already show clear contrasts of dry-stone wall feature pixels and their environment. Also, the Sobel algorithm based 'Edge extraction' operator showed the best results in the pre-test. Sobel calculates the gradient of the image followed by the detection of the gradient vector's magnitude (CNES 2018). In most cases the wall width of the pens corresponds to 2-3 pixels, accordingly a neighbourhood window of 3 x 3 pixels was chosen. In order to refine the results, the pixel value variance was investigated in a neighbourhood analysis, and displayed in a raster by using the GRASS 7.6 tool 'r.neighbors'. Due to their deviation, relative to the 3 x 3 pixels neighbourhood outstanding single pixels are integrated into a pixel group with a similar spectral signature. The result is a 'densified' edge extraction raster. For example, thus the environment has been smoothed, because single edge pixels, caused by the Hamada surface 3.1, are integrated in the surroundings. and a fragmented drywall, or rather pen structure is more clearly recognizable because close neighbourhood pixels (from the surroundings) are integrated into the structure. This raster was then reclassified with 'r.recode' of GRASS 7.6 to extract edge values greater than 6033, which was considered as a reasonable threshold. If the raster has integer values, 'r.reclass' is sufficient. If the raster values were stored in float format, such as in this case, 'r.recode' was used.

Whereas, it is possible to reclassify raster data based on the area of neighbouring pixels with the same class value, 'r.reclass.area.greater' of GRASS 7.6 was used to sieve the raster. This step removed noise, thus irrelevant data prior vectorisation. Here, contiguous pixel areas of less or equal to 10 m^2 were removed. These include, for example, small rocks and steppe vegetation such as shrubs. Due to their pen-like morphology, they produce similar but much smaller edges, and are therefore sources of error. Then the grid was vectorized ('Polygonize', GDAL 2.4.0), and the generated polygons were clipped to the size of the mask respectively the result of the first part of the analysis.

Clipping vector data (compare QGIS Development Team 2019) means

that only points, lines or polygons of one layer that overlay a polygon layer are included in a new output layer (De Smith et al. 2018: 132).

To reconnect fragmented pen structures and to dissolve them in one single polygon, a fixed distance vector buffer ('Shapes buffer', QGIS 2.18) of 1 m was applied. In addition, the 'Geometry checker' and 'Simplify geometries' of QGIS 2.18 were used to clean up the geometries, as described already in the last section. With the differences that a 50 m^2 threshold, to exclude too small polygons, was used here.

The third part of the analysis (see Analysis III, Fig. 17 and Appendix I) is based on a random forest classification (see Chapter 2.2). It was carried out in SNAP 6.0, a remote sensing data processing software by the European Space agency (ESA). The applied supervised 'Random forest classifier' (see Chapter 2.2) essentially works after the selection of a training pixel set size and the formation of decision trees. Both, the number of training pixels and the number of trees can be determined by the user. Training pixel areas per class must be defined in advance by ROI creation. The algorithm was adjusted based on the obtained class ROIs and with 10 000 training samples and 100 trees. These parameter values were considered to produce the best classification results in the pre-test. However, no livestock pens have been reliably detected. But the classification result turned out to be a good way to derive basic land cover characteristics such as the country road that extends from one end of the study area to the other. Therefore, the classification's target class 'Road' was then extracted in QGIS 2.18 with 'r.reclass' GRASS 7.6 from the classification results, and vectorised as previously described. Whereas, some classification confusion errors occurred, represented by small polygons spread over the study area, the 'Road' polygon have been separated using the tool 'Extract by Attribute' in QGIS 2.18. The polygon was then post-processed with a fixed distance vector buffer ('Shapes buffer' in QGIS 2.18), using a fixed distance of 10 m to maximise its extend to the hemming side strips. Then the road polygon area was subtracted from the result of the filtered edge extraction, which was already clipped with the slope and flow accumulation derived mask by using the 'Difference' tool of QGIS 2.18.

The fourth and last part of the analysis (see Analysis IV, Fig17 and Appendix I) focuses on the derivation of the vegetation cover in the study

area. For this purpose the NDVI (see Chapter 2.2) was calculated with the following formula (1):

$$\text{NDVI} = \frac{B_{Red\,edge} - B_{Red}}{B_{Red\,edge} + B_{Red}} \tag{1}$$

It was applied using the QGIS 2.18 'Raster calculator'. This tool uses raster datasets e.g. single bands, such as the multispectral WV-2 bands as input, enables data set-off, and other raster algebra functions (compare QGIS Development Team 2019). In this study the NDVI formula was applied to certain WV-2 bands.

The Red edge band (see B Rededge in equation 1) of the WV-2 data was considered to produce the most realistic vegetation cover results, and was therefore used as input for the equation. Three thresholds of 0.28, 0.4, and 0.5 were set, and the classes 0.28 – 0.39, 0.4 – 0.49, and 0.5 – 0.59 were extracted and reclassified using 'r.recode' GRASS 7.6. Then they were vectorised as described before and clipped to the same mask as the results of the edge structure detection. In addition, the geometries were cleaned as previously described but in this case areas smaller than 10 m^2 were removed. In a further step the curvature raster, produced in the first analysis part, was queried with the derived vegetation cover polygons using the QGIS 2.18 'Zonal statistics' plugin. As it allows the query of pixel values of a raster band via the spatial expansion of polygons or rather ROIs, this tool is especially useful for remote sensing data analyses. Various statistic such as count, sum, and average can be calculated for the raster values, and stored in the attribute table of the vector data set (compare QGIS Development Team 2019). Thus, it can be determined, which profile curvature form dominates in each of the three NDVI classes.

4.5 Accuracy assessment and statistic

To estimate the accuracy of the results of the structure detection, first an artificial vector grid with spacing of 1 x 1 km, and 30 cells was computed with the QGIS 2.18 'Create grid' tool. This has the advantage that, using this counting grid, in the next step an even distribution of GCPs over the entire

study area can be achieved (see Fig. 18). Thus, five GCPs per grid cell were created with the 'Editing' tool of QGIS 2.18, which meet the requirements of the target structure, or rather represent a livestock pen or a pen imprint. Thus, 88 GCPs were created for this purpose (see Fig. 18).

On this basis, the tool 'v.vect.stats' GRASS 7.6 was applied to query the livestock pen detection results and to add statistics, for example count and sum, to the GCP attributes per grid cell. The function queries vector data and used, if the spatial properties of a point set lying in a polygon should be determined (GRASS Development Team 2017). Thus, it can be determined how often a pen or pen imprint was matched by a GCP.

Moreover, the mentioned GCP set was used to query the original slope raster in order to investigate, if the assumption of livestock pen occurrence up to 20 ° can be verified. This step was performed with the 'Point sampling' tool of Jurgiel 2018, which can query raster and vector data. It is based on a user defined point set, in this case the 88 GCPs, to query a pixel or attribute value with the same coordinates (compare Jurgiel 2018).
In addition to the previously described counting grid method, an error matrix was calculated to determine the overall accuracy. Therefore, the GCP set used so far was extended by the same amount of random environment samples, collected from different surfaces in the study area that are not covered by livestock pens or herder camps in general. The pen detection results were again queried with the new amount of 176 GCPs. In the latter case, the GCP vector points were thereupon buffered with a fixed distance of 1 m (QGIS Development Team 2019) to create polygons out of them. This step is required to calculate a confusion matrix using the 'Compute Confusion Matrix' tool in OTB 6.6.1. Moreover, for this purpose the postprocessed pen detection result has to be converted back into raster format by the GDAL 2.4.0 'Rasterize' tool. To display the classification accuracy of the random forest classification described in the third analysis part, 30 GCPs were created for each class, and the confusion matrix was produced in the same way.

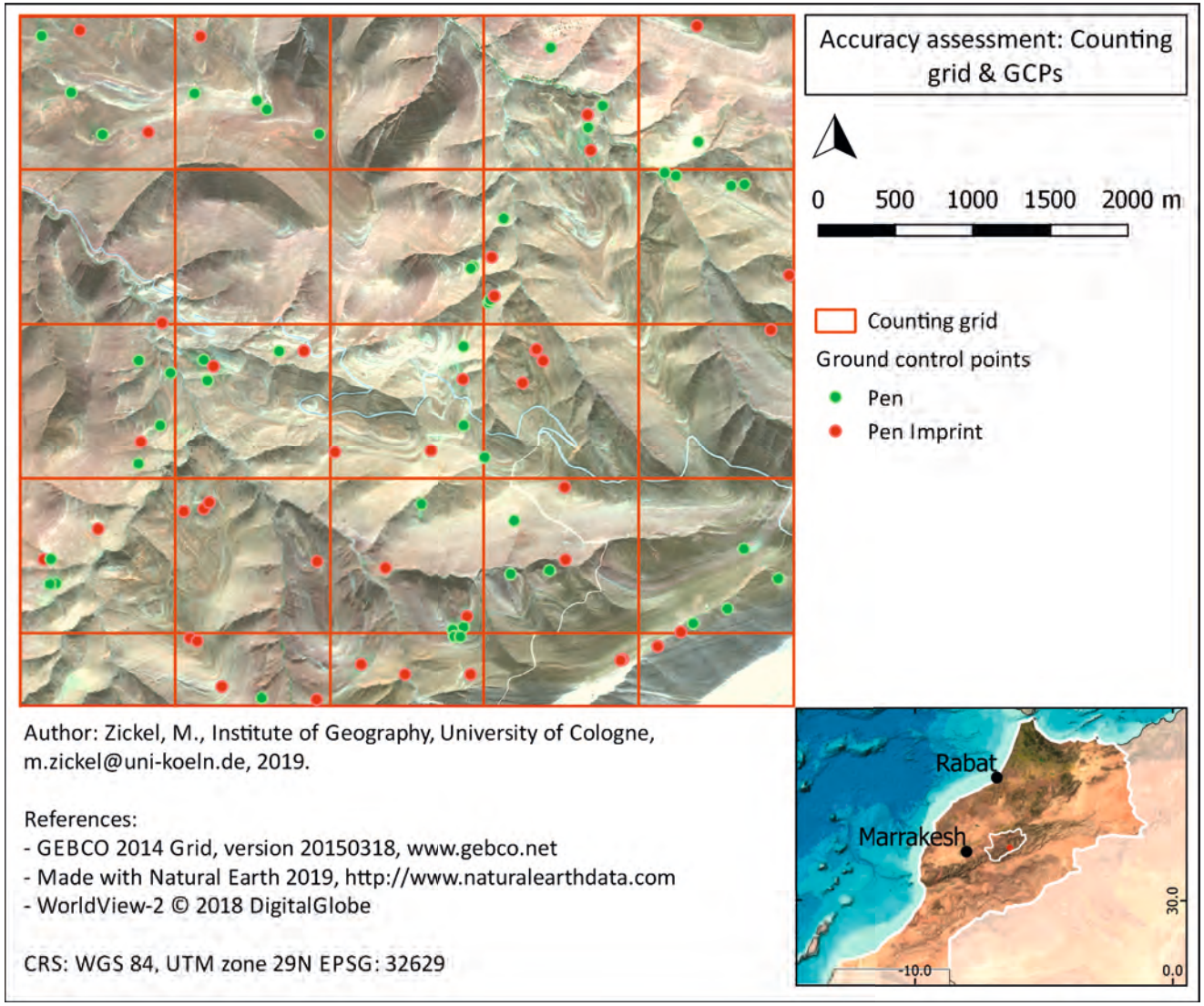

Figure 18: Counting grid and GCPs used to assess the detection accuracy.

Furthermore, to analyse the occurrence of livestock pen structures in relation to vegetation patches and to improve the estimation of detection error, an additional GCP set of 108 points was created. This assessment followed the same procedure as described at the beginning of this chapter, but the GCPs were created on the basis of the displayed pen detection result and vegetation patches in the QGIS 2.18 GUI.

According to the described procedure, most statistical information was embedded in vector geodata as attribute tables. Therefore, for further statistical analysis, the data sets were exported as spreadsheets from QGIS 2.18. The most important statistical intentions were briefly summarised in Fig. 17 (Chapter 4), and the results will be presented in the following chapter.

5 Results

The output of the study will be presented in the context of the two main results. These are successfully detected livestock pens and vegetation patches in the approx. 25 km^2 extensive remote sensing study area (as described in the beginning of Chapter 3). With the focus on this, the terrain parameters that delimit and represent the AOI (area of interest) mask will be examined first. In addition, the related terrain curvature properties of the vegetation patches will be emphasized. Based on the relationships between the partial results, a pastoral land use pattern can then be derived.

5.1 Area of interest definition

As described in the chapter's introduction, the AOI is essentially determined by confining terrain parameters that delimit possible livestock pen occurrence. The terrain of the study area is very mountainous. Therefore, some places were considered as not suitable for herder camps due to their steepness (more than 20° slope inclination) or the small flat area they offer. In addition, the occurrence of pens in river beds or on the country road, that runs through the study area can also be ruled out. As described in Chapter, Fig. 19 illustrates the dyed green AOI mask, which represents the outcome of the exclusion procedure described in Chapter 4.4. The pen detection results and the determined vegetation patches were circumcised with this mask.

In more detail, Fig. 19 displays areas of slope values that do not surpass 20 ° inclination. This threshold was set to 20 ° in accordance to field observation (Chapter 3.2) and the visual examination of the WV-2 scene. The persistence of the estimated slope threshold of 20 °, below which it was assumed that livestock pens were present, was confirmed by querying the computed slope raster with GCPs. Here, the same GCPs used to assess the detection accuracy of livestock pens (see Chapter 4.5) were used as the query set. The result of this query analysis is displayed in Fig. 20. Most of the values are below a slope inclination of 20 °. Therefore, most of the livestock pens occur on slopes of up to 20 °. Although outliers can be observed, apparently a few pens lying on slopes with more than 20 ° inclination.

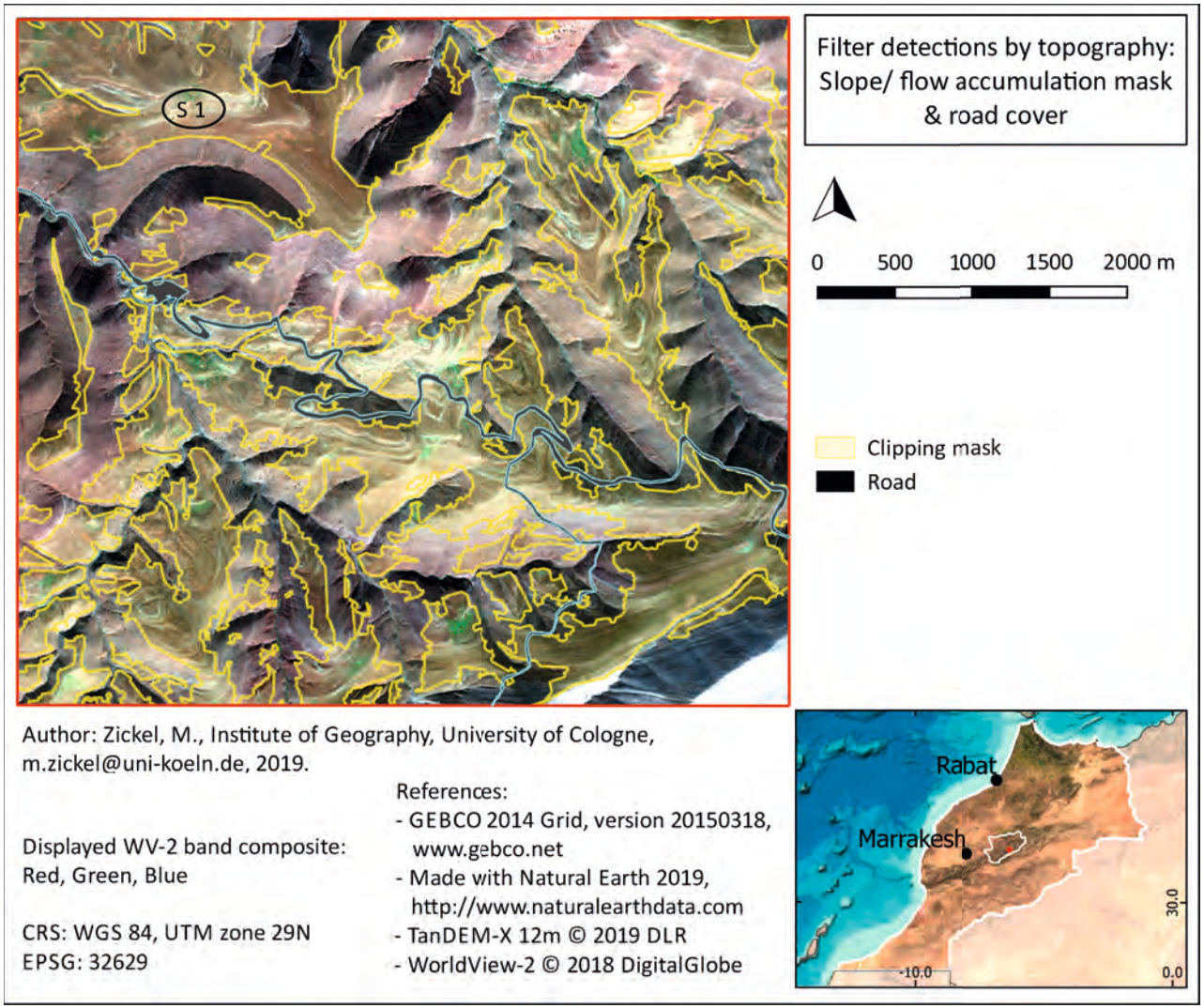

Figure 19: The terrain deterministic clipping mask (dyed green), which contains areas for possible herder camp or rather livestock pen locations.

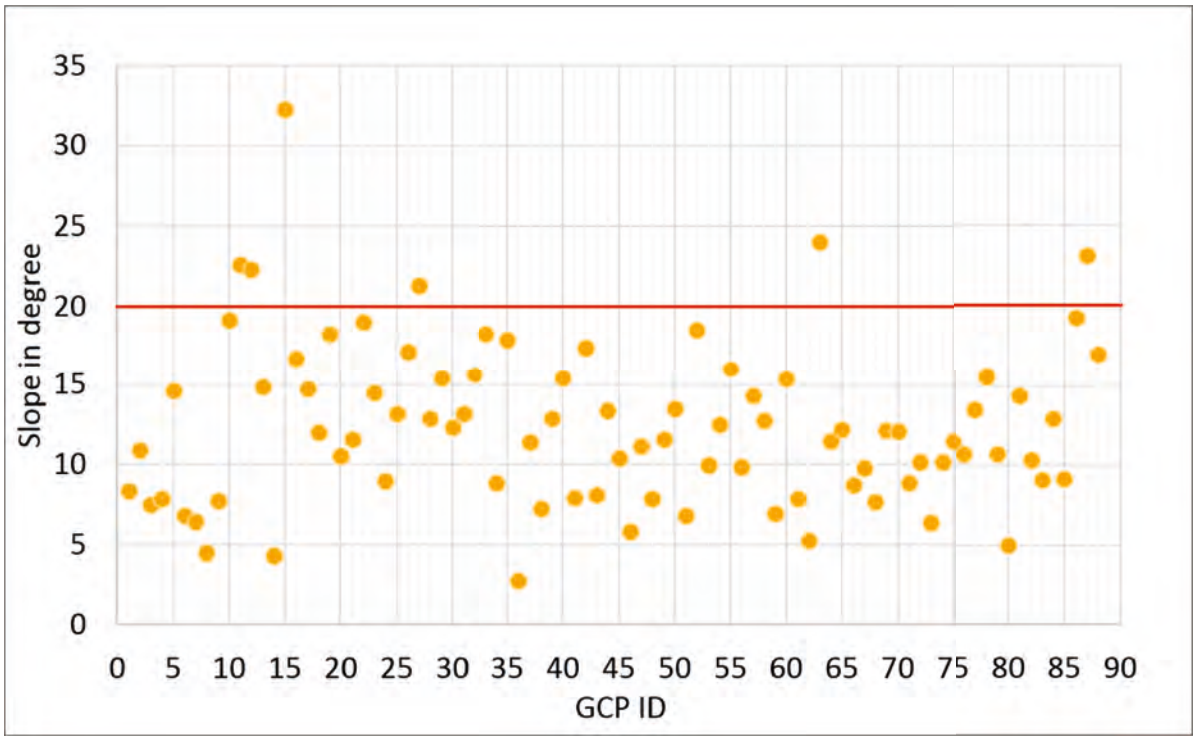

Figure 20: Slope values queried by livestock pen GCPs.

Further, areas below this slope threshold value or rather flat areas, that represent coarse natural terrain edges in the broad sense were excluded. This includes deeply carved river valleys, which was determined by the implementation of flow accumulation data as described at the beginning of Chapter 4.4.

The supervised random forest land cover classification was applied unsuccessfully with regard to the pen detection and the distinction between pens and abandoned pens respectively pen imprints (see Tab. 2). However, in the error matrix of the land cover classification, it can be seen, that the 'Road' class was classified most accurately relative to the other classes (see Tab. 2). Thus, besides the slope and flow accumulation-based mask, the vectorised class 'Road' (see Tab. 2) was used as an exclusion area too (see Fig. 19). Comprehensively, no recent herder camps are expected on the country road.

Table 2: Error matrix of the conducted random forest land cover classification.

Random forest classification		Classification					
		Pen Imprint	Pen Soil 2	Pen Soil 1	Pen	Road	Vegetation
Ground control	Pen imprint	258	0	18	0	0	0
	Pen Soil 2	253	20	0	0	0	0
	Pen Soil 1	241	0	20	0	0	7
	Pen	144	0	0	126	0	0
	Road	81	0	0	0	189	0
	Vegetation	236	0	0	1	0	33

5.2 Livestock pen detection

According to field data recorded in the herder camp that was investigated in 2017 (see Chapter 3.3), the linear dark signatures in the WV-2 image correspond to the dry-stone walls of the livestock pens observed in the field (Fig. 21). These field data points approximately mark the centres of livestock pens, which here exemplarily emphasise the objects that should become detected using the method described in Chapter 4.4.

Furthermore, Figure 21 shows that in case of this herder camp, most of the pen field data points are to find within the highlighted polygon areas, which represent the pen detection results. However, the positions of the field data points 'Pen 2' and 'Trench 1, Pen 1' are outside the detection polygons. Although the localities where pens occur were well detected, seven field data points are grouped in only three polygons. (see Fig. 21). Another aspect of the detection's performance displays Fig. 22, localised in the northwest of the study area (see tag 'S1', Fig. 19, Chapter 5.1). In contrast to the coarse morphological representation of pens in Fig. 21, the polygons that represent pens in Fig. 22 show a more linear morphology that follow the shape of the visible pen dry-stone wall.

Basically, the presented detection results, show that a detection of herder camps or pastoral livelihoods in the study area was successful. Especially, the highlighted areas (polygons) in Fig. 22, mainly mark dry-stone wall structures that are visible in the WV-2 base map. However, detection errors have to be emphasised too.

Besides correct detected pen structures, an example of an erroneous detection is displayed at the bottom right corner of Fig. 22. Probably, this detected structure represents a part of a natural drainage channel. The computed slope raster (see Chapter 4.4) shows increased slope inclination to the south of the linear structure, which reinforces this assumption. In the following, detection errors caused by natural surfaces summarized in the class 'Other'.

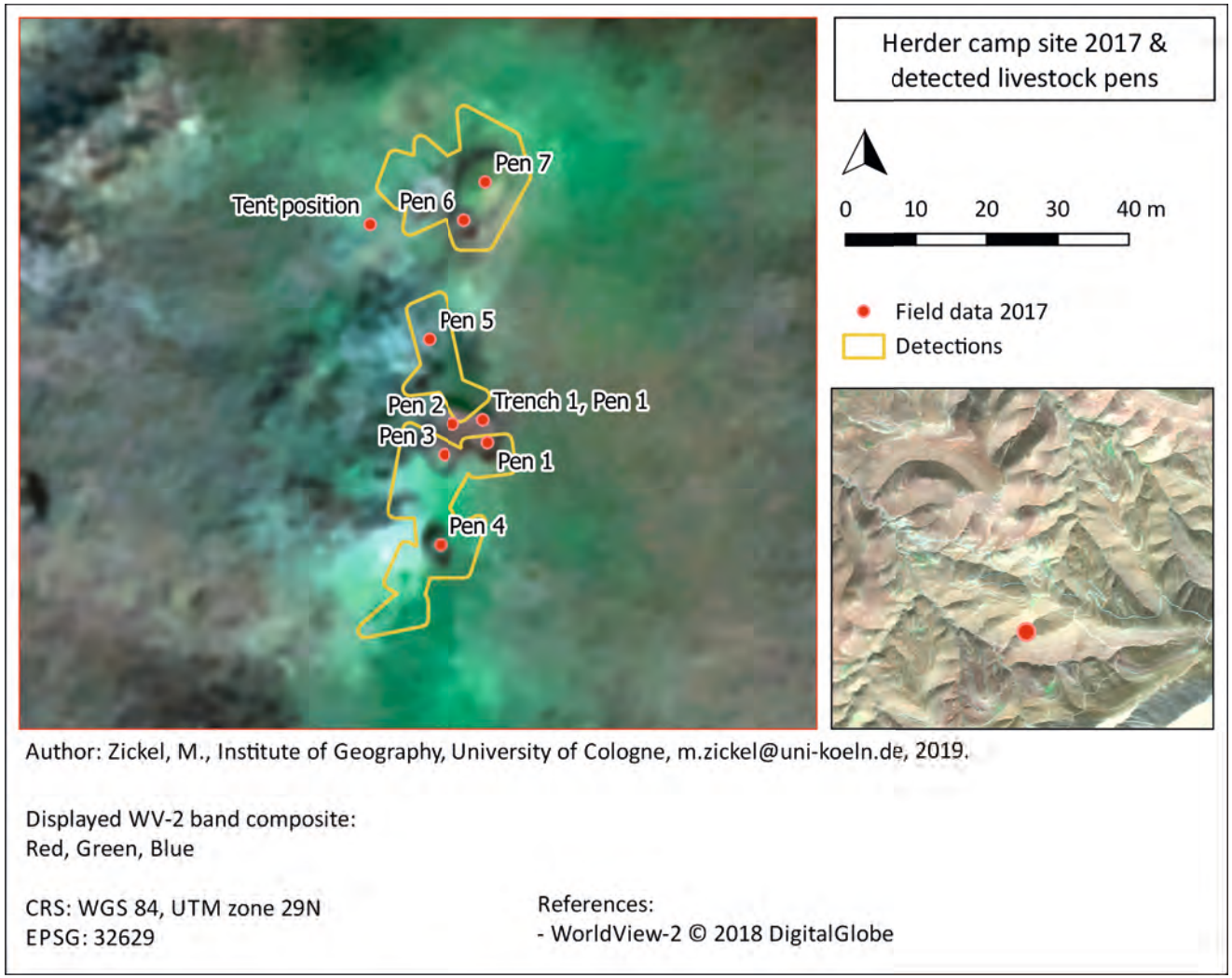

Figure 21: Comparison of the detection results with field data (GPS point coordinates) recorded in 2017.

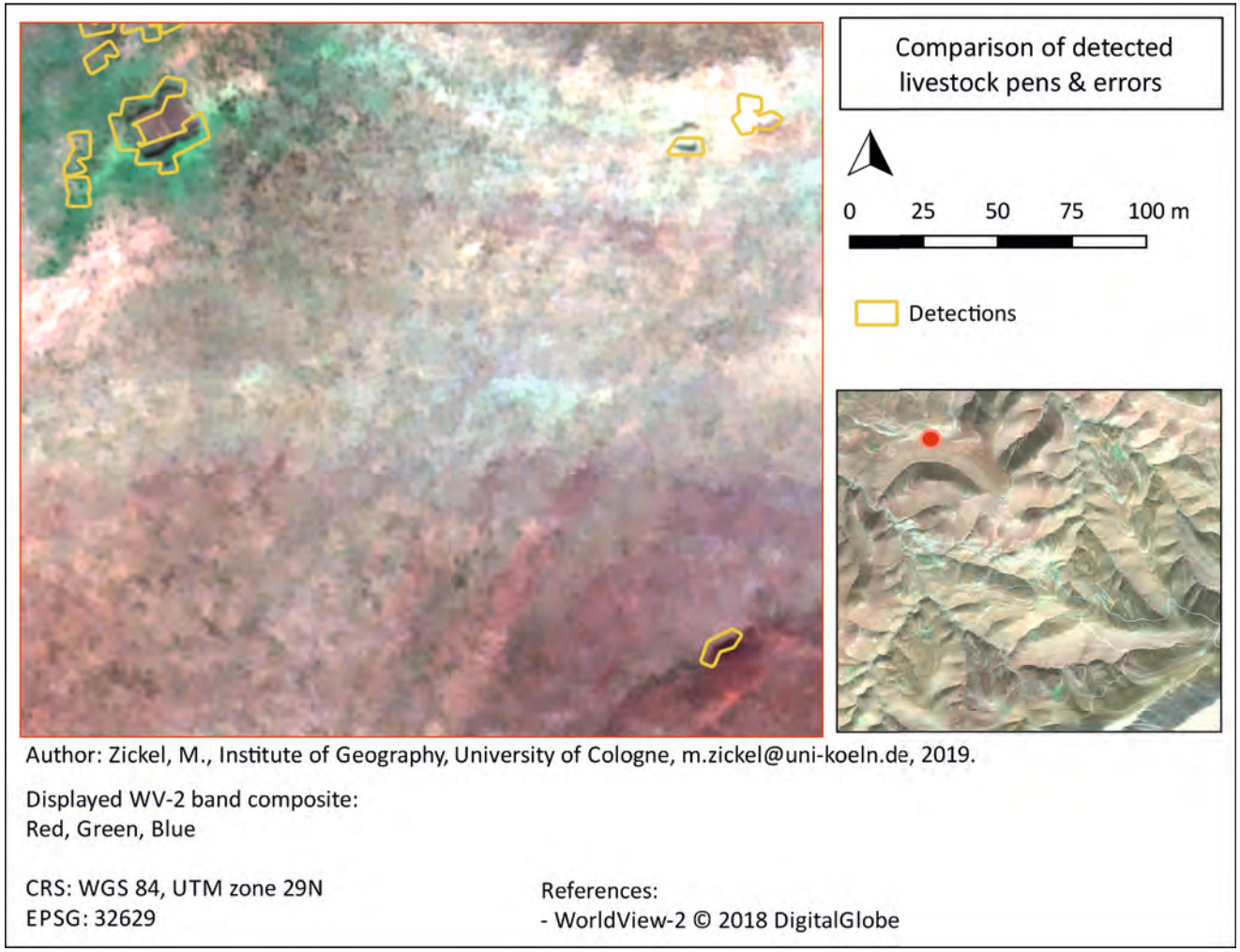

Figure 22: Examples of successful pen detections (top left corner) and an error detection (bottom right corner).

In general, with regard to the comparison of detection results to the GCPs, it is noteworthy that no detections can be found in the grid cells 4, 22, and 24. While the results of the ground control do not show pen detections in grid cell 4, one single pen imprint detection is displayed in each of the grid cells 22 and 24 (compare Fig. 23) In contrast, in grid cell 6 only detection errors ('Other') can be found whereas the ground control in Fig. 23 (bottom) shows that there are no pens or pen imprints to detect.

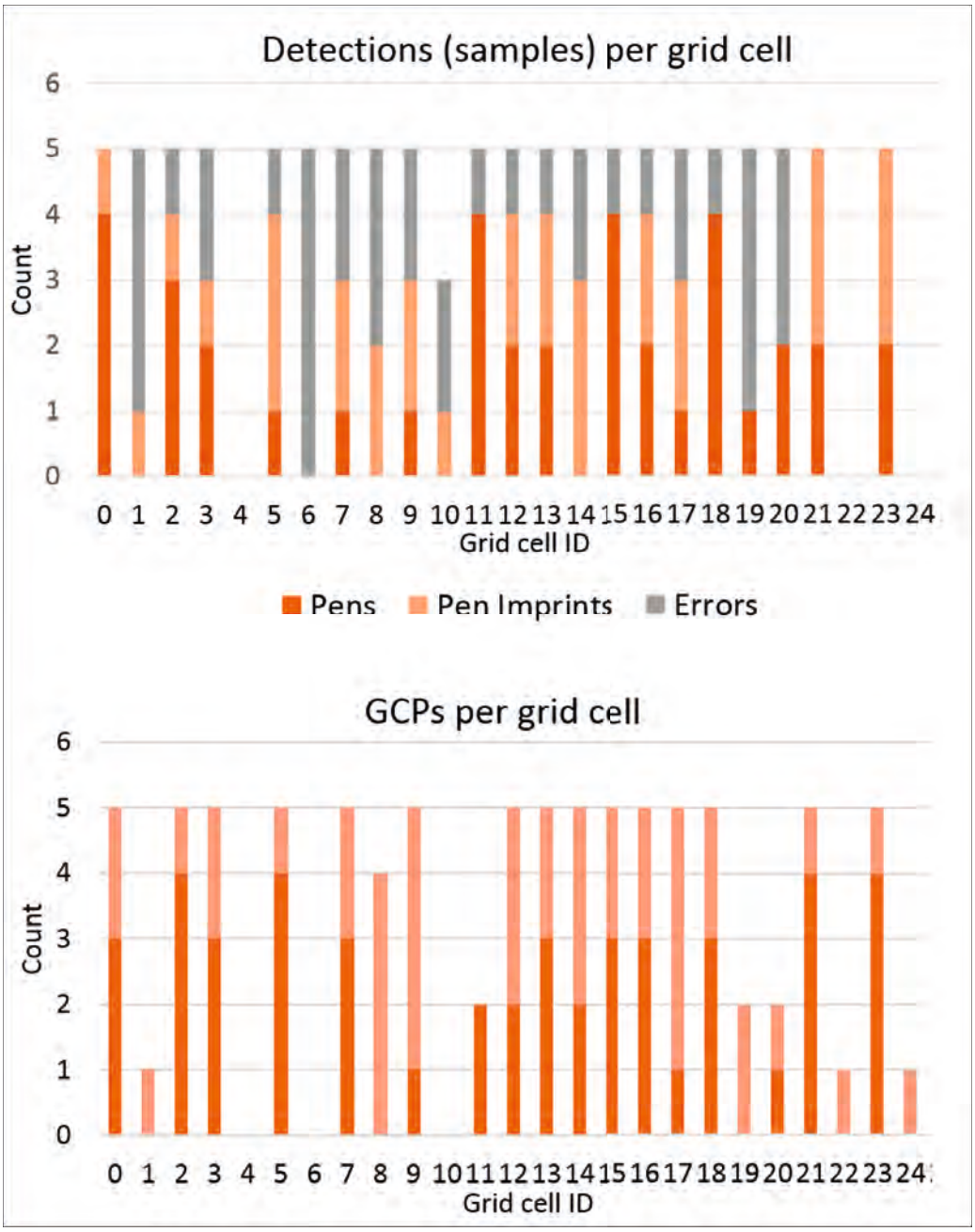

Figure 23: A first estimate of the detection accuracy. Comparison of detections (above) and GCP finds (bottom) per counting grid cell as described in Chapter 4.5.

In grid cell 10 a single pen imprint was found besides 2 errors (Other) whereas there are no ground control finds in the same grid cell.

The counting result for pens, pen imprints errors is illustrated per grid cell, by this representation also the spatial distribution of these classes could have been included. As mentioned above, it was not possible to distinguish between recently used livestock pens with intact dry-stone walls and imprints. However, while collecting GCPs for the accuracy assessment, it was possible to distinguish between pens with visible walls and places that had no or barely visible walls, but a comparable morphology and ground signature. On this basis, it was possible to estimate the pen to pen imprint ratio in the study area. Accordingly, after the subtraction of detection errors, and with regard to all correct pen detections, about 43 % are classified as pen imprints (compare Tab. 3). 23 pen imprints, out of 53, were successfully detected from totally 88 GCPs.

Table 3: Success and accuracy of the sampled detections in relation to total detections.

Class	**Sample count**	**%**	**Extrapolated to total detections**
Pens	30	34	407
Pen Imprints	23	26	312
Pens Total	53	60	719
Errors (Other)	35	40	475
Total GCPs:	88	100	Total detections: 1194

Furthermore, the overall detection accuracy (Tab. 3) shows, that about 60 % of all detections are successful pen detections. Accordingly, about 40 % are detection errors (Other) caused by natural surface morphology. If one extrapolates these percentages to the overall detections, it is possible to carefully estimate the amount of livestock pens in the study area. The result would be a quantity of 719 pens or pen imprints out of 1 194 detected objects (Tab. 3).

To gain a better understanding of the detection accuracy, an error matrix was calculated (see Chapter 4.5). For this purpose, the GCP set used so far was extended by the same amount of random environment samples, collected from different surfaces in the study area, that are not covered by livestock pens or herder camps in general. The pen detection result was then queried with the new set of 176 GCPs (see Chapter 4.5). The resulting error matrix in Tab. 4

shows slightly different results than the counting grid cell method (see Tab. 3).

Table 4: Error matrix of the pen detection result using 176 GCPs.

Pen detection error matrix		**Classification**		
		Pen	**Other**	**Total**
Ground control	**Pen**	174	106	280
	Other	0	267	267
	Total	174	373	547
Overall accuracy (%):	**88**	**80,6**	**GCPs (n):**	**176**

Considering this, it is possible to assess, if actual environment (Other) was predicted as detection (Pen), but it is not possible to see if actual pens are predicted as environment (see Tab. 4). The detection result includes successful pen detections and errors. All other land cover types in the study area are considered as environment or rather 'Other' where undetected pens can be included. Nevertheless, an overall accuracy of 80 % can be calculated.
Thus, including both results between 60 % and 80 % detection succeed can be reached with the method described in Chapter 4.5. However, the detection accuracy can still be differentiated with regard to additional herder camp characteristics, such as the noticeable green surface signature that is related to those.

5.3 Vegetation patches and terrain curvature

According to the result of the NDVI calculation (see Chapter 2.2), a large part of the study area is rather moderately covered by plants. Figure 24 shows a basic overview of the vegetation 'greenness' distribution in the study. The range of NDVI values has been classified to display lower values in light green, and higher values in dark green. Accordingly, remarkable vegetation patches emerge in areas such as river valleys (see tag 'W', Fig. 24) and terraced gardens (see tag 'T', Fig. 24). They are significantly 'greener', and more segregated than most surfaces overgrown with plants in the study area. These locations are characterised by above-average NDVI values. In addition, the map shows dark vegetation patches as exemplarily tagged 'S2' and 'S3' in Figure 24. Apparently, these patches have no direct relation to flowing water nor are they located in valleys. However, they correspond to the noticeable

green surface signature at herder camp sites (see Fig. 21 in Chapter 5.2), that was observed examining the RGB composite of the satellite imagery (see Chapter 1).

A closer look at one of these vegetation patches (see tag 'S2', Fig. 24), reveals a nearly concentric zoning of the index value ranges 0.28 to 0.39, 0.4 to 0.49, and 0.5 to 0.59 (Fig. 25). The threshold values of the classes mentioned, show increasing 'greenness' shows towards the vegetation patch centre. Against the background of comparatively high NDVI values summarised in the three classes, a frequent emergence of detected pens can be observed, as illustrated in Fig. 26. This figure corresponds to the tag 'S3' in Fig. 24, and shows a detailed view of the relation between vegetation patch and detected pens. This relation can be frequently found in the entire study area. Furthermore, livestock pens were detected in each part of the study area that showed a vegetation patch as described above (see Tab. 5 and Fig. 26).

Table 5: Result and ratio of querying the derived vegetation patches with samples of the pen detection result.

Detections & vegetation patches	**Sample count**	**%**	**% total**
Pens	16	14,8	19,4
Pen Imprints	5	4,6	
Pens & NDVI = 0.28 - 0.6	22	20,4	44,4
Pens Imprint & NDVI = 0.28 - 0.6	26	24,1	
Errors (Other)	39	36,1	36,1
Total	**108**		**100**

In addition to pens, pen imprints, and 'Other', pens in general that intersect the described vegetation patches were assessed using the counting grid method (see Chapter 4.5). The results obtained with the method show that 69 of 108 are actual pens or pen imprints. In total 48 pens or pen imprints, approximately 70 % of this number coincide with the vegetation patches described (see Tab. 5). It also shows that approximately half of successful detections are pens and the other half of are pen imprints that can be associated with vegetation patches.

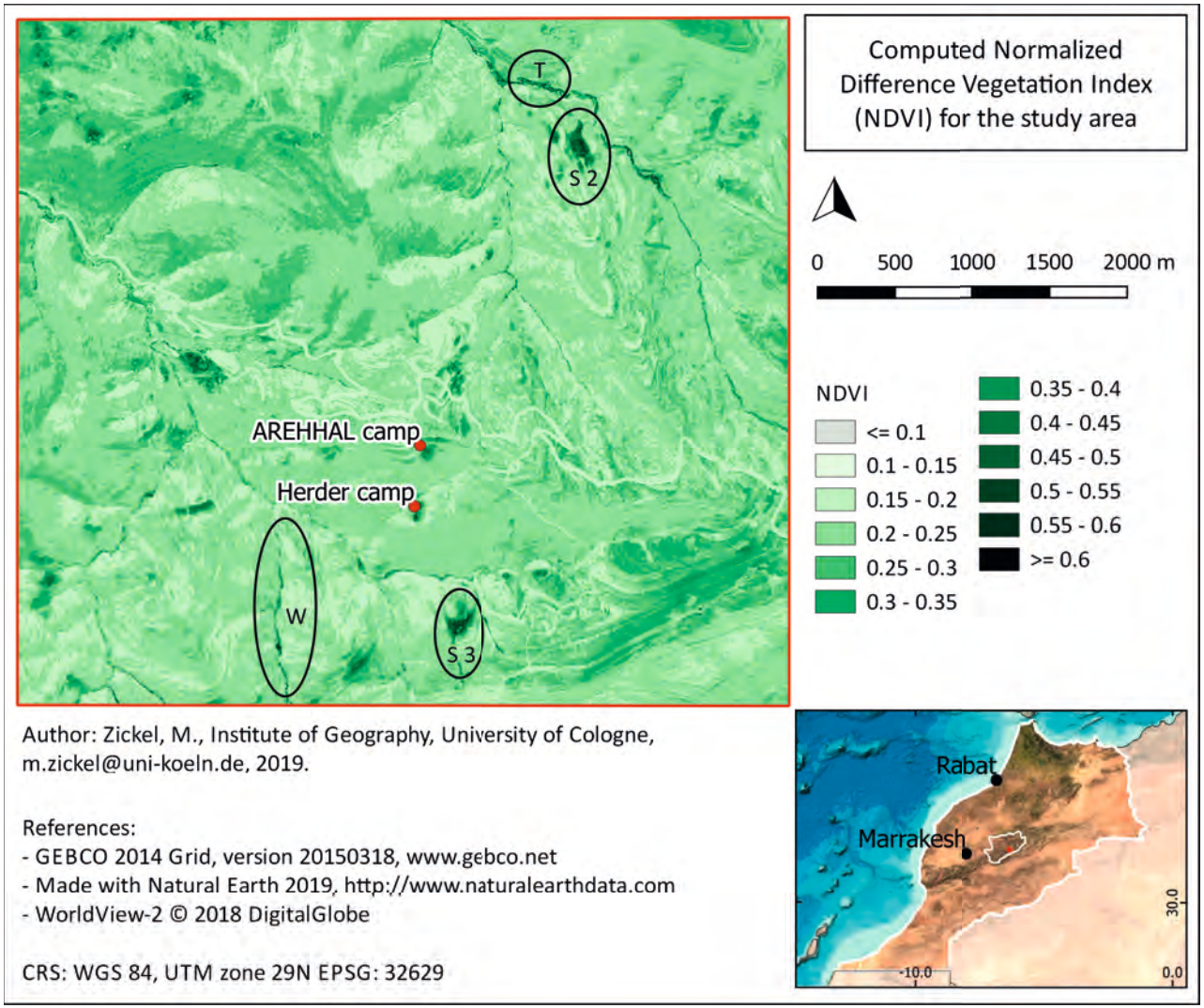

Figure 24: Vegetation greenness estimation for the study area represented by the NDVI vegetation index. 'W' shows a river valley, 'T' are terraced gardens, 'S2' and 'S3' are vegetation patches at herder camp sites.

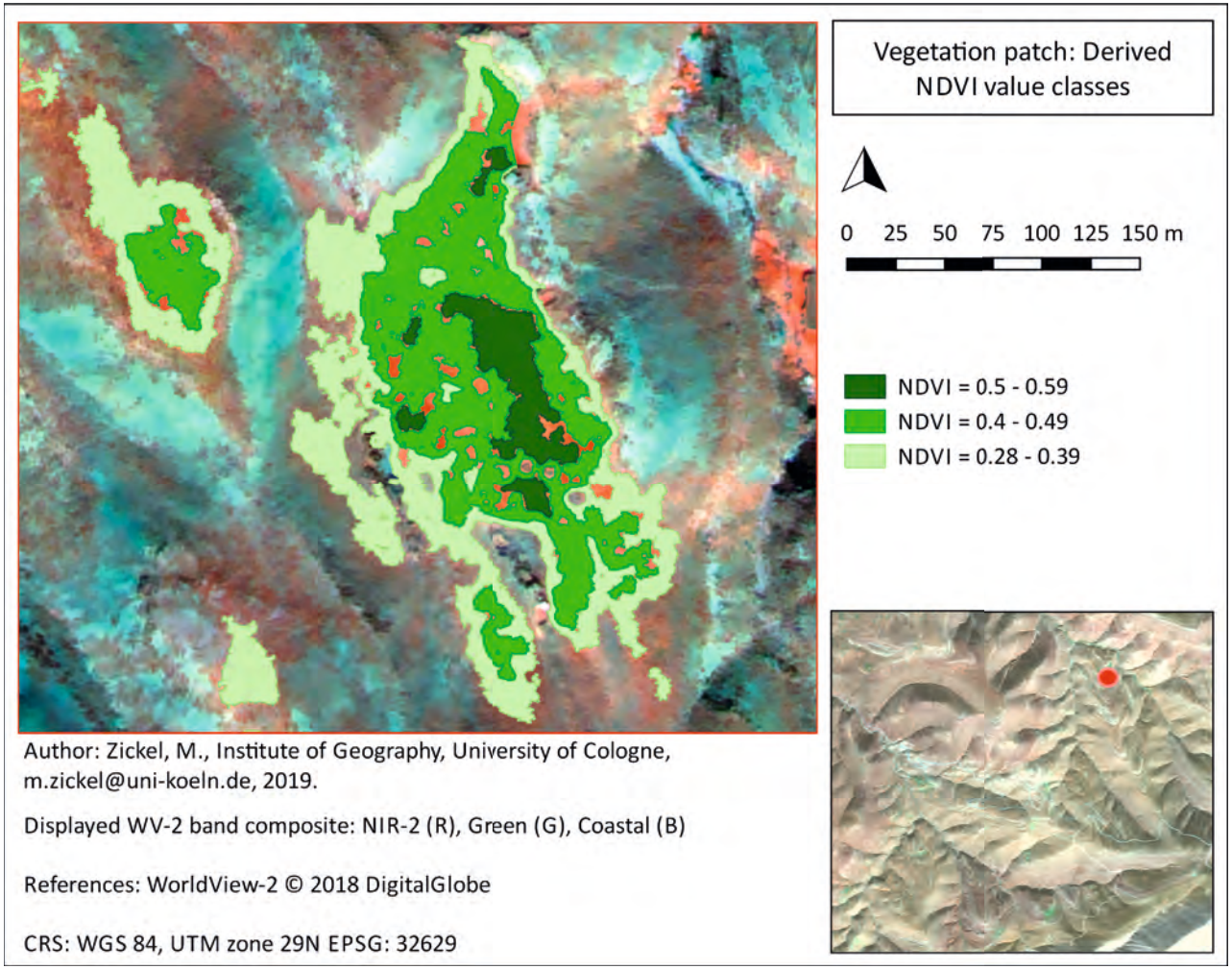

Figure 25: A detailed view of a vegetation patch associated with herder camps.

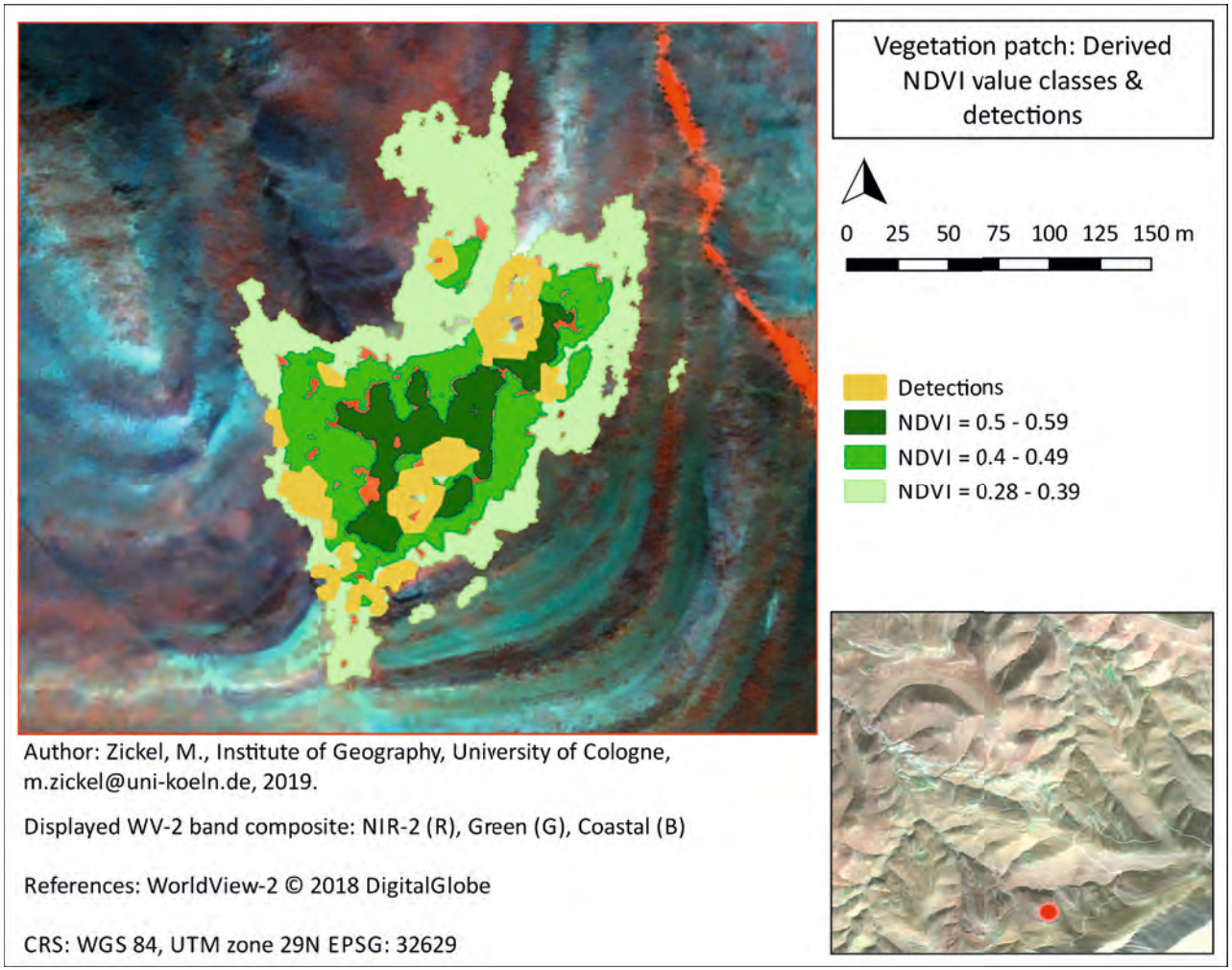

Figure 26: Vegetation patch and mapped pen detections.

Moreover, the integration of pen detection and vegetation pattern, querying the computed profile curvature (see Chapter 4.4) with the selected NDVI classes brought another aspect to the analysis. Figure 27 shows the result for each NDVI class of the vegetation patches. In the lower part of the figure, the diagram shows the number of pixels (n) of the specific NDVI class that have a concave or either convex equivalent value in the terrain profile curvature raster. A convex associated profile pixel has a negative value, whereas a concave pixel is identified by a positive value, which is represented by the two different colours. The percentage of concave to convex pixels in each NDVI class is plotted as a percentage on the Y-axis (see Fig. 27).

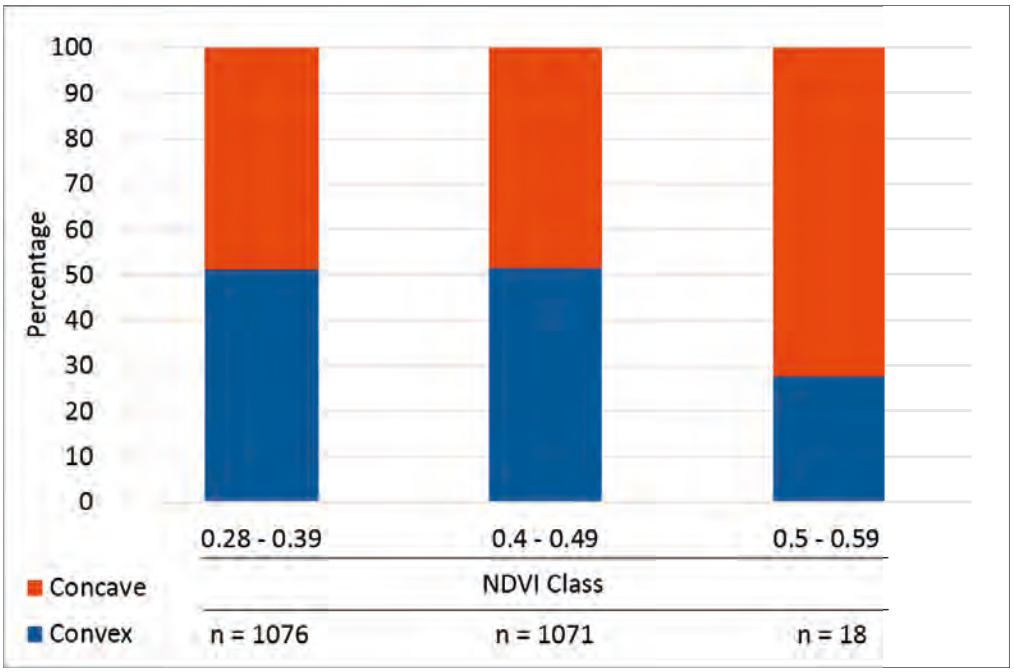

Figure 27: Result of querying the profile curvature raster with the derived vegetation patches.

For the two NDVI classes with relatively lower values, the ratio of concave to convex profile pixels is about 1 to 1 (approx. 50 %). But, convex pixels are most numerous in these two NDVI classes. Contrarily, the class with the highest NDVI values (0.5-0.59) counts less convex pixels than the two other NDVI classes. However, about three-quarters (72 %) of the count are concave pixel (see Fig. 27). It seems that the associated terrain's curvature change from the two lower NDVI classes up to the highest NDVI class is significant with regard to the concentric vegetation patch structures.

5.4 Pastoral land use pattern

Through the synthesis of the essential result parts described above, it is possible to get an impression of the distribution of pastoral livelihoods in the study area. Furthermore, the intensity of recent anthropogenic influence on the natural environment in the region can be estimated. Therefore, the resulting livestock pen detections and vegetation patches are combined and illustrated in Fig. 28. Additionally, the derived country road (see Chapter 5.1), that spatially distributes the study area is mapped on the TDX DEM. This elevation base map illustrates the altitudes where green vegetation or rather vegetation patches occur, and at which the mentioned dry-stone wall structures or mainly livestock pens were detected (see also Appendix III). Tag 'T' shown in Fig. 28 marks pen detections, but represents a place that is more related to agriculture, horticulture or rather terraced gardens (see tag 'T', in Fig. 24 in Chapter 5.3). However, besides other dry-stone wall structures in this location, livestock pens seem to be present as well. Probably these pens are not related to herder camps, but belong to agricultural livelihoods. Focusing on detections associated with vegetation patches, the map also shows the spatial distribution of probable herder camps. Close to the country road and in the map centre, an increased and denser occurrence of livestock pens (see tag 'C1' in Fig. 28) is evident. It appears, that this pattern can be found in many parts of the study area. The tags 'C2 to C4' mark further of such clusters of livestock pens or rather related herder camps. Often the individual clusters are widely separated from each other. The course of the mentioned road seems to play less of a segregating role than the terrain. Latter seems to divide the study area by deep valleys with steep slopes and mountain ridges. In any case, different catchment areas seem to exist. Furthermore, as mentioned above, pen detections coincide mainly with vegetation patches (see also Appendix III). Nevertheless, some isolated pens occur in the detection result too. However, tag 'E' in Fig. 28 shows another typical detection error (compare Chapter 5.3) that can be confused with livestock pen occurrence. This kind of detection error is situated on a steep sloping terrain edge on top of an approx. 2 700 m high mountain. With regard to the AOI mask presented in 19 (see Chapter 5.1), it seems that it is a relatively flat surface. However, the presented results and error sources will be discussed in the following chapter.

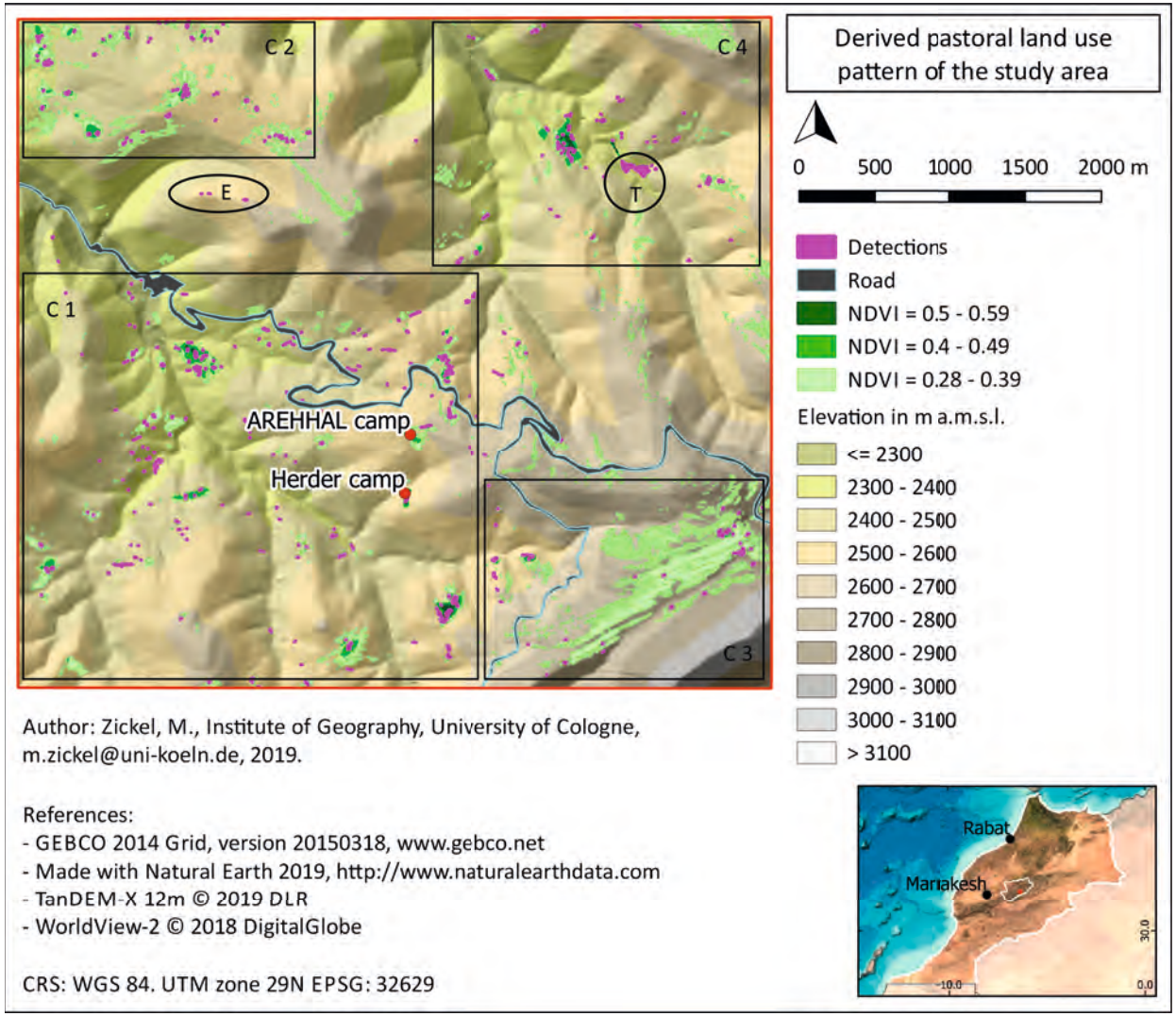

Figure 28: llustration of the analysis results in the study area. Tag 'T' marks terraced gardens, 'E' marks error detections, 'C1 to C4' are exemplary marked areas with an increased density of livestock pen occurrence.

6 Discussion

The focus of this work was the detection of herder camps, to examine their distribution, and to investigate the related green ground signature via remote sensing and GIS applications. The actual goal was to use this information to gain constant on-site clues of herder camps and their occurrence density in the form of spatial data in the study area. These should enable a selection of key sites, and moreover support subsequent geoarchaeological fieldwork. It was conducted by the detection of livestock pen structures, the collection of environmental data, and the determination of specific terrain properties, such as plant cover, slope, flow accumulation, and terrain curvature. In this chapter the analysis results are briefly summarised and discussed within the scientific context.

6.1 Challenges of site detection in digital geoarchaeology

Remote sensing is a common method to detect cultural heritage. However, many problems can be identified concerning satellite remote sensing-based detection of dry-stone wall enclosures or fortifications.

In general, the variation of structure size and shape is mentioned to be a challenge. Trier et al. 2009 investigated crop and soil marks induced from circular archaeological structures in the ground. Additionally, to size and shape variation, the small number of possible training sets was discussed there. Comprehensively, compared to urban areas or agricultural fields, in the archaeological context, the remains of structures on the surface or in the ground offer a far smaller sample size. Fortifications and enclosures, inclusive livestock pens, in recent as in archaeological context are often of low extension, narrow, fragmented, rather have (entrance) gaps, and are irregular in shape (see Trier et al. 2009: 1 and Lambers 2018: 117). Therefore, often they are poorly visible on the surfaces and difficult to detect, or rather classified in remotely sensed imagery data.

Within this study, similar challenges, as mentioned above, were identified. Especially, concerning the supervised classification of livestock pens with the random forest machine learning algorithm (see 6.2. With regard to the variability of geometric forms, terrain properties, the spectral similarity of

dry-stone walls and stones infrequently spreading on the surrounding surface, or rather a small sample size of the target objects, supervised classification was not suitable. The error matrix (see Tab. 2) of the random forest classification described in Chapter 5.1, displays these big differences in the confusion rate of the classes. The 'Random Forest Classifier' could produce good results with unbalanced data in other conditions, but still this depends on the training data set quality and size, as it is the case for other machine learning algorithms (Pal 2005: 221).

However, in contrast to the other classes, the class 'Road' was based on an artificial, homogenous and sharp bordered object, with a straight course, covering a comparingly large area. Possibly, this is the reason why it produces a comparably good classification result (compare Pal 2005). Moreover, its spectral signature is most consistent, its spatial extension is sharply bordered, thus it can be simply isolated too 4.4. According to the high confusion rate in the other classes, especially in the 'Pen' classes, just the class 'Road' was proceeded and implemented in the results.

The remaining classes can be confused easily among each other (compare Appendix II). Moreover, negative classification effects are mostly study site and target class specific. For example, the study area's steppe surface is spectrally very heterogenous (Grignetti et al. 1997: 1316). Probably, small spots of sparse xerophytic vegetation with relatively low reflectance in the NIR region can be easily confused with sediment or soil signals (see Chapter 5.1, Tab. 2).

Moreover, Zingman et al. 2016: 1, who worked on a comparable livestock pen detection project in the Alps, mentioned that spectral signatures of stone wall enclosures (livestock pens) show little contrast to their environment. He observed that livestock pens in the alpine study area are very low in height and stones or rocks on the surrounding surface can be spectrally confused with the walls that are made of these stones. The same case was observed in the High Atlas Mountain study area, where the dry-stone walls of the livestock pens are built of stones from the surroundings (see Chapter 2.6. Additionally, most of anthropogenic build-up structures, such as terraced gardens or farms (see Chapter 3.1) seem to be constructed of the same material that is highly available in the study area. The height of pen walls was observed to be relatively low, approximately between 0.5 to 1.2 m (see Chapter 3). Further,

the fragmentation grade and the wall height is varying. Although fragmented or low pen walls are poorly visible in the field (Chapter 3.1) the wall's imprint or a ground signature is visible in the WV-2 scene. Nevertheless, the ground signatures of livestock pen sediments seem to be very variable in the study area. Therefore, it was not possible to extract and classify a specific spectral signature to determine recently used pens and former pen sites.

The study site´s terrain, mountainous with steep slopes, brought additional challenges. Big parts of the WV-2 Scene are affected by shadows and sun glint spots. These effects depend on time and date of the image acquisition, nevertheless no other scene or satellite remote sensing product with similar, high-resolution, specifications were available for the remote location of the study area. Moreover, atmospheric corrections of the multispectral data did not improve the scene's quality (see Chapter 2.4). Shadows, for example at mountain slopes in particular are often spectrally confused with dry stone walls, as the wall´s shadow often covers a larger area that contains more pixels than the coverage of the wall.

In conclusion, a classification of exclusively spectral information was considered as not sufficient to fulfil the aim of this study. Moreover, an object-based image classification (compare Grippa et al. 2017) approach was considered, but during pre-processing the circular livestock pen shapes in the WV-2 imagery could not be isolated and were segmented in return.

However, Zingman et al. 2016 found a solution focusing on rectangular livestock pens, as they are common in alpine pastures. He used angle and convexity properties of the target objects derived from satellite and aerial images. Moreover, the mentioned problem of spectral confusion was widely solved in the application of morphological texture (MTC) and feature contrast (MFC). Thus, it was possible to filter grassland that has a specific texture, and which Zingman et al. 2016 relates exclusively to livestock pen occurrence. MTC also facilitates the distinction of forest, rock and glacier cover (compare Zingman et al. 2014 and Zingman et al. 2016).

6.2 The edge extraction-based detection approach

Whereas the targets, livestock pens, were the same in the High Atlas Mountains study area, the general conditions deviate strongly from Zingman et al. 2016's

study area and object. In contrast to the alps, most livestock pens in the Central High Atlas have a circular to oval shape (see Chapter 2.6) and they do not exclusively correspond to grassland, or rather low vegetation patches (compare Chapter 5.3). In this study, the solution was a combination of automated spectral edge extraction and a mask derived from herder camp associated environmental terrain characteristics (see Chapter 5.1).

Comparable to Zingman et al. 2014's approach, at first a noise reduction was achieved in the WV-2 multispectral dataset. Using local mean and variance matching (LMVM) in the pansharpening process, reduced the sprinkled texture caused by the stone pavement (Hamada) that covers the study area, and which lead to spectral confusion with the livestock pens (see Chapter 4.3). However, concerning LMVH algorithm's noise reduction, a possible loss of detail sharpness must be considered when configuring the alogirthm's parameters (see Chapter 4).

Facing the discussed problems of varying shape, size, and surface cover of pens, satellite data quality, spectral confusion and heterogeneous terrain in general, best pen detection results were achieved by applying the Sobel algorithm-based edge extraction on the WV-2's NIR-2 band. During the postprocessing, noise could be reduced once more due to a neighbourhood variance analysis (see Chapter 4.4). Besides noise reduction, this step resulted in more consistent, and therefore increased visibility of pens in the results, especially for highly fragmented pen walls. In this concern, it is of major importance to query the values of the edge extraction-based result with GCPs (ground control points) and to test several thresholds in order find a good balance of target object gain and loss. Moreover, the mentioned noise reduction and further processing steps (see Chapter 4.4) enable the possibility to adjust and refine the detection results on the one hand, but they also increase the degree of reality abstraction. Thus, as shape and size variation of the actual pens determine the pen detection results, the produced shape quality varies. As it was presented in Chapter 5.2, for instance in Fig. 21, in some locations the discussed method could lead to the merging of several pens and the inclusion of non-pen signatures. In other locations (see Fig. 22) where the derived pen polygon shape shows an increased fit, other pen walls are excluded from the results. In addition, terraced gardens framed by dry-stone walls have been

detected and some errors ('Other'), such as errors caused by drain channels at a hillslope (see Fig. 22) or by the occurrence of additional natural terrain edges. Although the actual shape of the pens is partly not well represented in the final dataset (see Chapter 5.4), sites of livestock pen occurrence, were successfully detected in most cases.

Furthermore, concerning the amount of detection errors, a major supplement to the analysis can be seen in the implementation of TDX high-resolution digital elevation data (see Chapters 2.3, 4.2). The availability of height information for the study area enabled the inclusion of detailed terrain characteristics in the GIS analysis. The majority of global DEMs have a far coarser spatial resolution (compare Grohmann 2018) and the executed analysis would probably not have been possible to the presented extent. In producing the DEM derived products 'Slope' and 'Flow Accumulation' it was possible to refine the edge extraction results and to exclude the mentioned detection errors. The related mask (see Chapter 5.1), which excludes river valleys and consists of areas with slopes up to 20 ° had a valuable influence on the rate of terrain caused detection errors. During the accuracy assessment the above-mentioned slope threshold was confirmed by querying the basic slope raster with GCPs (see Chapter 5.1). Mostly, herders in the study area seem to prefer areas with a maximum slope of 20 ° to build their campsites, or respectively build livestock pens there. In general, concerning the presented detection result, it can be assumed that between 60% and 80% of livestock pens in the study area were correctly detected.

The 'counting grid method' (see Chapter 4.5) was used to assess the pen detection accuracy. An approximately 60% verified detection rate can be determined in the sample size, applying this at least basic procedure. In addition, since this is a binary classification, the localisation error is the difference of 40%.

Collecting random environmental GCPs, an error matrix has been computed additionally (see Chapter 5.2). Therefore, it was possible to calculate a localisation overall accuracy of approximately 80%. The detection result includes pens and errors ('Other') that represent natural surfaces in the environment. Still the method to compute the error matrix, lacks the possibility to calculate a realistic false-negative value. However, whereas it is possible to

see if actual natural surfaces (environment GCPs) were predicted as livestock pen, it is not possible to check if actual pens were classified as 'environment'.

Nevertheless, computing a grid to ensure an evenly distributed selection of GCPs had the advantage to check if there are local divergences of detections and GCPs. For example, grid cell 4 shows that no detection was made in the cell because there are no actual pens. This is shown by the GCP count in this cell (compare Fig. 23 in Chapter 5.2). In contrast, in each of grid cell 22 and 24 a visible pen imprint was not detected. Also, there was one pen imprint detection in grid cell 10, but no imprint GCP. As described at the beginning of this chapter, the alleged pen imprints are particularly difficult to distinguish from their surroundings. First, this could imply that the contrast between the pen imprints and their immediate environment is low. Thus, corresponding pixels were possibly below the set threshold in the edge extraction output. Second, occasionally the contrast is very low, and some pen imprints were simply overlooked when the GCPs set was created. It illustrates that the pen imprints are a problematic detection target, regarding that it is not possible to isolate them in the detection results as well.

In general, it must be considered that the grid-based accuracy assessment, used a sample size of 5 GCPs per grid cell each. If more than 5 livestock pens occur in one grid cell, it is possible that the GCPs are tagging other pens than the selected pen detection results. The result is a probable underestimation of true detections.

Additionally, the extrapolation of the percentage to the basic population of the detections (see Tab. 3), proofed to be a good way to estimate the anthropogenic influence respectively the visibility of transhumant livelihoods in the landscape of the study area. However, the population of correct detections contains an unknown part of dry-stone wall structures that cannot be assigned to herder camps. Other dry-stone wall structures are common in the study area and partly included in the detection results. Their geometry is characteristic, such as the mentioned terraced gardens and therefore can be excluded by visual review. Nevertheless, probably the method works well in the selected study area, but not in other regions. For example, it will probably work less effective in regions with a higher subsistence diversity, where huts or detached houses can be confused with livestock pens of the same size. On

the other hand, in lowlands, the method could work even better due to the reduction of natural terrain edges.

In summary, one can say that the pure edge extraction-based detection, including the discussed limitations, works comparatively well. However, it was possible to significantly increase the herder camp evidence by the results of the NDVI analysis that will be discussed in the following. In combination with the vegetation patches, two independent features, livestock pen occurrence and increased plant growth, can be considered when the question arises whether a herder camp was detected or not.

6.3 Vegetation patches and the contextual role of terrain curvature

Looking at the results of the 'greenness' distribution analysis (see Chapter 5.3 and NDVI (see Chapter 2.2), it is comprehensible that the classified 'greeness' patches represent sparse, or rather a cover of low vegetation at herder camp sites. Respectively no tree or shrub canopy structures are present. Scattered trees, probably Juniperus thurifera (see Chapter 3.1), were detected mostly at steep hillslopes. Besides herder camp related vegetation patches, highlighted in this chapter, comparatively low NDVI values (0.28 to 0.39) occur in a broad context (see Fig. 24 in Chapter 5.3). NDVI values of 0.4 to 0.49 exclusively occur close to flowing water (rivers), terraced gardens that are probably artificially irrigated and/or fertilised, and in the near surroundings of livestock pens. NDVI values of 0.5 and higher can only be found where livestock pen detections are located too. This was observed when the dataset was queried with the pen detection results (see Chapter 5.3).

As displayed in the satellite imagery's RGB image (see Fig. 1 in Chapter 1) the detected vegetation patches mostly show a characteristic, homogenous, ground signature with high reflectance values in the red edge and NIR bands of the WV-2 data. The 'patch' like structure of the vegetation cover at herder camp sites shows that there is a certain difference between very low greenness intensity of the herder camp's surrounding environment (off-site) and a high greenness intensity on-site, near the livestock pens. The internal, concentric structure of the patches, made visible by the above mentioned NDVI classes, also shows that the greenness intensity decreases towards the patch edges. In the centre of the patches, where the highest NDVI values are found, there are

also livestock pens. Probably, ongoing soil formation processes (Anthrosol, see Chapter 2.7 and 3.3) within the livestock pens, increase local water storage ability and plant nutrient deposits are formed out of combusted dung. Thus, they can play a role in plant irrigation and fertilisation. Accordingly, it is possible that, regarding plant nutrients such as nitrogen, a concentric shift of plant species occurs, which are disparately adapted to high nutrient deposits. Thus, the different NDVI classes might represent different plant communities too. However, it is conceivable that plants favour these nutrient and water hotspots in the semiarid environment of the study area(see Chapter 2.6).

A comparable observation connected to pastoral activity is demonstrated in a very recent geoarchaeological study of (Marshall et al. 2018). Similar to pastoral societies of Morocco, in Marshall et al. 2018's study area, which is located in southwestern Kenya, it is common practice to pen livestock at night. It is concluded that this concept results in a concentration of herbivore excrements and thus represents a plant nutrient hotspot. The concentrated plant nutrients originate from biomass of the surrounding Savannah pasture lands Marshall et al. 2018: 387. These nutrient hotspots, or rather vegetation patches are as well visible in Landsat-7 satellite imagery (Marshall et al. 2018). Furthermore, Marshall et al. 2018 presents excavation results, which connects the locality of recent herder dwellings to former Neolithic occupation (Marshall et al. 2018: 389). With the results of geochemical, micromorphological, and isotopic analysis of these pen sediments, they could trace back pen occurrence to approximately 3 000 years before present. Thus, they excavated datable, long-term durable, dung originated plant nutrients at herder camp related vegetation patches in a semiarid environment. Obviously, the vegetation patches or long-term nutrient hotspots attract modern herders through the increased availability of fodder plants.

The example shows that a combination of prehistoric and modern dung deposits can result in vegetation patches. Thereby, pastoralists can enrich semiarid landscapes such as in Kenyan savannah landscapes (Marshall et al. 2018: 387).

In principle, Marshall et al. 2018's conclusions fit to the results of this study and observations during field work in 2017. The livestock pen stratigraphy that was investigated during field work (see Chapter 3.3) indicated

a significant enrichment of plant nutrients and possible long-term durability of the organic sediment components. Further, it is possible that generations of pastoralists favoured these places over a long period of time. Probably, such as in Marshall et al. 2018: 389, they create local, sustainable, long-term nutrient hotspots that enrich the floral landscape, and which can be tracked with geoarchaeological methods. However, this could explain the existence of vegetation patches on herder camp sites, which manifests in the sharply bordered green signatures in RGB images and the concentric zoning of comparatively high NDVI values on-site. Moreover, it is possible that local terrain properties, such as local terrain curvature variability, can be an additional reason for the concentric occurrence of greenness, or rather the zonation of NDVI-classes.

If one considers the terrain curvature type, on which the vegetation patches are located, it can result in a specific vegetation pattern too. Therefore the local terrain curvature properties were investigated in this study. Whereas NDVI values in the range of 0.28 to 0.49, the two lower classes, cover a convex terrain curvature slightly more often (see Fig. 29), the highest NDVI class cover mostly concave terrain. Even if the occurrence of NDVI values between 0.5 and 0.59 is much lower, the associated change in terrain curvature is significant. To illustrate the result, the possible profile of vegetation patch cover is displayed in a sketch on the bottom right of Fig. 29. Possibly, the result is biased, because the curvature raster was queried and cumulated per NDVI threshold class. Thus, the derivation of exact, local assumption would not be possible. Still it is an option that there is a change in local curvature related to the NDVI classes of a vegetation patch. This could be related to livestock trampling close to the livestock pens, which results in local soil compaction, a local natural depression onsite, or TDX underestimates the local terrain heights, which would result in locally incorrect DEM values.

However, the local role of concave terrain curvature related to the highest NDVI values seems still unclear. Whereas, the varying distribution of concave and convex curvature in the two lower NDVI classes displays that the occurrence of vegetation patches cannot be assigned to natural depressions in general. This reinforces the impression that the intense ‘greenness’ originates from local soil formation as mentioned above. As discussed, it is likely that there is

ongoing formation of Anthrosol in livestock pens, which is probably compacted by human and livestock trampling.

An additional advantage of the combination of 'edge extraction'-based pen detection results with the derived vegetation patches discussed in this chapter is displayed in Fig. 30. The visible white imprint in the Figure on the left was not detected by the 'edge extraction' approach, but a vegetation patch is present. It seems that the white imprint on the surface represents a structure in the ground. This imprint spectrally differs strongly from others, generally low reflective, pen imprints in the study area. It looks more alike circular stone structures in the ground, similar to buried structures that were represented by soil and crop marks, which were detected by Trier et al. 2009. In this case the origin of the ground signature, or rather soil mark is unclear. Probably it is caused by an anomaly in the ground, possibly rock, which is less moist and therefore influences the local plant growth pattern (compare Trier et al. 2009). In addition, a further indicator suggests a different temporal context than a relation to recent herder camps. The mapped stone artefact finds, discovered during field work, show likewise a close spatial relation to the site (see Fig. 30).

This last example particularly illustrates the powerful combination of different remote sensing approaches and geoarchaeological field work. Moreover, it also shows that the combined detection approach based on 'edge extraction' and NDVI has significant advantages over a single, linear method for this purpose. Furthermore, this is apparent regarding the derived pastoral land use pattern, which will be briefly discussed in the following chapter.

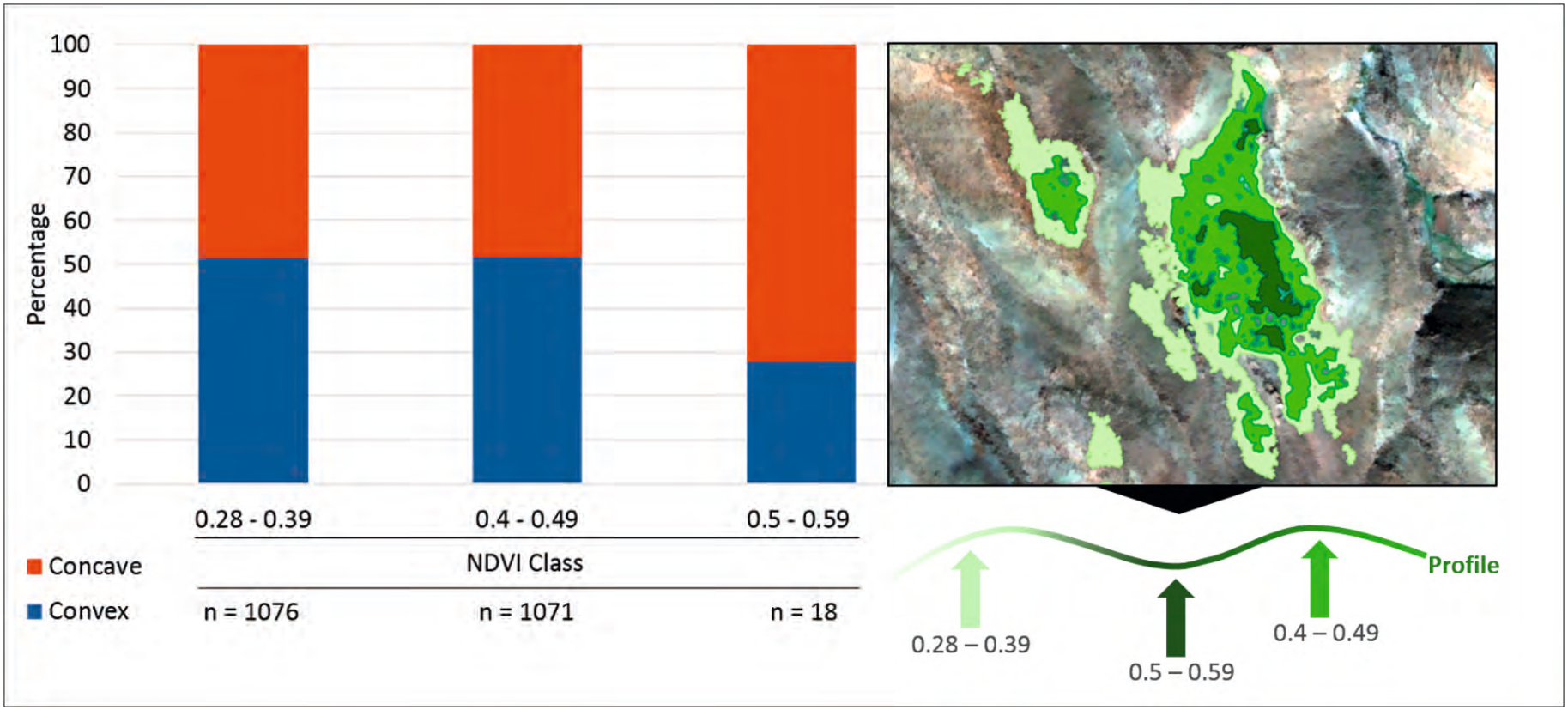

Figure 29: Result of the NDVI query of the terrain's profile curvature (left), Vegetation patch map view (upper right) and sketch of the associated vegetation patch profile view (bottom right).

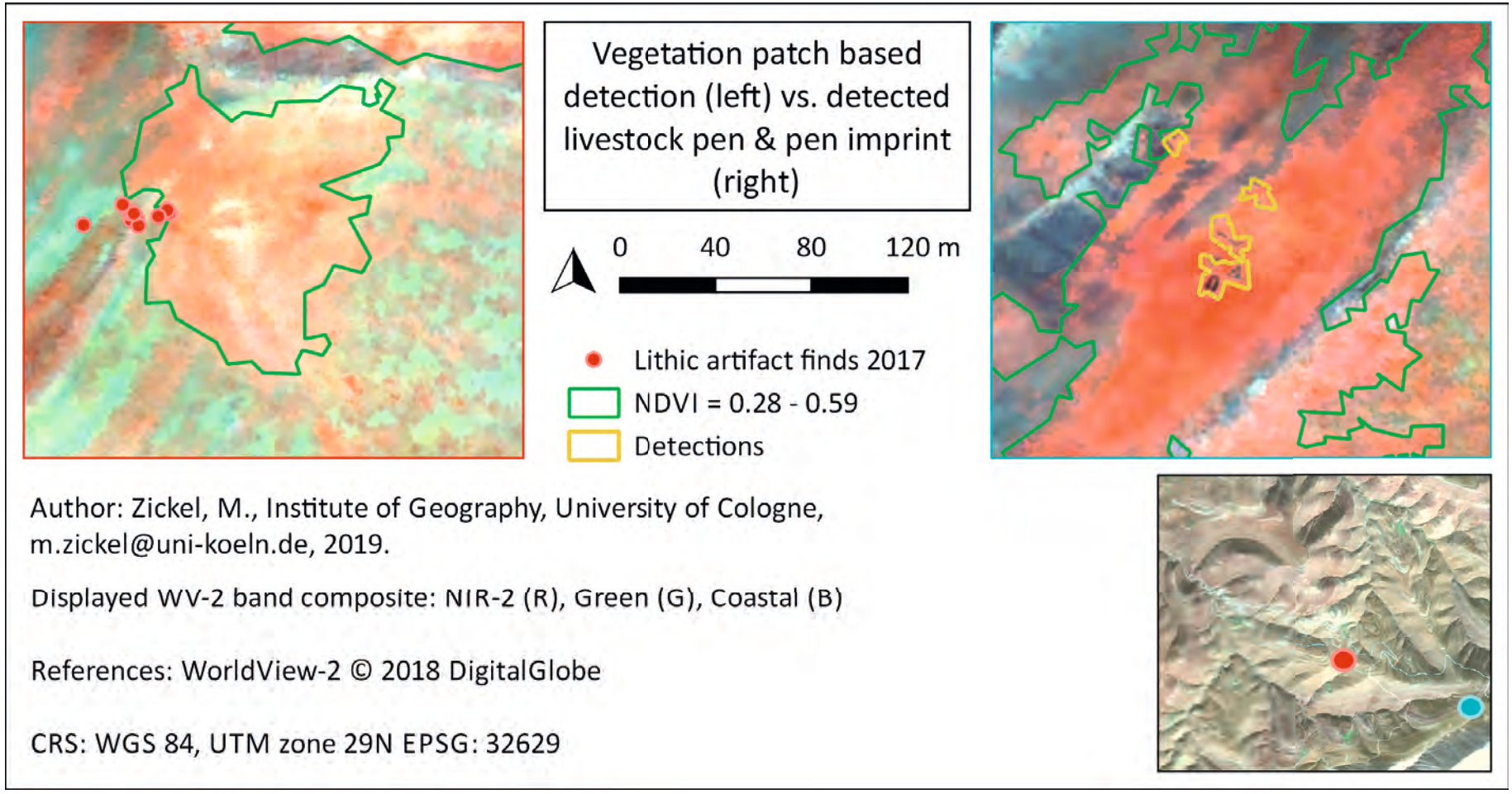

Figure 30: Comparison of non-detected, circular white object in the ground surrounded by a vegetation patch. Mapped lithic artefact finds from field data within the spatial context of the object (left). In contrast, dark, fragmented pens respectively pen imprints that are detectable by 'edge extraction' (right).

6.4 Pastoral land use in the study area

The derived geospatial data highlights herder camps and their distribution in relation to vegetation patch occurrence. The result is an overall view of primary recent pastoral livelihoods in the study area. Concerning the structure of the land use pattern (see Fig. 28 in Chapter 5.4), one assumption is a terrain-based segregation of areas occupied by pastoralists, or rather transhumant herders. In addition, related ethnographic data can be discussed in this context. As described in Chapter 3.2 the pastoral land use follows specific community-based laws, especially concerning transhumance. The study area covers an *Agdal* (see Chapter 2.6), a pasture land of the Aït Atta, but it can be assumed that the borders to the pasture lands of other ethnic groups play a delimiting role in the study area (see Hart 1981: 2 and Akasbi et al. 2012: 315). In addition to ethnicity, different livelihood types, such as agriculture or agropastoralism can be considered as a delimiting factor. For example, horticulture in terraced gardens was detected in the northeast of the study area (Fig. 24 in Chapter 5.3). Nevertheless, with regard to the detection distribution (see Fig. 28 in Chapter 5.4), the study area shows evidence of segregated land use. Whereas the mapped camp position of the accompanied Aït Atta family is located in the southern centre of the study area (see Chapter 3.2), the according catchment, possibly represents Aït Atta pasture land (compare Fig. 28 in Chapter 5.4).

In general, the results show that the study area unites characteristic aspects of an active cultural landscape. Furthermore, and with regard to the discussed study of Marshall et al. 2018, possibly the roots of this cultural landscapes go back to prehistoric times. Potentially, as Marshall et al. 2018 mentioned concerning the Kenyan study area, the Central High Atlas was frequented by pastoralists since Bronze Age or Neolithic times (see Chapter 3.3) and, due to ongoing long-term plant nutrient storage and the related pasture quality, still is today.

7 Conclusion

From a geoarchaeological perspective, the remote sensing and GIS analysis applied here is an essential contribution to future research in the study area. Many herder camps were identified by using the combined approach of livestock pen structure detection and NDVI-based vegetation patch analysis (see Fig. 28 in Chapter 5.4). The TDX DEM based terrain analysis proofed to be of major importance for this purpose.

According to the question to what extent livestock pens can successfully be detected in multispectral satellite imagery, this study shows that a pixel-based approach, cannot be exclusively used to reliably detect the narrow dry-stone walls of livestock pens (compare Fig. 1 in Chapter 1 and Appendix II). As previously discussed in Chapter 6.2, the majority of livestock pens only cover small areas, which results in a small amount of pixel values with low reflectance as a classificatory basis. Moreover, the pen shapes are often incoherent, structural discontinuities frequently occur, and no specific geometric feature (angle, etc.) was observed, that could have suggested a certain pattern. Another limitation, which emerged during the analysis was the difficult distinction between walls and the surrounding area, due to the fact that the building material of the dry-stone walls is taken from the vicinity. Taken all these limitations into account, the application of a supervised random forest classification resulted in an unproductive pixel-based land cover classification of the multispectral WV-2 data (see Tab. 2 in Chapter 5.1). However, the consistent 'Road' class, which was extracted in this step, was successfully processed and used in a following analysis step.

In contrast to the NDVI-based classification attempt, the second approach, the spectral edge extraction-based detection of livestock pens, was successful. The unsupervised classification with the Sobel algorithm, which was applied to the WV-2 NIR-2 band, performed well and proofed to be an effective method to extract spectral edges in general. Postprocessing this preliminary result was a major task and particularly enhanced by the use of TDX DEM derived terrain parameters (see Chapter 4.4). In combination with the above mentioned 'Road' land cover class, the slope and flow accumulation-based mask, specified the area of probable pen occurrences realistically (see Chapter 5.1).

Nevertheless, both approaches were unsuccessful in creating a spectral signature-based distinction between recently used pens and former pen sites (or rather pen imprints). A closer look at the selected methods shows, that these must possibly be revised to improve the accuracy of the detection results (see Chapter 4.5). The applied accuracy assessment does not allow a comparison with the overall accuracy of classification results from the scientific context. In contrast, taking into account the vast and mountainous terrain of the study area, it must be considered that the amount of probable key sites discovered, cannot be identified to such a large extent based on field survey data only.

The result of the NDVI (vegetation index) calculation and related definition of herder camp related vegetation patches (see Chapter 5.3) explains the green ground signature at herder camp sites (see Fig. 1 in Chapter 1). Furthermore, the discovered 'patch'-like, concentric structure of the derived vegetation pattern can probably be used as a primary tracer of pastoral livelihoods in the study area.

As it was presented in the Chapters 1, 2.7, and 3.3, livestock pen sediments are rich in potentially long-lasting organic matter. Possibly this results in increased local plant growth. In general, the investigation of the relations between terrain profile curvature and herder camp related vegetation patches, conclude that pen sediments probably are connected to the observed vegetation patterns. The concentric zonation of the vegetation patches can give an idea about the spatial extent of current soil formation processes and hence varying plant species compositions. This information can be specifically useful for micromorphological and archaeobotanical research. As discussed in Chapter 6.3 the presence of distinctive vegetation patches could demonstrate a successive occupation of recent herder camps in the study area. In contrast to the initial geoarchaeological research interest (see Chapter 1), it might therefore turn out that the newly discovered vegetation patches have a greater potential for future research than the distinction between recently used pens and pen imprints.

In general, the results derived from remote sensing data enable better insights in the spatial distribution of herder camps in the study area. As discussed before (see Chapter 6.4), occasional detection errors or dry-stone

structures belonging to other subsistence forms must be considered. However, the pastoral land use pattern presented in Fig. 28, Chapter 5.4 and Appendix III allows a detailed assessment of the distribution of pastoral livelihoods in the study area. Moreover, it can be concluded that the use of ethnographic data to the study, in particular the study of transhumance mobility of the Aït Atta and the consideration of specific *Agdal* land management practices, contributed to the interpretation of the results 6.4.

Concluding, it has been demonstrated that digital geoarchaeology, the triangulation of results from remote sensing, GIS, and geoarchaeological field data, can make a major contribution to the research of an interdisciplinary team of scientists. The results of this study give insights in a cultural landscape characterised by pastoral land use and enable a targeted course to study geoarchaeological sites in the study area.

8 Outlook

In general, the results presented and discussed fulfilled the research objective of this study, a remote sensing and GIS-based investigation of pastoral land use in the study area. On this basis, it is now possible to carry out targeted geoarchaeological research in the study area, which is concerned in the second section of the Chapter. However, the resulting pastoral land use map can certainly still be differentiated, and related processing steps can be approved.

Notes on methodological improvements

For example, it would be advantageous to detect watercourses in addition to the presented environmental geospatial data (see Chapter 5). Pastoralists need pasture lands as well as access to water (compare Hary et al. 1996: 3). Mountain rivers can be mapped to complete and differentiate the land use pattern. However, the spectral signature of water in the study area, which exclusively occurs in flowing form respectively in narrow mountain rivers, poses a challenge in satellite imagery classification. The analysis of C-Band SAR (compare Chapter 2.3) data, which is sensitive to water, for example of the Sentinel-1 mission (ESA 2019a) can be an advantage. In addition to the eight multispectral bands of WV-2 optical sensed SWIR bands, which indicate the absorption of water in this spectral region, such as of the Sentinel-2 mission (ESA 2019b) or the higher resolution SWIR data of WorldView-3 (DigitalGlobe 2019b) can be analysed. SWIR imagery can be used to classify different geological units, or rather sediments in the study area, which could be related to herder camp occurrence also.

Concerning the conducted pre-processing of the WV-2 imagery (see Chapter 4.3), local contrast enhancement and the Niblack's Method implemented by Trier et al. 2009 can be further investigated. Probably, this could enhance the visibility of livestock pen structures and therefore support their detection (see Trier et al. 2009: 6f).

The integration of the original TDX elevation information, which can be queried with the detected pens, can be a further approach to refine the conducted analysis. Whereas, the mountainous study area terrain contains high altitude areas that are potentially not suitable for herder camps, this could lead to a further limitation of realistic pen occurrence and decrease

error detections. Moreover, as discussed in Chapter 6.3, still it is possible that the terrain heights is underestimated and the TDX data is incorrect in some locations, such as at vegetation patches. However, an evaluation of the TDX DEM related to this phenomenon, would be a reasonable step.

In general, as discussed in Chapter 6.2 a more sophisticated accuracy assessment, such as described in Congalton & Green 2009, can be executed to achieve a better comparability to relatively similar detection approaches. For example, this is enabled by the calculation of Cohen's kappa coefficient (Congalton & Green 2009: 105). However, this would require the creation of a second reference detection raster. Instead of counting grid based GCP collection (see Chapter 4.5), referential polygon shapes of livestock pens could be created and rasterised for this purpose. The mentioned steps, would allow a more accurate, and above all, quantitative evaluation of the detection results (compareCongalton & Green 2009).

Besides, the calculation of vegetation indices, such as the NDVI, which was applied in this study, the structure of the derived vegetation patches can be possibly further differentiated. As discussed in Chapter 6.3, it is probable that various plant communities, with different nutrient requirements, grow at varying distances to the livestock pens and the related high nutrient availability. Therefore, detailed remote sensing based vegetation studies, for example, a distinction between plants species respectively their specific spectral signatures can be a contribution to subsequent research. Possibly the occurrence of certain plant species, which tolerate a very high nutrient content, can represent a further tracer for livestock pen sediments.

Notes on subsequent field work

In general, it would be important to review the established assumptions, concerning the discussed different land use catchments (see Chapter 6.4), in the field. In addition, detailed study of ethnographical data, such as the Aät Atta ethnography of Hart 1981 is required. The way borders between neighbouring *Agdal* are drawn in the study area today, can be of particular ethnoarchaeological interest. However, this can provide insights in the site selection of transhumant herders.

Since it could be related to an archaeological site, the origin of the white, circular ground signature discussed in Chapter 6.3, which shows a close spatial

relation to archaeological surface finds, will be a part of subsequent field work.

Concerning the presence of herder camp related vegetation patches, it appears that the ecological influence of livestock pen sediments, in which plant nutrients seem to be concentrated, is significant. Soil characteristics and related on-site processes will be further investigated. Related to this intention, comparable investigations of livestock pens, or rather pastoral sites imply a significant positive impact of herder camps on the local soil nutrient cycle (compare Muchiru et al. 2009: 329). In addition, similar to methods described in Mueller-Dombois & Ellenberg 1974: 90 a radial-transect method will be applied on the livestock pen environment. Different plant communities, which are possibly present within the vegetation patch can be determined and differentiated. Thus, the discussed concentric structure of the vegetation patches (see Chapter 6.3) will be further investigated.

Generally, comparable to the investigations in 2017 (see Chapter 3.3), the stratigraphy of selected livestock pens will be investigated and optionally sampled for further analysis under laboratory conditions (see 2.7). Probably methods described in Kothieringer et al. 2018 or in Marshall et al. 2018, can be applied to determine certain deposit age, deposition conditions, as well as related environmental conditions at the respective time of deposition. To conclude, the location of subsequent geoarchaeological field work in the study area is mainly based on the results of this study. The detection of herder camps enabled the selection of future geoarchaeological field work sites.

References

Akasbi, Z., Oldeland, J., Dengler, J., Finckh, M., 2012. Social and ecological constraints on decision making by transhumant pastoralists: a case study from the Moroccan Atlas Mountains. Journal of Mountain Science 9(3), 307–321.

Albertz, J., 2009. Einführung in die Fernerkundung: Grundlagen der Interpretation von Luft- und Satellitenbildern. Wiss. Buchges., Darmstadt, Germany.

Auclair, L., Lemjidi, A., Ewague, A., 2013. Paysages graves and 4000 ans de transhumance dans les alpages du haut atlas (Maroc). PAPERS XXV Valcamonica Symposium Conference, Valcamonica, Italy, Sept. 20–25, 2013.

Bartusch, M., Hajnsek, I., Janoth, J., Marschner, C., Moreira, A., Sparwasser, N., Zink, M., 2010. TanDEM-X The Earth and in three dimensions. `https://www.dlr.de/hr/en/Portaldata/32/Resources/dokumente/broschueren/TanDEM-X_web_Brochure2010.pdf`, 2019-4-15.

CNES, 2018. *Orfeo ToolBox, Version 6.6.1.* CNES - Centre national d'études spatiales und Open Source Geospatial Foundation. `https://www.orfeo-toolbox.org/CookBook/index_TOC.html`, 2019-5-4.

Congalton, R. G., Green, K., 2009. Assessing the Accuracy of Remotely Sensed Data - Principles and Practices Second edition. CRC Press, Taylor & Francis Group, Boca Raton, USA.

De Smith, M., Goodchild, M., Longley, P., 2018. Geospatial Analysis: A Comprehensive Guide to Principles, Techniques and Software Tools. Drumlin Security Ltd., London, UK.

DigitalGlobe, 2010. *The benefits of the eight spectral bands of WorldView-2.* `https://dg-cms-uploads-production.s3.amazonaws.com/uploads/document/file/35/DG-8SPECTRAL-WP_0.pdf`, 2019-4-15.

DigitalGlobe, 2019a. WorldView-2 satellite mission 2009 - 2019. `https://dg-cms-uploads-production.s3.amazonaws.com/uploads/document/file/98/WorldView2-DS-WV2-rev2.pdf`, 2019-4-29.

DigitalGlobe, 2019b. WorldView-3 satellite mission 2014 - 2019. `https://dg-cms-uploads-production.s3.amazonaws.com/uploads/document/file/95/DG2017_WorldView-3_DS.pdf`, 2019-4-29.

DLR, 2019. TanDEM-X satellite mission 2010 - 2019. https://www.dlr.de/dlr/en/Portaldata/1/Resources/documents/TanDEM-X_web.pdf, 2019-4-25.

Dominguez, P., 2013. L'agro-pastoralisme mobile des agdals du Haut Atlas. revista de recerca i formació en antropologia 18(2), 93–103.

Dominguez, P., Bourbouze, A., Demay, S., Genin, D., Kosoy, N., 2012. Diverse Ecological, Economic and Socio-Cultural Values of a Traditional Common Natural Resource Management System in the Moroccan High Atlas: The Aït Ikiss Tagdalts. Environmental Values 21, 277–296.

Dutilly-Diane, C., 2007. . Pastoral economics and marketing in North Africa: A literature review. Nomadic Peoples 11(1), 69–90.

Eitel, B., 2011. Formengemeinschaften der ariden und semiariden Gebiete. In: Gebhardt, H., Meyer, S., Glaser, R., Radtke, U., Reuber, P. (Eds.), Geographie: Physische Geographie und Humangeographie. Spektrum Akademischer Verlag, Heidelberg, Germany, 456–459.

ESA, 2019a. Sentinel-1 SAR satellite mission 2014 - 2019. ESA - European Space Agency. https://sentinel.esa.int/web/sentinel/technical-guides/sentinel-1-sar, 2019-5-28.

ESA, 2019b. Sentinel-2 MSI satellite mission 2015 - 2019. ESA - European Space Agency. https://sentinel.esa.int/web/sentinel/technical-guides/sentinel-2-msi, 2019-5-28.

FAO, 2015. World Reference Base for Soil Resources 2014, update 2015, International soil classification system for naming soils and creating legends for soil maps. World Soil Resources Reports, vol. 106. FAO. FAO, Rome, Italy.

Freeman, T., 1991. Calculating Catchment Area with Divergent Flow Based on a Regular Grid. Computers & Geosciences 17, 413–422.

GDAL 2.4.0, 2018. GDAL - Geospatial Data Abstraction Library, Version 2.4.0. GDAL Development Team. http://www.gdal.org, 2019-4-20.

GRASS 7.6, 2017. Geographic Resources Analysis Support System (GRASS GIS) Software, Version 7.6. GRASS Development Team. http://grass.osgeo.org, 2019-6-13.

GRASS Development Team, 2017. *Geographic Resources Analysis Support System (GRASS GIS) Software, Version 7.6.* Open Source Geospatial Foun-

dation. https://grass.osgeo.org/grass76/manuals/index.html, 2019-5-15.

Grignetti, A., Salvatori, R., Casacchia, R., Manes, F., 1997. Mediterranean vegetation analysis by multi-temporal satellite sensor data. International Journal of Remote Sensing 18(6), 1307–1318.

Grippa, T., Lennert, M., Beaumont, B., Vanhuysse, S., Stephenne, N., Wolff, E., 2017. An Open-Source Semi-Automated Processing Chain for Urban Object-Based Classification. Remote Sensing 9(358), 1–20.

Grohmann, C. H., 2018. Evaluation of TanDEM-X DEMs on selected Brazilian sites: Comparison with SRTM, ASTER GDEM and ALOS AW3D30. Remote Sensing of Environment 212(June 2018), 121–133.

Hart, D. M., 1981. Dadda 'Atta and his forty grandsons: The socio-political organisation of the Ait Atta of Southern Morocco. Menas Press, Wisbech, UK.

Hary, I., Schwartz, H.-J., Pielert, V. H., Mosler, C., 1996. Land degradation in African pastoral systems and the destocking controversy. Ecological Modelling 86(2-3), 227–233.

Hvezda, S., 2007. Wasser und Land im klassischen islamischen Recht unter besonderer Berücksichtigung der målikitischen Rechtsschule. Kölner Ethnologische Beiträge, Cologne, Germany.

Jensen, J. R., 2004. Introductory Digital Image Processing: A Remote Sensing Perspective. Prentice Hall Press, Upper Saddle River, NJ, USA.

Jones, C., 2000. Grazing management for healthy soils. Stipa Inaugural National Grasslands Conference 'Better Pastures Naturally', Mudges, Australia, Mar. 16–17, 2000. https://managingwholes.com/grazing-soils.htm/, 2019-5-29.

Jones, H., Vaughan, R., 2010. Remote Sensing of Vegetation: Principles, Techniques, and Applications. OUP Oxford, Oxford, UK.

Jurgiel, B., 2018. *Point Sampling Tool, Version 0.5.2*. Free Software Foundation. https://github.com/borysiasty/pointsamplingtool, 2019-5-13.

Kothieringer, K., Röpke, A., Reitmaier, T., Krause, R., 2018. Auf den Spuren prähistorischer Weidewirtschaft in (sub-)alpinen Böden: Erste Ergebnisse aus dem Montafon und der Silvretta (A/CH). Arbeitskreis Geoarchäologie Conference, Munich, Germany, May 3–5, 2018.

Krieger, G., Moreira, A., Fiedler, H., Hajnsek, I., Werner, M., Younis, M., Zink, M., 2007. TanDEM-X: A Satellite Formation for High-Resolution SAR Interferometry. IEEE Transactions on Geoscience and Remote Sensing 45(11), 3317–3341.

Lambers, K., 2018. Airborne and Spaceborne Remote Sensing and Digital Image Analysis in Archaeology. In: Siart, C., Forbriger, M., Bubenzer, O. (Eds.), Digital Geoarchaeology, Natural Science in Archaeology. 1st ed. Springer International Publishing, Basel, Switzerland, 109–122.

Lillesand, T., Kiefer, R., Chipman, J., 2015. Remote Sensing and Image Interpretation. John Wiley & Sons, Ltd., New York, USA.

Lloyd, C., 2010. Spatial Data Analysis: an Introduction for GIS Users. Oxford University Press, Oxford, UK.

Luo, L., Wang, X., Liu, C., Guo, H., Du, X., 2014. Integrated RS, GIS and GPS approaches to archaeological prospecting in the Hexi Corridor, NW China: a case study of the royal road to ancient Dunhuang. Journal of Archaeological Science 50, 178–190.

Macphail, R., Goldberg, P., 2018. Applied Soils and Micromorphology in Archaeology. Cambridge Manuals in Archaeology. Cambridge University Press, Cambridge, UK.

Maroc Météo, 2019. Le climat du Maroc. `http://www.marocmeteo.ma/?q=fr/climat_maroc`, 2019-5-18.

Marshall, F., Reid, R. E. B., Goldstein, S., Storozum, M., Wreschnig, A., Hu, L., Kiura, P., Shahack-Gross, R., Ambrose, S. H., 2018. Ancient herders enriched and restructured African grasslands. Nature 561(7723), 387–390.

Meier, L., 2017. Field sketches, AREHHAL campaign september 2017. `https://laurameier.allyou.net/9374319/ait-atta-nomad`, 2019-4-25.

Muchiru, A. N., Western, D., Reid, R. S., 2009. The impact of abandoned pastoral settlements on plant and nutrient succession in an African savanna ecosystem. Journal of Arid Environments 73(3), 322–331.

Mueller-Dombois, D., Ellenberg, H., 1974. Aims and Methods of Vegetation Ecology. John Wiley & Sons, Ltd., New York, USA.

OTB 6.6.1, 2018. Orfeo ToolBox, Version 6.6.1. CNES - Centre national d'études spatiales. `https://www.orfeo-toolbox.org`, 2019-5-15.

Pal, M., 2005. Random forest classifier for remote sensing classification. International Journal of Remote Sensing 26(1), 217–222.

Pastor, A., Gallello, G., Luisa Cervera, M., Guardia, M., 2016. Mineral soil composition interfacing archaeology and chemistry. TrAC Trends in Analytical Chemistry 78, 48–59.

Pelletier, J. D., 2008. Quantitative Modeling of Earth Surface Processes. Cambridge University Press, Cambridge, UK.

QGIS 2.18, 2019. *QGIS Geographic Information System, Version 2.18*. QGIS Development Team. `http://qgis.osgeo.org`, 2019-4-12.

QGIS Development Team, 2019. *QGIS Geographic Information System, Version 2.18*. Open Source Geospatial Foundation. `https://docs.qgis.org/2.18/en/docs/index.html`, 2019-4-12.

Ramankutty, N., Evan, A. T., Monfreda, C., Foley, J. A., 2008. Farming the planet: 1. Geographic distribution of global agricultural lands in the year 2000. Global Biogeochemical Cycles 22(1), 1–19.

Reitmaier, T., Alther, Y., Azizi, A., Benalla, A., Leib, S., Meier, L., Reitmaier, L., Romera, M. C., Walser, C., Zickel, M., 2017. «Arehhal» ein ethnoarchäologisches Pilotprojekt zum Nomadismus der Ait Atta in Marokko. SLSA Jahresbericht – Rapport annuel – Annual report, SLSA - Schweizerisch-Liechtensteinische Stiftung für archäologische Forschungen im Ausland. Zürich, Switzerland. `https://www.academia.edu/37298480/_Arehhal_ein_ethnoarch%C3%A4ologisches_Pilotprojekt_zum_Nomadismus_der_Ait_Atta_in_Marokko`, 2019-5-6.

Rubel, F., Kottek, M., 2010. Observed and projected climate shifts 1901-2100 depicted by world maps of the Köppen-Geiger climate classification. Meteorologische Zeitschrift 19(2), 135–141.

SAGA 2.3.2, 2016. System for Automated Geoscientific Analyses (SAGA) v. 2.3.2. SAGA Development Team. `http://www.saga-gis.org/en/index.html`, 2019-5-17.

Schlüter, T., 2006. Geological Atlas of Africa: With Notes on Stratigraphy, Tectonics, Economic Geology, Geohazards and Geosites of Each Country. ZEW economic studies. Springer Nature, Berlin/ Heidelberg, Germany.

SEOS, 2019a. Spectral signatures of soil, vegetation and water. Source: with modifications from Siegmund A & G Menz, 2005: Fernes nah gebracht -

Satelliten- und Luftbildeinsatz zur Analyse von Umweltveränderungen im Geographieunterricht In: Geographie und Schule, 154, 7. https://seos-project.eu/remotesensing/remotesensing-c01-p05.html, 2019-5-15.

SEOS, 2019b. The electromagnetic spectrum and atmospheric transmittance. Source: with modifications from Albertz, 2007 : Einführung in die Fernerkundung. Grundlagen der Interpretation von Luft- & Satellitenbildern. Darmstadt, 254. https://seos-project.eu/remotesensing/remotesensing-c01-p03.html, 2019-5-15.

Shahack-Gross, R., 2011. Herbivorous livestock dung: Formation, taphonomy, methods for identification, and archaeological significance. Journal of Archaeological Science Elsevier Ltd. 38, 205–218.

Shahack-Gross, R., 2017. Animal Gathering Enclosures. In: Cristiano Nicosia, G. S. (Ed.), Archaeological Soil and Sediment Micromorphology. John Wiley & Sons, Ltd, New York, USA. 265–280.

Siart, C., 2018. Digital Geoarchaeology: Bridging the Gap Between Archaeology, Geosciences and Computer Sciences. In: Siart, C., Forbriger, M., Bubenzer, O. (Eds.), Digital Geoarchaeology, Natural Science in Archaeology. Springer International Publishing, Basel, Switzerland, 1–7.

SNAP 6.0, 2018. ESA Sentinel Application Platform, Version 6.0. ESA - European Space Agency, Brockmann Consult - Array Systems Computing und C-S. https://step.esa.int/main/toolboxes/snap, 2019-5-15.

Spedding, C., 1971. Grassland ecology. Clarendon Press, Oxford, UK.

Trier, Ø., Larsen, S., Solberg, R., 2009. Automatic Detection of Circular Structures in High-resolution Satellite Images of Agricultural Land. Archaeological Prospection 16, 1–15.

Usery, E. L., 1993. Category Theory and the Structure of Features in Geographic Information Systems. Cartography and Geographic Information Systems 20(1), 5–12.

Verhagen, P., 2018. Spatial Analysis in Archaeology: Moving into New Territories. In: Siart, C., Forbriger, M., Bubenzer, O. (Eds.), Digital Geoarchaeology, Natural Science in Archaeology. 1st ed. Springer International Publishing, Basel, Switzerland, 11–25.

Zickel, M., Röpke, A., Reitmaier, T., 2018. Nomadismus im Hohen Altas, Marokko: Geo- und Ethnoarchäologie auf Weideplätzen. Arbeitskreis Geoarchäologie Conference, Munich, Germany, May 3–5, 2018.

Zingman, I., Saupe, D., Lambers, K., 2014. A Morphological Approach for Distinguishing Texture and Individual Features in Images. Pattern Recognition Letters 47, 129–138.

Zingman, I., Saupe, D., Penatti, O. A., Lambers, K., 2016. Detection of Fragmented Rectangular Enclosures in Very High Resolution Remote Sensing Images. IEEE Transactions on Geoscience and Remote Sensing 54(8), 4580–4593.

Appendix

Appendix I

Table 6: Tools applied in pre-processing, related toolbox provider, GUI and attached weblink to the respective tool documentation.

Pre-processing

Tool	**Purpose**	**Toolbox provider**	**Software (GUI)**	**Documentation**
Pansharpening	Combination of multispectral bands and high spatial resolution panchromatic band	(OTB 6.6.1 2018)	(OTB 6.6.1 2018)	https://www.orfeo-toolbox.org/CookBook/Applications/app_Pansharpening.html?highlight=pansharpen
r.resample	TanDEM-X interpolation	(GRASS 7.6 2017)	(QGIS 2.18 2019)	https://grass.osgeo.org/grass76/manuals/r.resample.html
OrthoRectification	Orthorectification with WorldVIew-2 geometric information (RPC) and TanDEM-X	(OTB 6.6.1 2018)	(OTB 6.6.1 2018)	https://www.orfeo-toolbox.org/CookBook/Applications/app_OrthoRectification.html
Georeferencer	Additional georeferenciation of Worldview-2 to TanDEM-X	(GDAL 2.4.0 2018)	(QGIS 2.18 2019)	https://docs.qgis.org/2.18/de/docs/user_manual/plugins/plugins_georeferencer.html
Clip (raster)	Clip the two datasets to study area extend	(GDAL 2.4.0 2018)	(QGIS 2.18 2019)	https://docs.qgis.org/2.8/en/docs/user_manual/processing_algs/gdalogr/gdal_extraction/cliprasterbymasklayer.html

Table 7: Tools applied in Analysis step I, related toolbox provider, GUI and attached weblink to the respective tool documentation.

Analysis I

Tool	**Purpose**	**Toolbox provider**	**Software (GUI)**	**Documentation**
r.slope.aspect	Slope and profile curvature	(GRASS 7.6 2017)	(QGIS 2.18 2019)	https://grass.osgeo.org/grass76/manuals/r.slope.aspect.html
Flow Accumulation (QM of ESP)	Detect valley bottoms	(SAGA 2.3.2 2016)	(QGIS 2.18 2019)	http://www.saga-gis.org/saga_tool_doc/2.3.0/sim_qm_of_esp_2.html
r.recode	Extract slope and flow accumulation thresholds	(GRASS 7.6 2017)	(QGIS 2.18 2019)	https://grass.osgeo.org/grass76/manuals/r.recode.html
Polygonize (raster to vector)	Vectorise slope and flow accumulation thresholds	(GDAL 2.4.0 2018)	(QGIS 2.18 2019)	https://docs.qgis.org/2.18/en/docs/user_manual/processing_algs/gdalogr/gdal_conversion.html
Shapes buffer (fixed distance)	Increase valley bottom coverage	(QGIS 2.18 2019)	(QGIS 2.18 2019)	https://docs.qgis.org/2.18/en/docs/user_manual/processing_algs/saga/shapes_tools.html#shapes-buffer
Simplify geometries	Smooth slope and valley bottom geometries	(QGIS 2.18 2019)	(QGIS 2.18 2019)	https://docs.qgis.org/2.18/en/docs/user_manual/processing_algs/qgis/vector_geometry_tools.html#simplify-geometries
Geometry checker	Remove slivers and very small polygons	(QGIS 2.18 2019)	(QGIS 2.18 2019)	https://docs.qgis.org/2.18/en/docs/user_manual/plugins/plugins_geometry_checker.html
Difference	Intersect slope and flow accumulation polygons	(QGIS 2.18 2019)	(QGIS 2.18 2019)	https://docs.qgis.org/2.18/en/docs/user_manual/processing_algs/qgis/vector_overlay_tools.html#difference

Table 8: Tools applied in Analysis step II, related toolbox provider, GUI and attached weblink to the respective tool documentation.

Analysis II

Tool	**Purpose**	**Toolbox provider**	**Software (GUI)**	**Documentation**
Edge Extraction (sobel)	Extract spectral edges of WolrdView-2 band 8	(OTB 6.6.1 2018)	(OTB 6.6.1 2018)	https://www.orfeo-toolbox.org/CookBook/Applications/app_EdgeExtraction.html?highlight=edge%20extraction
r.neighbors	Produce a pixel value variance raster	(GRASS 7.6 2017)	(QGIS 2.18 2019)	https://grass.osgeo.org/grass76/manuals/r.neighbors.html
r.recode	Extract edge variance threshold	(GRASS 7.6 2017)	(QGIS 2.18 2019)	https://grass.osgeo.org/grass76/manuals/r.recode.html
r.reclass. area.greater	Sieve raster, exlude too small areas	(GRASS 7.6 2017)	(QGIS 2.18 2019)	https://grass.osgeo.org/grass76/manuals/r.reclass.area.html
Polygonize (raster to vector)	Vectorise the edge raster	(GDAL 2.4.0 2018)	(QGIS 2.18 2019)	https://docs.qgis.org/2.18/en/docs/user_manual/processing_algs/gdalogr/gdal_conversion.html
Clip (vector)	Intersect edge polygons with the slope/ flow accumul. derived mask	(QGIS 2.18 2019)	(QGIS 2.18 2019)	https://docs.qgis.org/2.18/en/docs/user_manual/processing_algs/qgis/vector_overlay_tools.html
Shapes buffer (fixed distance)	Reconnect fragmented structures and dissolve them	(QGIS 2.18 2019)	(QGIS 2.18 2019)	https://docs.qgis.org/2.18/en/docs/user_manual/processing_algs/saga/shapes_tools.html#shapes-buffer
Geometry checker	Remove slivers and very small polygons	(QGIS 2.18 2019)	(QGIS 2.18 2019)	https://docs.qgis.org/2.18/en/docs/user_manual/plugins/plugins_geometry_checker.html
Simplify geometries	Smooth geometries of the detection result	(QGIS 2.18 2019)	(QGIS 2.18 2019)	https://docs.qgis.org/2.18/en/docs/user_manual/processing_algs/qgis/vector_geometry_tools.html#simplify-geometries

Table 9: Tools applied in Analysis step III, related toolbox provider, GUI and attached weblink to the respective tool documentation.

Analysis III

Tool	**Purpose**	**Toolbox provider**	**Software (GUI)**	**Documentation**
Random Forest Classifier	Classify areas covered by the road	(SNAP 6.0 2018)	(SNAP 6.0 2018)	https://github.com/senbox-org/snap-engine/blob/master/snap-classification/src/main/java/org/esa/snap/classification/gpf/randomForest/RandomForestClassifierOp.java
r.reclass	Extract road class	(GRASS 7.6 2017)	(QGIS 2.18 2019)	https://grass.osgeo.org/grass76/manuals/r.reclass.html
Polygonize (raster to vector)	Vectorise road class	(GDAL 2.4.0 2018)	(QGIS 2.18 2019)	https://docs.qgis.org/2.18/en/docs/user_manual/processing_algs/gdalogr/gdal_conversion.html
Extract by attribute	Extract road polygon	(QGIS 2.18 2019)	(QGIS 2.18 2019)	https://docs.qgis.org/2.18/en/docs/user_manual/processing_algs/qgis/vector_selection_tools.html
Shapes buffer (fixed distance)	Buffer road polygon	(QGIS 2.18 2019)	(QGIS 2.18 2019)	https://docs.qgis.org/2.18/en/docs/user_manual/processing_algs/saga/shapes_tools.html#shapes-buffer
Difference	Intersect road with detection result	(QGIS 2.18 2019)	(QGIS 2.18 2019)	https://docs.qgis.org/2.18/en/docs/user_manual/processing_algs/qgis/vector_overlay_tools.html#difference

Table 10: Tools applied in Analysis step IV, related toolbox provider, GUI and attached weblink to the respective tool documentation.

Analysis IV

Tool	**Purpose**	**Toolbox provider**	**Software (GUI)**	**Documentation**
Raster calculator	Calculate NDVI vegetation index	(QGIS 2.18 2019)	(QGIS 2.18 2019)	https://docs.qgis.org/2.18/en/docs/user_manual/working_with_raster/raster_calculator.html
r.recode	Set NDVI thresholds	(GRASS 7.6 2017)	(QGIS 2.18 2019)	https://grass.osgeo.org/grass76/manuals/r.recode.html
Polygonize (raster to vector)	Vectorise NDVI classes	(GDAL 2.4.0 2018)	(QGIS 2.18 2019)	https://docs.qgis.org/2.18/en/docs/user_manual/processing_algs/gdalogr/gdal_conversion.html
Clip (vector)	Clip NDVI polygons with the slope/ flow accumulation dervied mask	(QGIS 2.18 2019)	(QGIS 2.18 2019)	https://docs.qgis.org/2.18/en/docs/user_manual/processing_algs/qgis/vector_overlay_tools.html
Geometry checker	Remove slivers and very small polygons	(QGIS 2.18 2019)	(QGIS 2.18 2019)	https://docs.qgis.org/2.18/en/docs/user_manual/plugins/plugins_geometry_checker.html
Zonal statistics	Query curvature raster with NDVI polygons	(QGIS 2.18 2019)	(QGIS 2.18 2019)	https://docs.qgis.org/2.18/en/docs/user_manual/plugins/plugins_zonal_statistics.html

Table 11: Tools applied to access the accuracy of the conducted approach, related toolbox provider, GUI and attached weblink to the respective tool documentation.

Accuracy assessment

Tool	**Purpose**	**Toolbox provider**	**Software (GUI)**	**Documentation**
Create grid	Create counting grid cells	(QGIS 2.18 2019)	(QGIS 2.18 2019)	https://docs.qgis.org/2.8/en/docs/user_manual/processing_algs/qgis/vector_creation_tools/creategrid.html
Editing	Create GCP and reference ROIs for the random forest classifcation result	(QGIS 2.18 2019)	(QGIS 2.18 2019)	https://docs.qgis.org/2.18/en/docs/user_manual/working_with_vector/editing_geometry_attributes.html
v.vect.stats	Count GCP per grid cell	(GRASS 7.6 2017)	(QGIS 2.18 2019)	https://grass.osgeo.org/grass76/manuals/v.vect.stats.html
Point sampling tool	Query slope with GCP	(Jurgiel 2018)	(QGIS 2.18 2019)	https://plugins.qgis.org/plugins/pointsamplingtool/
Shapes buffer (fixed distance)	Buffer GCP to create polygons	(QGIS 2.18 2019)	(QGIS 2.18 2019)	https://docs.qgis.org/2.18/en/docs/user_manual/processing_algs/saga/shapes_tools.html#shapes-buffer
Rasterize (vector to raster)	Rasterise detection result	(GDAL 2.4.0 2018)	(QGIS 2.18 2019)	https://docs.qgis.org/2.18/en/docs/user_manual/processing_algs/gdalogr/gdal_conversion.html
Compute Confusion Matrix	Calculate confusion matrix for detection result and random forest classification	(OTB 6.6.1 2018)	(OTB 6.6.1 2018)	https://www.orfeo-toolbox.org/CookBook/Applications/app_ComputeConfusionMatrix.html?highlight=confusion%20matrix

Appendix II

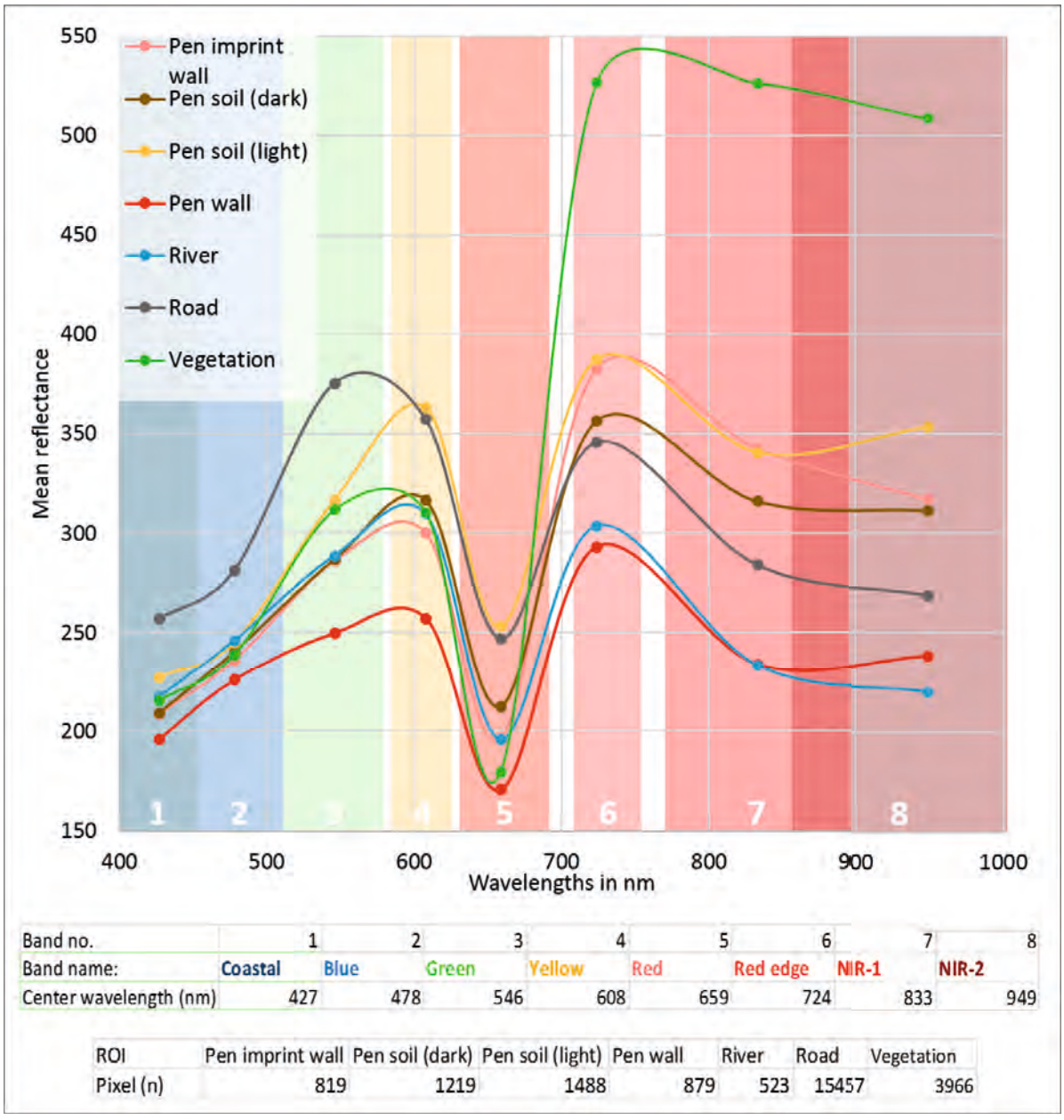

Band no.	1	2	3	4	5	6	7	8
Band name:	Coastal	Blue	Green	Yellow	Red	Red edge	NIR-1	NIR-2
Center wavelength (nm)	427	478	546	608	659	724	833	949

ROI	Pen imprint wall	Pen soil (dark)	Pen soil (light)	Pen wall	River	Road	Vegetation
Pixel (n)	819	1219	1488	879	523	15457	3966

Figure 31: Spectral signatures (mean values of the class ROIs) of different land cover types in the WorldView-2 scene that was used in this study.

Appendix III

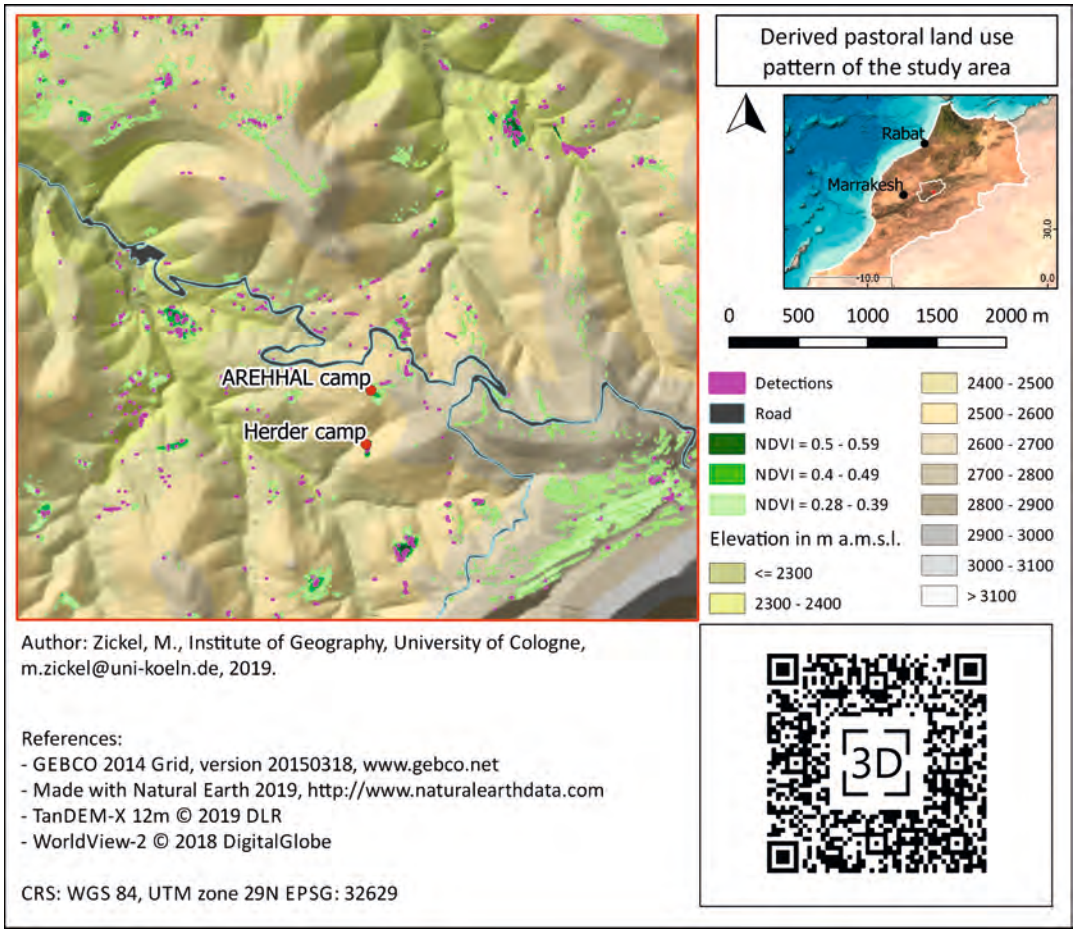

Figure 32: 3D model based on the Tandem-X DEM and mapped pastoral land use pattern of the study area (use QR code or `http://archaeobotanik.phil-fak.uni-koeln.de/sites/archaeobotanik/MZ_MA_3D/HAC-maroc-pastoral.html`).

KÖLNER ETHNOLOGISCHE BEITRÄGE
HERAUSGEGEBEN VON MICHAEL J. CASIMIR

HEFT 1 **BABET NAEFE 2002**
Die Kormoranfischer vom Erhai-See
Eine südwest-chinesische Wirtschaftsweise im Wandel

HEFT 2 **ANNIKA WIEKHORST 2002**
Die Verwendung von Pflanzen in der traditionellen Medizin bei drei Baka Gruppen in Südost Kamerun

HEFT 3 **IRENE HILGERS 2002**
Transformationsprozeß im Norden Kirgistans
Sozio-ökonomischer Wandel am Beispiel eines Dorfes

HEFT 4 **BRITTA FUCHS 2002**
Wenn der Muezzin rufen will
Diskurse über ein Moscheebauprojekt im Kölner Stadtteil Chorweiler

HEFT 5 **KERSTIN HADJER 2003**
Illegalisierte Identitäten
Auswirkungen der Sans Papiers-Problematik auf den Alltag afrikanischer Migranten in Pariser Wohnheimen (Foyers)

HEFT 6 **FLORIAN STAMMLER 2003**
Überlebensstrategien im postsozialistischen Russland
Das Beispiel der rentierzüchtenden Chanty und Nentsy in Nordwestsibirien

HEFT 7 **CLAUDIA LIEBELT 2003**
Die Wasserwirtschaft im südmarokkanischen Dratal im Spannungsfeld von lokaler und staatlicher Ressourcenkontrolle

HEFT 8 **NADIA CORNELIUS 2003**
Genese und Wandel von Festbräuchen und Ritualen in Deutschland von 1933 bis 1945

HEFT 9 **HENRICA VAN DER BEHRENS 2003**
Gartenbau der Himba
Ackerbauliche Bodennutzung einer pastoralnomadischen Gruppe im Nordwesten Namibias und Wandel von Festbräuchen und Ritualen

HEFT 10 **TOBIAS SCHMIDTNER 2004**
Ressourcenmanagement und kollektives Handeln
Wirtschaft und soziale Organisation bei einer Gemeinschaft namibianischer small miners in der Erongo-Region

HEFT 11 **NATASCHA GARVIN 2004**
„La vara es recta, no es torcida“
Der Alcalde Auxiliar als lokale Autorität in einer indigenen Gemeinde Guatemalas

HEFT 12 **SEBASTIAN T. ELLERICH 2004**
Der Yaqona-Markt in Fidschi
Zustand, Probleme, Bemühungen

HEFT 13 **ANNE SCHADY 2004**
"Community Participation" and "Peer Education"
A critique of key-concepts in HIV/AIDS prevention in Swaziland

HEFT 14 **THEKLA HOHMANN 2004**
Transformationen kommunalen Ressourcenmanagements im Tsumkwe Distrikt (Nordost-Namibia)

KÖLNER ETHNOLOGISCHE BEITRÄGE
HERAUSGEGEBEN VON MICHAEL J. CASIMIR

HEFT 15 **BETTINA ZIESS 2004**
Weide, Wasser, Wild.
Ressourcennutzung und Konfliktmanagement in einer Conservancy im Norden Namibias.

HEFT 16 **DEIKE EULENSTEIN 2004**
Die Ernährungssituation und Ernährungsweise in der DDR (1949-1989) und die Veränderungen nach der Wiedervereinigung am Beispiel Thüringens

HEFT 17 **SONJA GIERSE-ARSTEN 2005**
CHRIST CRUSHES HIV-CRISIS
Umgang namibischer Pfingstkirchen mit der HIV/AIDS Epidemie

HEFT 18 **JANA JAHNKE 2006**
Lokale Interessen, Staatlichkeit und Naturschutz in einem globalen Kontext
Untersuchung eines Projektes der Weltbank zur Einrichtung von geschützten Gebieten in Peru mit Management durch indigene Bevölkerungsgruppen

HEFT 19 **MONIKA ZÍKOVÁ 2006**
Die kulturspezifische Formung des Gefühls
Japan im interkulturellen Vergleich

HEFT 20 **BJÖRN THEIS 2006**
DISKRETION UND DIFFAMIE
Innensicht und Fremdbild am Beispiel der Freimaurerei

HEFT 21 **LAURA E. BLECKMANN 2007**
Zur Verräumlichung kollektiver Erinnerung
Landschaften in Preisgedichten der Herero/Himba im Nordwesten Namibias

HEFT 22 **SUSANNE HVEZDA 2007**
Wasser und Land im klassischen islamischen Recht unter besonderer Berücksichtigung der mālikitischen Rechtsschule

HEFT 23 **SILKE TÖNSJOST 2007**
Plants and Pastures
Local knowledge on livestock - environment relationships among OvaHerero pastoralists in north - western Namibia

HEFT 24 **TAIYA MIKISCH 2007**
Stolz und Stigma
Tanz und Geschlechterrollen in Zagora, Südmarokko

HEFT 25 **FRANZISKA BEDORF 2007**
We don't have a culture
"Being coloured" in Namibia als Konstruktion und Praxis

HEFT 26 **FRANK WILDAUER 2007**
Zur Genese ethnischer Konflikte
Die Konkomba-Kriege im Norden Ghanas

HEFT 27 **MARTIN BÖKE 2008**
Die Rolle der Emotionen im traditionellen chinesischen Medizinsystem

HEFT 28 **NICOLAI SPIEß 2008**
Die Tempel von Khajuraho (Indien) und ihre erotischen Skulpturen in den Augen ihrer Betrachter

KÖLNER ETHNOLOGISCHE BEITRÄGE
HERAUSGEGEBEN VON MICHAEL J. CASIMIR

HEFT 29 **ELISA TRÄGER 2008**
Bioprospektion und indigene Rechte
Der Konflikt um die Nutzung von Bioressourcen

HEFT 30 **KATRIN SCHAUMBURG 2008**
Maponya's in Transition - The Social Production and Construction of an Urban Place in Soweto, Johannesburg (South Africa)

HEFT 31 **LINA GANDRAS 2009**
Warum Bio?
Eine Untersuchung zum Kaufverhalten im Lebensmittelbereich

HEFT 32 **LEANDROS FISCHER 2009**
Landscape and Identities
Palestinian Refugees in Lebanon

HEFT 33 **MICHAEL J. CASIMIR 2010**
Growing up in a Pastoral Society
Socialisation among Pashtu Nomads in Western Afghanistan

HEFT 34 **KATHARINA GRAF 2010**
Drinking Water Supply in the Middle Drâa Valley, South Morocco
Options for Action in the Context of Water Scarcity and Institutional Constraints

HEFT 35 **BARBARA SOLICH 2010**
Increasing Malaria Risk in Eastern Africa
A Multi-Causal Analysis

HEFT 36 **IBRAHIM ANKAOĞLUAR 2011**
Das Haus im Fokus Austronesischera Orientierungssysteme

HEFT 37 **CHRIS FREIHAUT 2011**
Community Forestry
Instrument des globalen Klimaschutzes oder lokale Maßnahme zu Empowerment?

HEFT 38 **HEIDRUN MEZGER 2011**
Zur Weberei der Dogon in Mali
Eine komparative und historische Perspektive

HEFT 39 **DIEGO AUGUSTO MENESTREY SCHWIEGER 2012**
Institutions and Conflict:
An Ethnographic Study of Communal Water Management in North-West Namibia

HEFT 40 **CAROLIN MAEVIS 2012**
Die Vermittlung von Unmittelbarkeit
Bilder und Erleben „ursprünglicher Natur" von Safari-TouristInnen am Naivashasee, Kenia

HEFT 41 **FABIENNE BRAUKMANN 2012**
Nilpferdjäger, Weber, Salzhändler
Wirtschaftliche Strategien und soziale Organisation der Haro Südäthiopiens im Wandel

HEFT 42 **ANNE TURIN 2014**
Imperiale Jagd und europäische Expansion im Oranje-Freistaat, 1800-1890
A.H. Bain, Prinz Alfreds Jagd und die Rettung des Weißschwanzgnus

HEFT 43 **LENA MUCHA 2014**
Friedlicher ziviler Widerstand im Kontext des urbanen Konfliktes im Stadtteil *Comuna 13* in Medellín (Kolumbien)

KÖLNER ETHNOLOGISCHE BEITRÄGE
HERAUSGEGEBEN VON MICHAEL J. CASIMIR

HEFT 44 **DUŠKO BAŠIĆ 2015**
The United Nations of Football
South-South Migration, Transnational Ties and Denationalization in the National Football Teams of Equatorial Guinea and Togo

HEFT 45 **ANNA KALINA KRÄMER 2016**
Das „Anthropozän" als Wendepunkt zu einem neuen wissenschaftlichen Bewusstsein?
Eine Untersuchung aus ethnologischer Perspektive zur Bedeutung und Verwendung des Konzeptes.

HEFT 46 **THOMAS WIDLOK 2017**
Wir Staatsmenschen
Das Feld, die Stadt und der Staat in der Kulturanthropologie Afrikas

HEFT 47 **KATHARINA HAGER 2017**
Vom Arme-Leute-Essen zum andinen Superfood.
Quinua in Bolivien im Spannungsfeld zwischen Revitalisierung, Ernährungssicherung und internationalem Quinuaboom.

HEFT 48 **DOREH TAGHAVI 2017**
EXPLORING FALLISM:
Student Protests and the Decolonization of Education in South Africa

HEFT 49 **CATERINA REINKER 2017**
Life on Sauerkraut Hill
Representation and Practices of Freedom and Constriction among German Immigrants in Cape Town, South Africa

HEFT 50 **SONJA ESTERS 2017**
Schwarz-Weiß im Dunkeln
Zur Aushandlung von Gender, Hautfarbe und Ethnizität in Kölner Tanzclubs

HEFT 51 **ALINA ZIEGLER 2018**
„Ausländer-Time"
Zur Konstruktion und Inszenierung sozialer Identitäten durch Schülerinnen und Schüler an einer Realschule in Köln

HEFT 52 **TABEA SCHIEFER 2019**
Whiskykonsum als Multisensorisches und Identitätsstiftendes Erlebnis
Ergebnisse einer empirischen Untersuchung in Deutschland und in Schottland

HEFT 53 **CAROLA JACOBS 2019**
Practicing Belonging and Navigating Uncertainties:
The Case of Congolese Diasporans in South Africa

HEFT 54 **PAULINA PEGA 2019**
Die Tataren
Geschichte, Fremd- und Eigenbild einer muslimischen Gemeinschaft in Ostpolen

HEFT 55 **ANNA KALINKA KRÄMER 2020**
Satsaṅg, Saṅgha, Sādhana
Zur Verortung von Spiritualität im indischen Rishikesh

HEFT 56 **MARIA LASSAK 2020**
***Unconditional Cash Transfer* als staatliches Instrument der Armutslinderung inTansania am Beispiel des Bezirks Kilombero, Südwest-Tansania**

Druck und Bindung: Hundt Druck GmbH, Köln
Tel: +49 (0) 221 940 68-0 · www.hundt-druck.de

KÖLNER ETHNOLOGISCHE BEITRÄGE
HERAUSGEGEBEN VON MICHAEL J. CASIMIR

ISSN 1611 - 4531